



Air Quality Modeling Final Rule
Technical Support Document

2015 Ozone NAAQS Good Neighbor Plan

Office of Air Quality Planning and Standards
United States Environmental Protection Agency

1. Introduction

In this technical support document (TSD) we describe the air quality modeling performed to support the EPA’s final Good Neighbor Plan for the 2015 Ozone National Ambient Air Quality Standards (NAAQS) (i.e., final rule). For this final rule, air quality modeling is used to project ozone design values¹ at individual monitoring sites to the 2023 and 2026 analytic years² and to estimate state-by-state contributions to ozone design values at individual monitoring sites in these future years. The projected ozone design values are evaluated to identify ozone monitoring sites that are expected to have nonattainment or maintenance problems for the 2015 ozone National Ambient Air Quality Standards (NAAQS) in the future (i.e., nonattainment and maintenance receptors).³ Ozone contribution data for 2023 and 2026 are used to quantify projected interstate contributions from emissions in each upwind state to ozone design values at projected nonattainment and maintenance receptors in other states (i.e., in downwind states). The contributions from individual states to nonattainment and maintenance receptors in other states (i.e., upwind states and downwind states, respectively) are evaluated to identify upwind states that contribute greater than or equal to 1 percent of the 2015 ozone NAAQS (i.e., 1 percent of 70 ppb which is 0.70 ppb) to one or more downwind receptors. Upwind states that contribute at or above this threshold to particular receptors are referred to as being “linked” to these receptors. In this final rule the EPA is making a finding that interstate transport of ozone precursor emissions from 23 upwind states (Alabama, Arkansas, California, Illinois, Indiana, Kentucky, Louisiana, Maryland, Michigan, Minnesota, Mississippi, Missouri, Nevada, New Jersey, New York, Ohio, Oklahoma, Pennsylvania, Texas, Utah, Virginia, West Virginia, and Wisconsin) are significantly contributing to nonattainment or interfering with maintenance of the 2015 ozone NAAQS in downwind states, based on projected ozone precursor emissions in the 2023 ozone season.

As described in this TSD, the EPA performed air quality modeling for the 2016 base year and 2023 and 2026 future years to project 2016-centered base period design values to each of these future years. Ozone source apportionment modeling was performed using emissions projected to 2023 and 2026 to determine the contributions of total anthropogenic emissions from each state to projected

¹ The ozone design value for a monitoring site is the 3-year average of the annual fourth-highest daily maximum 8-hour average ozone concentrations at the site.

² The rationale for using 2023 and 2026 as applicable future analytic years for this transport assessment is described in the preamble for this final rule.

³ As described in section 3, the EPA also identified an additional type of maintenance-only receptors based on recent measured data that exceed the NAAQS.

ozone design values at individual monitoring sites nationwide for each of these years. The modeling for 2023 and 2026 was used to identify receptors and upwind/downwind linkages to inform Step 1 and Step 2 of the 4-step interstate transport framework, respectively.⁴ In addition, modeling was performed for the 2026 EGU plus non-EGU final rule control case that is analyzed in the Regulatory Impact Analysis (RIA).

The remaining sections of this TSD are as follows. Section 2 describes the air quality modeling platform and the evaluation of model predictions of maximum daily average 8-hour (MDA8) ozone concentrations using measured (i.e., observed) data. Section 3 describes the procedures for projecting ozone design value concentrations and the approach for identifying monitoring sites projected to have nonattainment and/or maintenance problems in 2023 and 2026. Section 4 describes (1) the source apportionment modeling, (2) the procedures for quantifying contributions to individual monitoring sites including nonattainment and/or maintenance receptors, and (3) the evaluation of upwind state contributions to individual receptors in downwind states. In Section 5 we present the results of the 2026 control case model run. Section 6 describes a back-trajectory analysis for selected receptors in 2023. Appendix A describes the results of a sensitivity analysis designed to investigate the possible causes of ozone under prediction in the 2016v2 modeling for the purpose of improving model performance in the 2016v3 modeling for this final rule. Appendix B provides model performance statistics and graphics for maximum daily average 8-hour (MDA8) ozone concentrations based on the 2016v3 base year modeling. Appendix C includes tables containing the ozone contributions to each receptor from each state and other individual source “tags” tracked in the source apportionment modeling for 2023 and for 2026. Appendix D contains tables which provide the total upwind state contribution as a percent of the 2023 ozone average design value and as a percent of ozone formed from total U.S. anthropogenic emissions at each receptor. Appendix E contains tables which identify which upwind states are linked to individual downwind receptors in 2023 and 2026. Appendix F contains graphics which display the spatial distribution of top 10-day average contributions from individual states covered by this final rule based on modeling for 2023.

⁴ See the preamble for a detailed description of the 4-step interstate transport framework. In summary, for Step 1: identify monitoring sites that are projected to have problems attaining and/or maintaining the NAAQS (i.e., nonattainment and/or maintenance receptors); Step 2: identify states that impact those air quality problems in other (i.e., downwind) states sufficiently such that the states are considered “linked” and therefore warrant further review and analysis; Step 3: identify the emissions reductions necessary (if any), applying a multifactor analysis, to eliminate each linked upwind state’s significant contribution to nonattainment or interference with maintenance of the NAAQS at the locations identified in Step 1; and Step 4: adopt permanent and enforceable measures needed to achieve those emissions reductions.

The input and output modeling files for the 2016, 2023 and 2026 modeling to support this final rule are available on data drives in the EPA docket office.⁵ A copy of the air quality model input and/or output data can also be obtained by contacting Norm Possiel at possiel.norm@epa.gov.

2. Air Quality Modeling Platform

The EPA used version 3 of the 2016-based air quality modeling platform (i.e., 2016v3) to provide the foundational model-input data sets for 2016, 2023, and 2026. In addition to emissions data for 2016, 2023, and 2026, this platform includes meteorology, initial and boundary condition concentrations, and other inputs representative of the 2016 base year. In response to public comments on the 2016v2 base year and projected emissions inventories, the 2016v3 emissions platform includes numerous updates to both anthropogenic and biogenic emissions and the addition of NO_x emissions from lightning strikes. These updates are described in the document *Preparation of Emissions Inventories for the 2016v3 North American Emissions Modeling Platform* available in the docket for this final rule.

2.1 Air Quality Model Configuration and Model Simulations

The photochemical model simulations performed for this final rule used the Comprehensive Air Quality Model with Extensions (CAMx version 7.10, Ramboll, 2021). CAMx is a three-dimensional grid-based Eulerian air quality model designed to simulate the formation and fate of oxidant precursors, primary and secondary particulate matter concentrations, and deposition over regional and urban spatial scales (e.g., the contiguous U.S.). Consideration of the different processes (e.g., transport and deposition) that affect primary (directly emitted) and secondary (formed by atmospheric chemical processes) pollutants at the regional scale in different locations is fundamental to understanding and assessing the effects of emissions on air quality concentrations. For this final rule, as in the CSAPR Update, Revised CSAPR Update, and the proposed disapprovals, the EPA used the CAMx Ozone Source Apportionment Technology/Anthropogenic Precursor Culpability Analysis (OSAT/APCA) technique⁶ to model ozone contributions, as described below in section 4.

The geographic extent of the modeling domains that were used for air quality modeling in this analysis are shown in Figure 2-1. The large outer domain covers the 48 contiguous states along with most of Canada and all of Mexico with a horizontal resolution of 36 x 36 km (i.e., 36 km domain).

⁵ A list of available model input and output data is provided in the file “Air Quality Modeling Files_2016v3 Platform” which can be found in the docket for this final rule.

⁶ As part of this technique, ozone formed from reactions between biogenic VOC and NO_x with anthropogenic NO_x and VOC are assigned to the source of anthropogenic emissions.

The inner domain covers the 48 contiguous states along with adjacent portions of Canada and Mexico at 12 x 12 km resolution (i.e., 12 km domain).

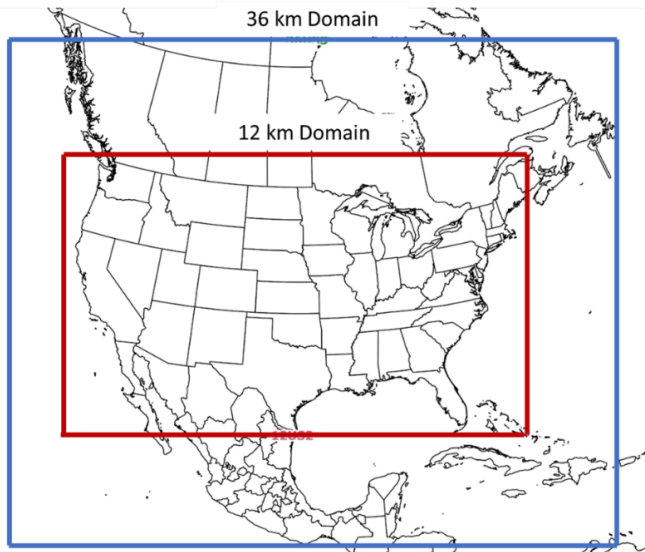


Figure 2-1. Air quality modeling domains.

CAMx requires a variety of input files that contain information pertaining to the modeling domain and simulation period. These include gridded, hourly emissions estimates and meteorological data, and initial and boundary concentrations. Separate emissions inventories were prepared for the 2016 base year and the 2023 and 2026 projection years. All other inputs (i.e., meteorological fields, initial concentrations, ozone column, photolysis rates, and boundary concentrations) were specified for the 2016 base year model application and remained unchanged for the projection-year model simulation.⁷

The 12 km CAMx model simulations performed for this final rule are listed in Table 2-1. The simulation period for each run was preceded by a 15-day ramp-up period.

Table 2-1. Model run name, case name and simulation period for each model run.⁸

<i>Analytic Year</i>	<i>Model Run</i>	<i>Case Name</i>	<i>Simulation Period</i>
2016	2016 baseline	2016gf	Annual
2023	2023 baseline	2023gf	Annual

⁷ The EPA used the CAMx7.1chemparam.CB6r5_CF2E chemical parameter file for all the CAMx model runs described in this TSD.

⁸ Because the model simulations run in Greenwich Mean Time (GMT), the actual simulation period included October 1 in order to obtain MDA8 ozone concentrations based on local time for September 30.

<i>Analytic Year</i>	<i>Model Run</i>	<i>Case Name</i>	<i>Simulation Period</i>
	2023 state total anthropogenic contributions	2023gf_ussa	May - September
2026	2026 baseline	2026gf	Annual
	2026 control case	2026gf_cntl	Annual
	2026 state total anthropogenic contributions	2026gf_ussa	May - September

2.2 Meteorological Data for 2016

This section describes the meteorological modeling that was performed to provide meteorological data for 2016 for input to air quality modeling. Note that the EPA used the same meteorological data for the 2016v3 air quality modeling as was used for the 2016v2 air quality modeling.

The 2016 meteorological data were derived from running Version 3.8 of the Weather Research Forecasting Model (WRF) (Skamarock, et al., 2008). The meteorological outputs from WRF include hourly-varying horizontal wind components (i.e., speed and direction), temperature, moisture, vertical diffusion rates, and rainfall rates for each grid cell in each vertical layer. Selected physics options used in the WRF simulations include Pleim-Xiu land surface model (Xiu and Pleim, 2001; Pleim and Xiu, 2003), Asymmetric Convective Model version 2 planetary boundary layer scheme (Pleim 2007a,b), Kain-Fritsch cumulus parameterization (Kain, 2004) utilizing the moisture-advection trigger (Ma and Tan, 2009), Morrison double moment microphysics (Morrison et al., 2005; Morrison and Gettelman, 2008), and RRTMG longwave and shortwave radiation schemes (Iacono et.al., 2008).

Both the 36 km and 12 km WRF model simulations utilize a Lambert conformal projection centered at (-97,40) with true latitudes of 33 and 45 degrees north. The 36 km domain contains 184 cells in the X direction and 160 cells in the Y direction. The 12 km domain contains 412 cells in the X direction and 372 cells in the Y direction. The atmosphere is resolved with 35 vertical layers up to 50 mb (see Table 2-2), with the thinnest layers being nearest the surface to better resolve the planetary boundary layer (PBL).

The 36 km WRF model simulation was initialized using the 0.25-degree Global Forecast System (GFS) analysis and 3-hour forecast from the 00 GMT, 06 GMT, 12 GMT, and 18 GMT simulations. The 12 km model was initialized using the 12 km North American Model (12NAM) analysis product provided by National Climatic Data Center (NCDC).⁹ The 40 km Eta Data

⁹ <https://www.ncdc.noaa.gov/data-access/model-data/model-datasets/north-american-mesoscale-forecast-system-nam>

Assimilation System (EDAS) analysis (ds609.2) from the National Center for Atmospheric Research (NCAR) was used where 12NAM data was unavailable.¹⁰ Analysis nudging for temperature, wind, and moisture was applied above the boundary layer only. The model simulations were conducted continuously. The ‘ipxwrf’ program was used to initialize deep soil moisture at the start of the run using a 10-day spin-up period (Gilliam and Pleim, 2010). Land use and land cover data were based on the USGS for the 36NOAM simulation and the 2011 National Land Cover Database (NLCD 2011) for the 12US simulation. Sea surface temperatures (SST) were ingested from the Group for High Resolution Sea Surface Temperatures (GHRSSST) (Stammer et al., 2003) 1 km resolution SST data. Additionally, lightning data assimilation was utilized to suppress (force) deep convection where lightning is absent (present) in observational data. This method is described by Heath et al. (2016) and was employed to help improve precipitation estimates generated by the model.

Table 2-2. Vertical layers and their approximate height above ground level.

WRF Layer	Height (m)	Pressure (mb)	Sigma
35	17,556	5000	0.000
34	14,780	9750	0.050
33	12,822	14500	0.100
32	11,282	19250	0.150
31	10,002	24000	0.200
30	8,901	28750	0.250
29	7,932	33500	0.300
28	7,064	38250	0.350
27	6,275	43000	0.400
26	5,553	47750	0.450
25	4,885	52500	0.500
24	4,264	57250	0.550
23	3,683	62000	0.600
22	3,136	66750	0.650
21	2,619	71500	0.700
20	2,226	75300	0.740
19	1,941	78150	0.770
18	1,665	81000	0.800
17	1,485	82900	0.820
16	1,308	84800	0.840
15	1,134	86700	0.860
14	964	88600	0.880
13	797	90500	0.900
12	714	91450	0.910
11	632	92400	0.920
10	551	93350	0.930
9	470	94300	0.940
8	390	95250	0.950

¹⁰ <https://www.ready.noaa.gov/edas40.php>.

WRF Layer	Height (m)	Pressure (mb)	Sigma
7	311	96200	0.960
6	232	97150	0.970
5	154	98100	0.980
4	115	98575	0.985
3	77	99050	0.990
2	38	99525	0.995
1	19	99763	0.9975
Surface	0	100000	1.000

Details of the annual 2016 meteorological model simulation and evaluation are provided in a separate technical support document, which can be found in the docket for this final rule.¹¹

The meteorological data generated by the WRF simulations were processed using wrfcamx v4.7 (Ramboll 2021) meteorological data processing program to create 35-layer gridded model-ready meteorological inputs to CAMx. In running wrfcamx, vertical eddy diffusivities (Kv) were calculated using the Yonsei University (YSU) (Hong and Dudhia, 2006) mixing scheme. We used a minimum Kv of 0.1 m²/sec except for urban grid cells where the minimum Kv was reset to 1.0 m²/sec within the lowest 200 m of the surface in order to enhance mixing associated with the nighttime “urban heat island” effect. In addition, we invoked the subgrid convection and subgrid stratoform cloud options in our wrfcamx run for 2016.

2.3 Initial and Boundary Concentrations

The lateral boundary and initial species concentrations for the 36 km simulations were derived from outputs of a three-dimensional global atmospheric chemistry model, GEOS-Chem global model (I. Bey, et al., 2001) which was run for 2016. The GEOS-Chem predictions were used to provide one-way dynamic boundary concentrations at one-hour intervals and an initial concentration field for the 36 km CAMx simulations for 2016, 2023 and 2026. In the 2016v2 modeling for the proposed rule, the EPA used the hemispheric version of the Community Multi-scale Air Quality Model (H-CMAQ).¹² The basis for selecting GEOS-Chem for the 2016v3 modeling is discussed in Appendix A.

Air quality modeling for the 36 km domain was used to provide initial and boundary conditions for the nested 12 km domain model simulations. Both the 36 km and 12 km modeling domains have 35 vertical layers with a top at about 17,550 meters, or 50 millibars (mb). The model

¹¹ Meteorological Modeling for 2016.docx.

¹² More information about the H-CMAQ model and other applications using this tool is available at: <https://www.epa.gov/cmaq/hemispheric-scale-applications>. Note that the EPA used the same initial and boundary conditions for the 2016v2 air quality modeling as was used for the 2016v1 air quality modeling.

simulations produce hourly air quality concentrations for each grid cell across each modeling domain. Modeling for the 36 km domain was performed for 2016 and 2023. Outputs from the 2016 36 km simulation were used to provide initial and boundary conditions for the 2016 12 km model simulation. Outputs from the 2023 36 km simulation were used to provide initial and boundary conditions for the 2023 and 2026 12 km simulations.

2.5 Air Quality Model Evaluation

An operational model performance evaluation for ozone was conducted to examine the ability of the 2016v3 CAMx modeling system to simulate 2016 measured MDA8 ozone concentrations. This evaluation focused on graphical analyses and statistical metrics of model predictions versus observations. Details on the evaluation methodology, the calculation of performance statistics, and results are provided in Appendix B. Overall, the ozone model performance statistics for the CAMx 2016v3 simulation are within the ranges found in other recent peer-reviewed applications (e.g., Simon et al, 2012 and Emory et al, 2017). As described in Appendix B, model performance for the 2016v3 platform is notably improved compared to model performance for the 2016v2 platform. The model performance results demonstrate the scientific credibility of our 2016v3 modeling platform. These results provide confidence in the ability of the modeling platform to provide a reasonable projection of expected future year ozone concentrations and contributions. Model performance statistics for individual monitoring sites for the period May through September are provided in a spreadsheet file in the docket for this final rule.¹³

3. Identification of Future Nonattainment and Maintenance Receptors in 2023

3.1 Definition of Nonattainment and Maintenance Receptors

The ozone predictions from the 2016 base year and future case CAMx model simulations were used to calculate average and maximum ozone design values for the 2023 and 2026 analytic years using the approach described in this section. Following the approach used for the proposed rule, we evaluated projected average and maximum design values in conjunction with the most recent measured ozone design values (i.e., 2021)¹⁴ to identify nonattainment or maintenance sites in each of the three future years. Those monitoring sites with future year average design values that

¹³ CAMx 2016v3 MDA8 O3 Model Performance Stats by Site.

¹⁴ The 2021 design values are the most current official design values available for use in this final rule. The 2021 ozone design values, by monitoring site, can be found in the following file in the docket: Final GNP O3 DVs_Contributions.

exceed the NAAQS (i.e., average design values of 71 ppb or greater)¹⁵ and that are currently measuring nonattainment are considered to be nonattainment receptors. Similarly, monitoring sites with a projected maximum design value that exceeds the NAAQS are projected to be maintenance receptors. Maintenance-only receptors include those monitoring sites where the projected average design value is below the NAAQS, but the maximum design value is above the NAAQS, and monitoring sites with projected average design values that exceed the NAAQS, but for which current design values based on measured data do not exceed the NAAQS.¹⁶ In addition, as described in the preamble for this final rule, the EPA received comments stating that our methodology to identify receptors in 2023 appears overly optimistic in light of current measured data. These commenters suggest that the EPA give greater weight to current measured data as part of the method for identifying projected receptors. In response to these comments the EPA has developed an additional maintenance-only receptor category, which includes what we refer to as “violating monitor” receptors. Specifically, the EPA has identified “violating monitor” receptors as those monitoring sites with measured 2021 and preliminary 2022 design values *and* 4th high maximum daily MDA8 ozone concentrations in both 2021 and 2022 (preliminary data) that exceed the NAAQS, although model-projected design values for 2023 are below the NAAQS.¹⁷

The procedures for calculating projected average and maximum design values are described below. The monitoring sites that are projected to be nonattainment and/or maintenance-only receptors for the ozone NAAQS in 2023 and 2026 are used for assessing the contribution of emissions in upwind states to downwind nonattainment and maintenance of the 2015 ozone NAAQS as part of this final rule.

3.2 Approach for Projecting Ozone Design Values

The ozone predictions from the 2016, 2023, and 2026 model simulations were used to project ambient (i.e., measured) ozone design values (DVs) to 2023 and 2026 based on an approach that

¹⁵ In determining compliance with the NAAQS, ozone design values are truncated to integer values. For example, a design value of 70.9 parts per billion (ppb) is truncated to 70 ppb which is attainment. In this manner, design values at or above 71.0 ppb are considered to be violations of the NAAQS.

¹⁶ The EPA’s modeling guidance notes that projecting the highest (i.e., maximum) design value from the base period provides an approach for evaluating attainment in periods with meteorological conditions especially conducive to high ozone concentrations.

¹⁷ 2021 4th high MDA8 ozone concentrations and preliminary 2022 design values and 4th high MDA8 ozone concentrations for violating monitor receptors are provided in Table 3-3. Daily MDA8 ozone concentrations which can be used to identify the 4th values in 2021 and the preliminary 4th high values in 2022 for other monitoring sites can be in the file Final GNP O3 DVs_Contributions.xls in the docket for this rule.

follows from the EPA’s guidance for attainment demonstration modeling (US EPA, 2018),¹⁸ as summarized here. The modeling guidance recommends using 5-year weighted average ambient design values centered on the base modeling year as the starting point for projecting average design values to the future. Because 2016 is the base emissions year, we used the average ambient 8-hour ozone design values for the period 2014 through 2018 (i.e., the average of design values for 2014-2016, 2015-2017 and 2016-2018) to calculate the 5-year weighted average design values (i.e., 2016-centered design values). The 5-year weighted average ambient design value at each site was projected to 2023 and 2026 using the Software for Model Attainment Test Software – Community Edition (SMAT-CE)¹⁹. This program calculates the 5-year weighted average design value based on observed data and projects future year values using the relative response predicted by the model. Equation (3-1) describes the recommended model attainment test in its simplest form, as applied for monitoring site *i*:

$$(DVF)_i = (RRF)_i * (DVB)_i \quad \text{Equation 3-1}$$

DVF_i is the estimated design value for the future year at monitoring site *i*; RRF_i is the relative response factor for monitoring site *i*; and DVB_i is the base period design value monitored at site *i*. The relative response factor for each monitoring site (RRF_i) is the fractional change in MDA8 ozone between the base and future year. The RRF is based on the average ozone on model-predicted “high” ozone days in grid cells in the vicinity of the monitoring site. The modeling guidance recommends calculating RRFs based on the highest 10 modeled ozone days in the base year simulation at each monitoring site. Specifically, the RRF for an individual monitoring site is the ratio of the average MDA8 ozone concentration in the future year to the average MDA8 concentration in the 2016 base year. The average values are calculated using MDA8 model predictions in the future year and in 2016 for the 10 highest days in the 2016 base year modeling. For cases in which the base year model simulation does not have 10 days with ozone values ≥ 60 ppb at a site, we use all days with ozone

¹⁸ The EPA’s ozone attainment demonstration modeling guidance is referred to as “the modeling guidance” in the remainder of this document.

¹⁹ Software download information and documentation are available at <https://www.epa.gov/scram/photochemical-modeling-tools>

≥ 60 ppb, as long as there were at least 5 days that meet this criterion. At monitor locations with less than 5 days with modeled 2016 base year ozone ≥ 60 ppb, no RRF or DVF is calculated for the site and the monitor in question was not included in this analysis.

The modeling guidance recommends calculating the RRF using the base year and future year model predictions from the cells immediately surrounding the monitoring site along with the grid cell in which the monitor is located. In this approach the RRF is based on a 3 x 3 array of 12 km grid cells centered on the location of the grid cell containing the monitor.

As in the proposal, the EPA also projects design values based on a modified version of the “3 x 3” approach for those monitoring sites located in coastal areas. In this alternative approach, the EPA eliminated from the RRF calculations the modeling data in those grid cells that are dominated by water (i.e., more than 50 percent of the area in the grid cell is water) and that do not contain a monitoring site (i.e., if a grid cell is more than 50 percent water but contains an air quality monitor, the data from that cell would remain in the calculation). The choice of more than 50 percent of the grid cell area as water as the criteria for identifying overwater grid cells is based on the treatment of land use in the Weather Research and Forecasting model (WRF).²⁰ Specifically, in the WRF meteorological model those grid cells that are greater than 50 percent overwater are treated as being 100 percent overwater. In such cases the meteorological conditions in the entire grid cell reflect the vertical mixing and winds over water, even if part of the grid cell also happens to be over land with land-based emissions, as can often be the case for coastal areas. Overlaying land-based emissions with overwater meteorology may be representative of conditions at coastal monitors during times of on-shore flow associated with synoptic conditions and/or sea-breeze or lake-breeze wind flows. But there may be other times, particularly with off-shore wind flow when vertical mixing of land-based emissions may be too limited due to the presence of overwater meteorology. Thus, for this modeling projected average and maximum design values were calculated for individual monitoring sites based on both the “3 x 3” approach as well as the alternative approach that eliminates overwater cells in the RRF calculation for near-coastal areas (i.e., “no water” approach).

For both the “3 x 3” approach and the “no water” approach, the grid cell with the highest base year MDA8 ozone concentration on each day in the applicable array of grid cells surrounding the

²⁰ <https://www.mmm.ucar.edu/weather-research-and-forecasting-model>.

location of the monitoring site²¹ is used for both the base and future components of the RRF calculation. That is, the base and future year data are paired in space for the grid cell that has the highest MDA8 concentration on the given day.

The approach for calculating projected maximum design values is similar to the approach for calculating the projected average design values. To calculate projected maximum design values we start with the highest (i.e., maximum) ambient design value from the 2016-centered 5-year period (i.e., the maximum of design values from 2014-2016, 2014-2017, and 2016-2018). The base period maximum design value at each site is projected to 2023 and 2026 using the site-specific RRFs, as determined using the procedures for calculating RRFs described above.

For this final rule, the EPA is relying upon design values based on the “no water” approach for identifying nonattainment and maintenance receptors and for calculating contributions, as described in section 4, below.

Consistent with the truncation and rounding procedures for the 8-hour ozone NAAQS, the projected design values are truncated to integers in units of ppb.²² Therefore, projected design values that are greater than or equal to 71 ppb are considered to be violating the 2015 ozone NAAQS. For those sites that are projected to be violating the NAAQS based on the projected average design values, we examined the design values for 2021, which are the most recent concurred measured design values at the time of this final action.²³ As noted above, we identify nonattainment receptors as those sites that are violating the NAAQS based on current measured air quality and also have projected average design values of 71 ppb or greater. Maintenance-only receptors identified based on monitoring plus modeling include both (1) those sites with projected average design values above the NAAQS that are currently measuring clean data and (2) those sites with projected average design values below the level of the NAAQS, but with projected maximum design values of 71 ppb or greater.²⁴ As noted above, the EPA also identified as maintenance-only receptors those monitoring sites with measured 2021 and preliminary 2022 design values *and* 4th high maximum daily MDA8

²¹ For the “3 x 3” approach the applicable array contains the 9 grid cells that surround and include the grid cell containing the monitoring site. The applicable array for the “no water” approach includes the grid cell containing the monitoring site along with the subset of the “3 x 3” grid cells that are not classified as “water” grid cells using the criteria described in this TSD.

²² 40 CFR Part 50, Appendix U to Part 50 – Interpretation of the Primary and Secondary National Ambient Air Quality Standards for Ozone.

²³ Official, concurred ozone design values for 2021 are provided in the file Final GNP O3 DVs_Contributions which can be found in the docket for this final rule.

²⁴ In addition to the maintenance-only receptors, the projected nonattainment receptors are also maintenance receptors because the maximum design values for each of these sites is always greater than or equal to the average design value.

ozone concentrations in both 2021 and 2022 (preliminary data) that exceed the NAAQS, although model-projected design values for 2023 are below the NAAQS.

The 2016-centered base period average and maximum design values, the projected average and maximum design values for 2023 and the 2021 design values for monitoring sites that are projected to be nonattainment or maintenance-only receptors in 2023 based on monitoring and modeling using the “no water” approach are provided in Tables 3-1 and 3-2, respectively.²⁵ In total, in the 2023 base case there are a total of 33 projected modeling-based receptors nationwide including 14 nonattainment receptors in 9 different counties and 19 maintenance-only receptors in 13 additional counties (Harris County, TX has both nonattainment and maintenance-only receptors).²⁶

The projected average and maximum design values for 2023 and the 2021 and preliminary 2022 design values and the 2021 and preliminary 2022 4th high values for monitoring sites that are identified as “violating monitor” maintenance-only receptors in 2023 are provided in Tables 3-3. There are 49 monitoring sites that are identified as “violating-monitor” maintenance-only receptors in 2023.²⁷ As noted earlier in this section, the EPA uses the approach of considering “violating-monitor” maintenance-only receptors as confirmatory of the proposal’s identification of receptors and does not implicate additional linked states in this final rule. Rather, using this approach serves to strengthen the analytical basis for our Step 2 findings by establishing that many upwind states covered in this rule are also projected to contribute above 1 percent of the NAAQS to these additional “violating monitor” maintenance-only receptors.

²⁵ The “3 x 3” approach and the “no water” approach result in the same set of receptors. That is, the receptors identified based on the “3 x 3” approach are also the receptors identified based on the “no water” approach. However, using design values from the “3 x 3” approach, the maintenance-only receptor at site 550590019 in Kenosha County, WI would become a nonattainment receptor because the average design value with the “3 x 3” approach is 72.0 ppb versus 70.8 ppb with the “no water” approach. In addition, the maintenance-only receptor at site 090099002 in New Haven County, CT would become a nonattainment receptor using the “no water” approach because the average design value with the “3 x 3” approach is 71.2 ppb versus 70.5 ppb with the “no water” approach.

Projected design values for 2023 based on both the “3 x 3” and “no water” approaches for individual monitoring sites nationwide are provided in the file “2016v3_Final FIP_DVs_state_contributions” which can be found in the docket for this final rule.

²⁶ The EPA’s modeling also projects that three monitoring sites in the Uinta Basin (i.e., monitor 490472003 in Uintah County, Utah and monitors 490130002 and 490137011 in Duchesne County, Utah) will have average design values above the NAAQS in 2023. However, as noted in the proposed rule, the Uinta Basin nonattainment area was designated as nonattainment for the 2015 ozone NAAQS not because of an ongoing problem with summertime ozone (as is usually the case in other parts of the country), but instead because it violates the ozone NAAQS in winter. The main causes of the Uinta Basin’s wintertime ozone are sources located at low elevations within the Basin, the Basin’s unique topography, and the influence of the wintertime meteorologic inversions that keep ozone and ozone precursors near the Basin floor and restrict air flow in the Basin. Because of the localized nature of the ozone problem at these sites the EPA has not identified these three monitors as receptors in Step 1 of this proposed rule.

²⁷ The list of violating monitors in Table 3-3 does not include two such monitors in California (i.e., monitor site 060430006 in Mariposa County and monitoring site 061112002 in Ventura County).

The average and maximum design values for nonattainment and maintenance receptors in 2026 are provided in Tables 3-5 and 3-6, respectively. There are 7 nonattainment receptors and 12 monitored plus modeled maintenance-only receptors in 2026.

Table 3-1. Average and maximum 2016-centered and 2023 base case 8-hour ozone design values and 2021 design values (ppb) at projected nonattainment receptors in 2023.

<i>Monitor ID</i>	<i>State</i>	<i>County</i>	<i>2016 Centered Average</i>	<i>2016 Centered Maximum</i>	<i>2023 Average</i>	<i>2023 Maximum</i>	<i>2021</i>
060650016	CA	Riverside	79.0	80	72.2	73.1	78
060651016	CA	Riverside	99.7	101	91.0	92.2	95
080350004	CO	Douglas	77.3	78	71.3	71.9	83
080590006	CO	Jefferson	77.3	78	72.8	73.5	81
080590011	CO	Jefferson	79.3	80	73.5	74.1	83
090010017	CT	Fairfield	79.3	80	71.6	72.2	79
090013007	CT	Fairfield	82.0	83	72.9	73.8	81
090019003	CT	Fairfield	82.7	83	73.3	73.6	80
481671034	TX	Galveston	75.7	77	71.5	72.8	72
482010024	TX	Harris	79.3	81	75.1	76.7	74
490110004	UT	Davis	75.7	78	72.0	74.2	78
490353006	UT	Salt Lake	76.3	78	72.6	74.2	76
490353013	UT	Salt Lake	76.5	77	73.3	73.8	76
551170006	WI	Sheboygan	80.0	81	72.7	73.6	72

Table 3-2. Average and maximum 2016-centered and 2023 base case 8-hour ozone design values and 2021 design values (ppb) at projected maintenance-only receptors.

<i>Monitor ID</i>	<i>State</i>	<i>County</i>	<i>2016 Centered Average</i>	<i>2016 Centered Maximum</i>	<i>2023 Average</i>	<i>2023 Maximum</i>	<i>2021</i>
40278011	AZ	Yuma	72.3	74	70.4	72.1	67
80690011	CO	Larimer	75.7	77	70.9	72.1	77
90099002	CT	New Haven	79.7	82	70.5	72.6	82
170310001	IL	Cook	73.0	77	68.2	71.9	71
170314201	IL	Cook	73.3	77	68.0	71.5	74
170317002	IL	Cook	74.0	77	68.5	71.3	73
350130021	NM	Dona Ana	72.7	74	70.8	72.1	80
350130022	NM	Dona Ana	71.3	74	69.7	72.4	75
350151005	NM	Eddy	69.7	74	69.7	74.1	77
350250008	NM	Lea	67.7	70	69.8	72.2	66
480391004	TX	Brazoria	74.7	77	70.4	72.5	75

<i>Monitor ID</i>	<i>State</i>	<i>County</i>	<i>2016 Centered Average</i>	<i>2016 Centered Maximum</i>	<i>2023 Average</i>	<i>2023 Maximum</i>	<i>2021</i>
481210034	TX	Denton	78.0	80	69.8	71.6	74
481410037	TX	El Paso	71.3	73	69.8	71.4	75
482010055	TX	Harris	76.0	77	70.9	71.9	77
482011034	TX	Harris	73.7	75	70.1	71.3	71
482011035	TX	Harris	71.3	75	67.8	71.3	71
530330023	WA	King	73.3	77	67.6	71.0	64
550590019	WI	Kenosha	78.0	79	70.8	71.7	74
551010020	WI	Racine	76.0	78	69.7	71.5	73

Table 3-3. Average and maximum 2023 design values, and 2021 and preliminary 2022 design values and 4th high values at violating monitors (ppb).*

<i>Monitor ID</i>	<i>State</i>	<i>County</i>	<i>2023 Average</i>	<i>2023 Maximum</i>	<i>2021</i>	<i>2022 P*</i>	<i>2021 4th High</i>	<i>2022 P* 4th High</i>
040070010	AZ	Gila	67.9	69.5	77	76	75	74
040130019	AZ	Maricopa	69.8	70.0	75	77	78	76
040131003	AZ	Maricopa	70.1	70.7	80	80	83	78
040131004	AZ	Maricopa	70.2	70.8	80	81	81	77
040131010	AZ	Maricopa	68.3	69.2	79	80	80	78
040132001	AZ	Maricopa	63.8	64.1	74	78	79	81
040132005	AZ	Maricopa	69.6	70.5	78	79	79	77
040133002	AZ	Maricopa	65.8	65.8	75	75	81	72
040134004	AZ	Maricopa	65.7	66.6	73	73	73	71
040134005	AZ	Maricopa	62.3	62.3	73	75	79	73
040134008	AZ	Maricopa	65.6	66.5	74	74	74	71
040134010	AZ	Maricopa	63.8	66.9	74	76	77	75
040137020	AZ	Maricopa	67.0	67.0	76	77	77	75
040137021	AZ	Maricopa	69.8	70.1	77	77	78	75
040137022	AZ	Maricopa	68.2	69.1	76	78	76	79
040137024	AZ	Maricopa	67.0	67.9	74	76	74	77
040139702	AZ	Maricopa	66.9	68.1	75	77	72	77
040139704	AZ	Maricopa	65.3	66.2	74	77	76	76
040139997	AZ	Maricopa	70.5	70.5	76	79	82	76
040218001	AZ	Pinal	67.8	69.0	75	76	73	77
080013001	CO	Adams	63.0	63.0	72	77	79	75
080050002	CO	Arapahoe	68.0	68.0	80	80	84	73
080310002	CO	Denver	63.6	64.8	72	74	77	71
080310026	CO	Denver	64.5	64.8	75	77	83	72

<i>Monitor ID</i>	<i>State</i>	<i>County</i>	<i>2023 Average</i>	<i>2023 Maximum</i>	<i>2021</i>	<i>2022 P*</i>	<i>2021 4th High</i>	<i>2022 P* 4th High</i>
090079007	CT	Middlesex	68.7	69.0	74	73	78	73
090110124	CT	New London	65.5	67.0	73	72	75	71
170310032	IL	Cook	67.3	69.8	75	75	77	72
170311601	IL	Cook	63.8	64.5	72	73	72	71
181270024	IN	Porter	63.4	64.6	72	73	72	73
260050003	MI	Allegan	66.2	67.4	75	75	78	73
261210039	MI	Muskegon	67.5	68.4	74	79	75	82
320030043	NV	Clark	68.4	69.4	73	75	74	74
350011012	NM	Bernalillo	63.8	66.0	72	73	76	74
350130008	NM	Dona Ana	65.6	66.3	72	76	79	78
361030002	NY	Suffolk	66.2	68.0	73	74	79	74
390850003	OH	Lake	64.3	64.6	72	74	72	76
480290052	TX	Bexar	67.1	67.8	73	74	78	72
480850005	TX	Collin	65.4	66.0	75	74	81	73
481130075	TX	Dallas	65.3	66.5	71	71	73	72
481211032	TX	Denton	65.9	67.7	76	77	85	77
482010051	TX	Harris	65.3	66.3	74	73	83	72
482010416	TX	Harris	68.8	70.4	73	73	78	71
484390075	TX	Tarrant	63.8	64.7	75	76	76	77
484391002	TX	Tarrant	64.1	65.7	72	77	76	80
484392003	TX	Tarrant	65.2	65.9	72	72	74	72
484393009	TX	Tarrant	67.5	68.1	74	75	75	75
490571003	UT	Weber	69.3	70.3	71	74	77	71
550590025	WI	Kenosha	67.6	70.7	72	73	72	71
550890008	WI	Ozaukee	65.2	65.8	71	72	72	72

* 2022 preliminary design values are based on 2022 measured MDA8 concentrations provided by state air agencies to the EPA's Air Quality System (AQS), as of January 3, 2023.

Table 3-4. Average and maximum 2016-centered and 2026 base case 8-hour ozone design values and 2021 design values (ppb) at projected nonattainment receptors in 2026.

<i>Monitor ID</i>	<i>State</i>	<i>County</i>	<i>2016 Centered Average</i>	<i>2016 Centered Maximum</i>	<i>2026 Average</i>	<i>2026 Maximum</i>
060650016	CA	Riverside	79.0	80	71.4	72.4
060651016	CA	Riverside	99.7	101	90.0	91.2
080590006	CO	Jefferson	77.3	78	72.0	72.6
080590011	CO	Jefferson	79.3	80	72.4	73.0
090019003	CT	Fairfield	82.7	83	71.3	71.5
482010024	TX	Harris	79.3	81	73.9	75.5
490353013	UT	Salt Lake	76.5	77	71.9	72.3

Table 3-5. Average and maximum 2016-centered and 2026 base case 8-hour ozone design values and 2021 design values (ppb) at projected maintenance-only receptors in 2026.

<i>Monitor ID</i>	<i>State</i>	<i>County</i>	<i>2016 Centered Average</i>	<i>2016 Centered Maximum</i>	<i>2026 Average</i>	<i>2026 Maximum</i>
040278011	AZ	Yuma	72.3	74	69.9	71.5
080690011	CO	Larimer	75.7	77	70.0	71.2
090013007	CT	Fairfield	82.0	83	70.9	71.7
350130021	NM	Dona Ana	72.7	74	69.9	71.2
350130022	NM	Dona Ana	71.3	74	69.0	71.6
350151005	NM	Eddy	69.7	74	69.1	73.4
350250008	NM	Lea	67.7	70	69.2	71.6
480391004	TX	Brazoria	74.7	77	69.1	71.2
481671034	TX	Galveston	75.7	77	70.2	71.4
490110004	UT	Davis	75.7	78	69.9	72.1
490353006	UT	Salt Lake	76.3	78	70.5	72.1
551170006	WI	Sheboygan	80.0	81	70.8	71.7

4. Ozone Contribution Modeling

As noted above, the EPA performed nationwide, state-level ozone source apportionment modeling using the CAMx OSAT/APCA technique to provide data on the contribution of projected 2023 NO_x and VOC emissions from anthropogenic source sectors in each state. The state-by-state anthropogenic source apportionment modeling is described in section 4.1. In section 4.2 we describe the method for calculating the average contribution metric for each source apportionment model run and in section 4.3 we present the results of the state-by-state all anthropogenic modeling.

4.1 State-by-State All Anthropogenic Modeling

In the state-by-state source apportionment model run, we tracked the ozone formed from each of the following contribution categories (i.e., “tags”):

- States – anthropogenic NO_x and VOC emissions from each of the contiguous 48 states and the District of Columbia tracked individually (emissions from all anthropogenic sectors in a given state were combined);
- Biogenics – biogenic NO_x and VOC emissions domain-wide;
- Initial and Boundary Concentrations – air quality concentrations used to initialize the 12 km

model simulation and air quality concentrations transported into the 12 km modeling domain from the lateral boundaries;

- Tribes – the collective emissions from those tribal lands for which we have point source inventory data in the 2016v3 emissions platform (we did not model the contributions from individual tribes);
- Canada and Mexico – collective anthropogenic emissions from sources in the portions of Canada and Mexico that are within the 12 km modeling domain (contributions from Canada and Mexico were not modeled separately);
- Fires – combined emissions from wild and prescribed fires domain-wide within the 12 km modeling domain;
- Offshore – total emissions from offshore marine vessels and offshore drilling platforms; and
- NO_x emissions from lightning strikes.

The above-listed tagged sources account for all ozone sources simulated by the model such that the sum of tagged ozone contributions adds to the total modeled ozone at each hour and grid cell. The source apportionment modeling provides hourly contributions to ozone from anthropogenic NO_x and VOC emissions in each state, individually, to ozone concentrations in each model grid cell. The contributions to ozone from chemical reactions between biogenic NO_x and biogenic VOC emissions were modeled and assigned to the “biogenic” category. The contributions from wildfire and prescribed fire NO_x and VOC emissions were modeled and assigned to the “fires” category. The contributions from the “biogenic”, “offshore”, and “fires” categories are not assigned to individual states nor are they included in the state contributions.

4.2 Method for Calculating the Contribution Metric

As noted above, CAMx state-by-state source apportionment model runs for 2023 and 2026 were performed to obtain contributions for the period May through September using the projected 2023 and 2026 emissions and 2016 meteorology. The resulting hourly contributions²⁸ from each tag were processed to calculate an 8-hour average contribution metric value for each tag at each monitoring site. The contribution metric values at each individual monitoring site are calculated using model predictions for the grid cell containing the monitoring site. The process for calculating the average contribution metric uses the source apportionment outputs in a “relative sense” to apportion

²⁸ Contributions from anthropogenic emissions under “NO_x-limited” and “VOC-limited” chemical regimes were combined to obtain the net contribution from NO_x and VOC anthropogenic emissions in each state.

the projected average design value at each monitoring location into contributions from each individual tag. This process is similar in concept to the approach described above for using model predictions to calculate future year ozone design values.

The basic approach used to calculate the average contribution metric values for 2023 is described by the following steps:

- (1) For the model grid cells containing an ozone monitoring site, calculate the 8-hour average contribution from each source tag to each monitoring site for the time period of the 2023 modeled MDA8 ozone concentration on each day:
- (2) Average the MDA8 concentrations for the top 10 modeled ozone concentration days in 2023 and average the 8-hour contributions for each of these same days for each tag;
- (3) Divide the 10-day average contribution for each tag by the corresponding 10-day average concentration to obtain a Relative Contribution Factor (RCF) for each tag at each monitor; and
- (4) Multiply the 2023 average design values by the corresponding RCF to produce the average contribution metric value for each tag at each monitoring site in 2023.

These steps are written out mathematically in Equation 4-1 where $C_{t,i}$ represents the contribution metric value from tag, t , to monitor, i , $DVF_{2023,i}$ represents the projected 2023 future year average DV at monitor, i , $O3C_{t,top10,i}$ is the average ozone *contribution* to MDA8 ozone from tag, t , across the top-10 future year MDA8 modeled days at monitor, i , and, $O3_{top10,i}$ is the average ozone *concentration* across the top-10 future year MDA8 modeled days at monitor, i .

$$C_{t,i} = DVF_{2023,i} \times \frac{O3C_{t,top10,i}}{O3_{top10,i}} \quad \text{Equation 4-1}$$

The contribution metric values calculated from step 4 are truncated to two digits to the right of the decimal (e.g., a calculated contribution of 0.78963... is truncated to 0.78 ppb). As a result of truncation, the tabulated contributions may not always sum to the future year average design value at individual monitoring sites. In addition, when calculating the contribution metric values we applied a criteria that 5 or more of the top 10 model-predicted concentration days must have MDA8 concentrations ≥ 60 ppb in the future year in order to calculate a valid contribution metric. The criterion of having at least 5 days with MDA8 ozone concentrations ≥ 60 ppb was chosen to avoid including contributions on days that are well below the NAAQS in the calculation of the contribution metric. Using a minimum of 5 days up to a maximum of 10 days with MDA8 ozone ≥ 60 ppb aligns with recommendations in the EPA’s air quality modeling guidance for projecting future year design values, as described above.

To calculate contribution metric values from the 2026 source apportionment model runs, we followed the same approach as described above for 2023, except that we calculated the average contribution metric values for 2026 using the 2026 MDA8 concentrations and 2026 8-hour average contributions for the same dates that were used to calculate the contribution metric values in 2023. Even though 2026 is only 3 years beyond 2023, it is possible that changes in projected emissions between 2023 and 2026 could potentially result in a change in the ranking of days based on model predicted MDA8 ozone concentrations in 2026 compared to 2023 at some monitoring sites. Using modeled contribution data from the same set of dates when calculating contribution metric values for 2023 and 2026 provides consistency in terms of the meteorology associated with the contributions that are used to calculate contribution metric values in both years at individual monitoring sites. The contribution metric values for monitoring sites nationwide for the 2023 and 2026 state-by-state source apportionment model runs are provided in the file “Final GNP O3 DVs_Contributions” which can be found in the docket of this final rule. Note that this file contains data for monitoring sites that meet the criteria for calculating valid contribution metric values, as described above.²⁹

4.3 Results of State-by-State All Anthropogenic Modeling

The largest contribution from each state to monitoring plus modeled downwind receptors in 2023 is provided in Table 4-1.³⁰ The largest contribution from each state to “violating monitor” receptors in 2023 is provided in Table 4-2. The largest contribution from each state to receptors in 2026 is provided in Table 4-3.

The contribution metric values from each state and the other source tags at individual nonattainment and maintenance-only sites in the 2023 and 2026 are provided in Appendix C. A table with the total upwind state collective contribution expressed as the percent of the 2023 ozone design value and as a percent of total U.S. anthropogenic ozone is provided in Appendix D. The upwind states linked to each downwind receptor in 2023 and in 2026 are identified in Appendix E. The spatial fields of top 10-day average contributions from individual states covered by this final rule are provided in Appendix F.

²⁹ Contribution metric values were not calculated for the receptor in King County, Washington because there were fewer than 5 days with future year MDA8 ozone concentrations ≥ 60 ppb at this receptor.

³⁰ For California the largest contribution to a downwind receptor in 2023 is the contribution to monitoring site 060651016, which is a nonattainment receptor located on the Morongo Band of Mission Indians reservation in Riverside County, California. See the preamble for information on how the EPA considers transport to receptors on tribal lands in this final rule.

Table 4-1. Largest contribution from each state to downwind nonattainment and maintenance-only receptors in 2023 (ppb).

<i>Upwind State</i>	<i>Largest Contribution to Downwind Nonattainment Receptors</i>	<i>Largest Contribution to Downwind Maintenance-Only Receptors</i>
Alabama	0.75	0.65
Arizona	0.54	1.69
Arkansas	0.94	1.21
California	35.27	6.31
Colorado	0.14	0.18
Connecticut	0.01	0.01
Delaware	0.44	0.56
District of Columbia	0.03	0.04
Florida	0.50	0.54
Georgia	0.18	0.17
Idaho	0.42	0.41
Illinois	13.89	19.09
Indiana	8.90	10.03
Iowa	0.67	0.90
Kansas	0.46	0.52
Kentucky	0.84	0.79
Louisiana	9.51	5.62
Maine	0.02	0.01
Maryland	1.13	1.28
Massachusetts	0.33	0.15
Michigan	1.59	1.56
Minnesota	0.36	0.85
Mississippi	1.32	0.91
Missouri	1.87	1.39
Montana	0.08	0.10
Nebraska	0.20	0.36
Nevada	1.11	1.13
New Hampshire	0.10	0.02
New Jersey	8.38	5.79
New Mexico	0.36	1.59
New York	16.10	11.29
North Carolina	0.45	0.66
North Dakota	0.18	0.45

<i>Upwind State</i>	<i>Largest Contribution to Downwind Nonattainment Receptors</i>	<i>Largest Contribution to Downwind Maintenance-Only Receptors</i>
Ohio	2.05	1.98
Oklahoma	0.79	1.01
Oregon	0.46	0.31
Pennsylvania	6.00	4.36
Rhode Island	0.04	0.01
South Carolina	0.16	0.18
South Dakota	0.05	0.08
Tennessee	0.60	0.68
Texas	1.03	4.74
Utah	1.29	0.98
Vermont	0.02	0.01
Virginia	1.16	1.76
Washington	0.16	0.09
West Virginia	1.37	1.49
Wisconsin	0.21	2.86
Wyoming	0.68	0.67

Table 4-2. Largest contribution to downwind 8-hour ozone “violating monitor” maintenance-only receptors in 2023 (ppb).

<i>Upwind State</i>	<i>Largest Contribution to Downwind Violating Monitor Maintenance-Only Receptors</i>
Alabama	0.79
Arizona	1.62
Arkansas	1.16
California	6.97
Colorado	0.39
Connecticut	0.17
Delaware	0.42
District of Columbia	0.03
Florida	0.50
Georgia	0.31
Idaho	0.46
Illinois	16.53
Indiana	9.39

<i>Upwind State</i>	<i>Largest Contribution to Downwind Violating Monitor Maintenance-Only Receptors</i>
Iowa	1.13
Kansas	0.82
Kentucky	1.57
Louisiana	5.06
Maine	0.02
Maryland	1.14
Massachusetts	0.39
Michigan	3.47
Minnesota	0.64
Mississippi	1.02
Missouri	2.95
Montana	0.12
Nebraska	0.43
Nevada	1.11
New Hampshire	0.10
New Jersey	8.00
New Mexico	0.34
New York	12.08
North Carolina	0.65
North Dakota	0.35
Ohio	2.25
Oklahoma	1.57
Oregon	0.36
Pennsylvania	5.20
Rhode Island	0.08
South Carolina	0.23
South Dakota	0.12
Tennessee	0.86
Texas	3.83
Utah	1.46
Vermont	0.03
Virginia	1.39
Washington	0.11
West Virginia	1.79
Wisconsin	5.10
Wyoming	0.42

Table 4-3. Largest contribution from each state to downwind nonattainment and maintenance-only receptors in 2026 (ppb).

<i>Upwind State</i>	<i>Largest Contribution to Downwind Nonattainment Receptors</i>	<i>Largest Contribution to Downwind Maintenance-Only Receptors</i>
Alabama	0.20	0.69
Arizona	0.44	1.34
Arkansas	0.53	1.16
California	34.03	6.16
Colorado	0.04	0.17
Connecticut	0.00	0.01
Delaware	0.43	0.41
District of Columbia	0.03	0.02
Florida	0.46	0.17
Georgia	0.13	0.16
Idaho	0.27	0.36
Illinois	0.63	13.57
Indiana	1.06	8.53
Iowa	0.14	0.62
Kansas	0.14	0.42
Kentucky	0.79	0.76
Louisiana	4.57	9.37
Maine	0.00	0.01
Maryland	1.06	0.92
Massachusetts	0.06	0.31
Michigan	1.39	1.47
Minnesota	0.15	0.32
Mississippi	0.29	1.15
Missouri	0.29	1.68
Montana	0.06	0.07
Nebraska	0.09	0.19
Nevada	0.67	0.90
New Hampshire	0.01	0.09
New Jersey	8.10	7.04
New Mexico	0.35	0.46
New York	12.65	12.34
North Carolina	0.40	0.42
North Dakota	0.09	0.17
Ohio	1.95	1.93
Oklahoma	0.19	0.74

<i>Upwind State</i>	<i>Largest Contribution to Downwind Nonattainment Receptors</i>	<i>Largest Contribution to Downwind Maintenance-Only Receptors</i>
Oregon	0.26	0.41
Pennsylvania	5.47	4.94
Rhode Island	0.00	0.03
South Carolina	0.14	0.15
South Dakota	0.03	0.04
Tennessee	0.24	0.54
Texas	0.48	4.34
Utah	1.05	0.81
Vermont	0.01	0.02
Virginia	1.09	1.10
Washington	0.10	0.14
West Virginia	1.36	1.34
Wisconsin	0.17	0.18
Wyoming	0.40	0.59

In CSAPR, the CSAPR Update, and the Revised CSAPR Update, and in the proposal for this final rule the EPA used a contribution screening threshold of 1 percent of the NAAQS to identify upwind states that may significantly contribute to downwind nonattainment and/or maintenance problems and which warrant further analysis to determine if emissions reductions might be required from each state to address the downwind air quality problem. The EPA determined that 1 percent was an appropriate threshold to use in Step 2 because there were important, even if relatively small, contributions to identified nonattainment and maintenance receptors from multiple upwind states. The EPA has historically found that the 1 percent threshold is appropriate for identifying interstate transport linkages for states collectively contributing to downwind ozone nonattainment or maintenance problems because that threshold captures a high percentage of the total pollution transport affecting downwind receptors. The EPA received numerous comments on the use of the 1 percent screening threshold. Responses to these comments can be found in the preamble and in the Response to Comments (RTC) document for this final rule.

Based on the maximum downwind contribution data in Table 4-1, the following 21 states contribute at or above the 0.70 ppb threshold to downwind nonattainment receptors in 2023: Alabama, Arkansas, California, Illinois, Indiana, Kentucky, Louisiana, Maryland, Michigan, Mississippi, Missouri, Nevada, New Jersey, New York, Ohio, Oklahoma, Pennsylvania, Texas, Utah, Virginia, and West Virginia. Based on the maximum downwind contribution data also in

Table 4-1, the following 23 states contribute at or above the 0.70 ppb threshold to downwind monitoring plus modeled maintenance-only receptors in 2023: Arizona, Arkansas, California, Illinois, Indiana, Iowa, Kentucky, Louisiana, Maryland, Michigan, Minnesota, Mississippi, Missouri, Nevada, New Jersey, New Mexico, New York, Ohio, Oklahoma, Texas, Virginia, West Virginia, and Wisconsin. Finally, based on the maximum downwind contribution in Table 4-2, the following additional states contribute at or above the 0.70 ppb threshold to downwind violating monitor maintenance-only receptors in 2023: Kansas and Tennessee. Note that Arizona, Iowa, Kansas, New Mexico, Tennessee, and Wyoming fall into one of two categories: (a) not linked to downwind receptors based on the 2016v2 modeling for the proposal, but that are now linked based on the 2016v3 modeling or are linked to a violating monitor; or (b) were linked to downwind receptors based on 2016v2 modeling for the proposal, but that are now not linked to any receptors based on the 2016v3 modeling or under the definition of receptors used at proposal.

Based on the maximum downwind contribution data in Table 4-3, the following 13 states contribute at or above the 0.70 ppb threshold to downwind nonattainment receptors in 2026: California, Indiana, Kentucky, Louisiana, Maryland, New Jersey, New York, Ohio, Pennsylvania, Utah, Virginia, West Virginia. Based on the maximum downwind contribution data also in Table 4-3, the following 8 states contribute at or above the 0.70 ppb threshold to downwind monitoring plus modeled maintenance-only receptors in 2026: Arizona, Arkansas, Illinois, Mississippi, Missouri, Nevada, Oklahoma, and Texas.

The contributions for individual upwind/downwind linkages for each upwind state are provided in Appendix C. The upwind states linked to each receptor are provided in Appendix E.

5. 2026 Control Case Modeling

In this section we provide the results of the 2026 control case modeling. The control case reflects the estimated emissions reductions expected to result from this final rule. The components of the final rule control case are described in the RIA. The change in NO_x emissions between the 2026 base case and the 2026 control case are provided, by state in Table 5-1. Note that negative values in this table denote a reduction in emissions whereas positive values denote an increase in emissions.³¹ The impacts on emissions are rank ordered by the amount of emissions reduction (i.e., negative

³¹ The imposition of the final rule results in changes in regional electricity flows, resulting in changes in net imports. As a result, some states (even those not subject to the rule) may see changes in emissions as a result of generation shifting.

values are at the top). That is, in Table 5-1 the states with the largest NO_x emissions reductions in the final rule case are at the top of the list.

The “ppb” impacts on ozone design values at individual monitoring sites are shown in Figure 5-1. The spatial field of impacts on the modeled top 10-day average MDA8 ozone concentrations in 2026 is shown in Figure 5-2. Both figures indicate that the NO_x emissions reductions in the control case are expected to reduce ozone concentrations across broad regions of the eastern and western U.S within and downwind of the states covered by this final rule.

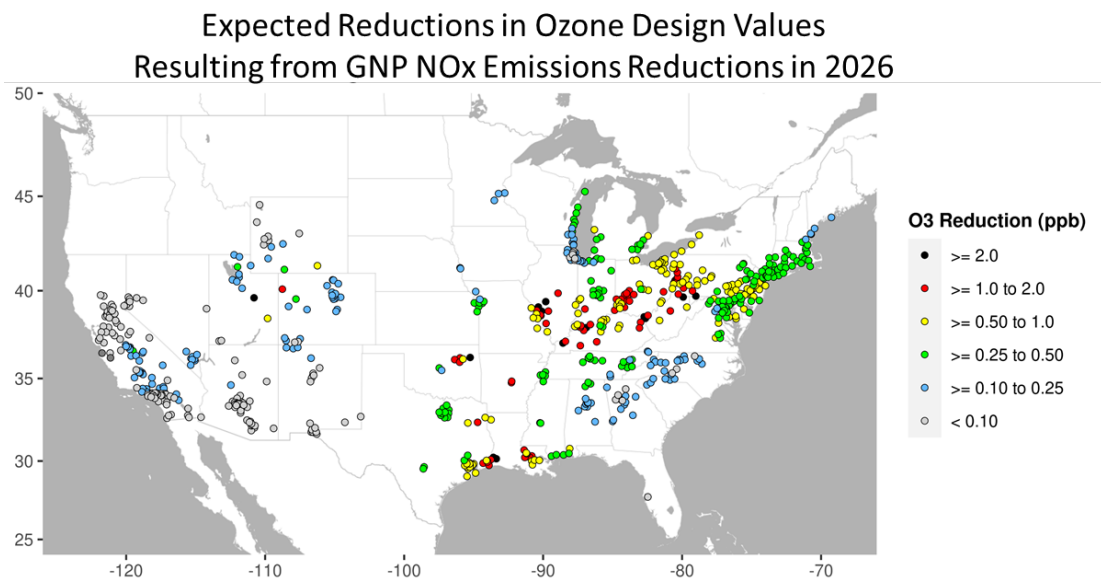


Figure 5-1. Reduction in design value concentrations at individual monitoring sites.

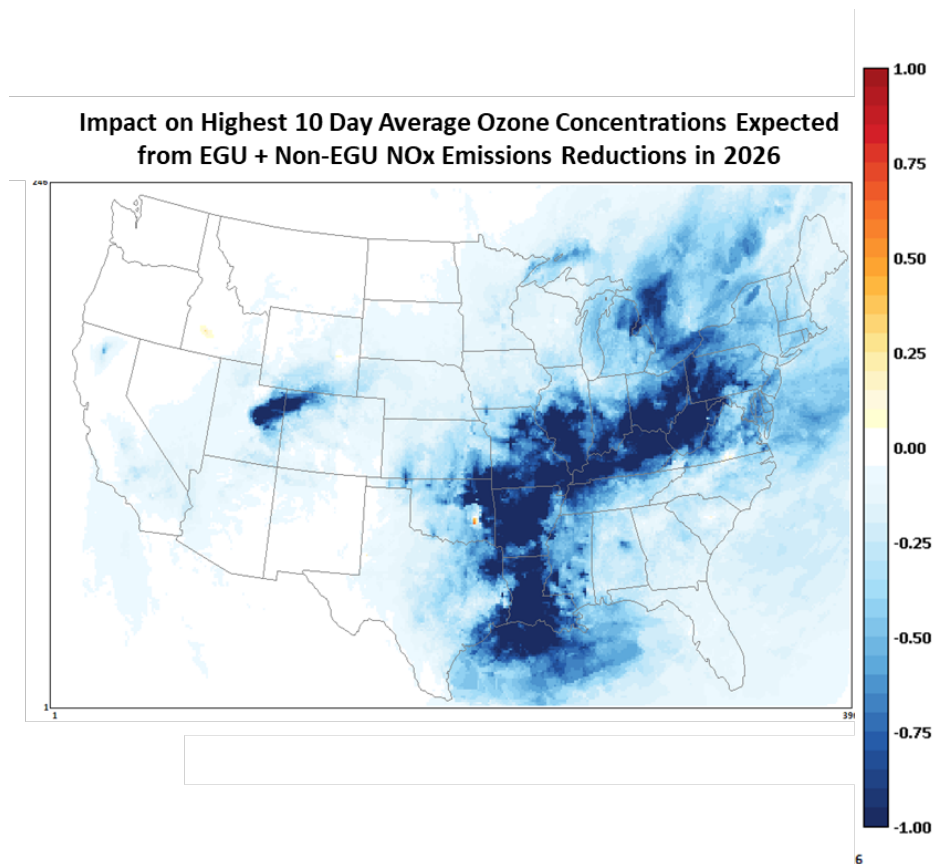


Figure 5-2. Impact of the control case NOx emissions reductions on the top 10-day average MDA8 ozone concentrations (ppb) in 2026.

The estimated “ppb” impacts on projected 2026 ozone design values for those monitoring sites that are identified as monitored plus modeled receptors in 2026 and/or in 2023 are provided in Table 5-2. Table 5-3 provides the same information for the violating monitor-based maintenance-only receptors in 2023.³² Examining the emissions data in Table 5-1 together with the ppb impacts in Table 5-2 and 5-3 indicates that the largest reductions in receptor ozone design values are predicted to occur in the Houston-Galveston-Brazoria, Texas area. In this area the reductions from the final rule case range from 0.7 to 0.9 ppb. At most of the receptors in both the Dallas/Ft Worth and the New York/Coastal Connecticut areas the reductions in ozone design values range from 0.4 to 0.5 ppb. At receptors in Indiana, Michigan, and Wisconsin near the shoreline of Lake Michigan, ozone design values are projected to decline by 0.3 to 0.4 ppb, but by as much as 0.5 ppb at the receptor in Muskegon, MI. Lesser reductions of 0.1 ppb are predicted in the urban and near-urban receptors in Chicago. In the West, reductions in ozone design values just under 0.2 ppb are predicted at receptors

³² The approaches for identifying receptors are described in Section 3.

in Denver with slightly greater reductions, just above 0.2 ppb, at receptors in Salt Lake City. At receptors in Phoenix, California, El Paso/Las Cruces, and southeast New Mexico the reductions in ozone design values are predicted to be less than 0.1 ppb.

Table 5-1. Impact on EGU and Non-EGU Ozone Season NO_x Emissions by State in the 2026 Modeled Control Case (1,000 tons).

<i>State</i>	<i>Final - Baseline</i>
Louisiana	-12.6
Oklahoma	-9.9
Texas	-7.7
Arkansas	-7.3
Missouri	-6.9
Michigan	-5.3
Kentucky	-5.3
Utah	-5.2
Ohio	-4.9
West Virginia	-3.7
Indiana	-3.1
Mississippi	-3.0
Pennsylvania	-2.1
Illinois	-2.1
California	-1.7
Virginia	-1.6
Tribal	-1.3
Minnesota	-1.2
New York	-1.2
New Jersey	-0.3
Arizona	-0.3
Alabama	-0.2
Maryland	-0.1
Nevada	0.0
Rhode Island	0.0
Florida	0.0
Maine	0.0
Oregon	0.0
Vermont	0.0
District of Columbia	0.0
Washington	0.0
Montana	0.0
Delaware	0.0

<i>State</i>	<i>Final - Baseline</i>
Massachusetts	0.0
New Hampshire	0.0
New Mexico	0.0
Connecticut	0.0
Tennessee	0.0
South Dakota	0.0
Georgia	0.0
Nebraska	0.1
Idaho	0.1
Colorado	0.1
North Dakota	0.1
Wisconsin	0.1
South Carolina	0.2
Iowa	0.3
North Carolina	0.4
Kansas	0.4
Wyoming	0.5

Table 5-2. Ozone Impacts at Projected 2023 Nonattainment and Maintenance-Only Receptors (ppb) for the Final Rule Modeled Control Case in 2026.

<i>Site ID</i>	<i>State</i>	<i>County</i>	<i>Final Rule Case</i>
40278011	Arizona	Yuma	-0.06
60650016	California	Riverside	-0.06
60651016	California	Riverside	-0.08
80350004	Colorado	Douglas	-0.17
80590006	Colorado	Jefferson	-0.14
80590011	Colorado	Jefferson	-0.11
80690011	Colorado	Larimer	-0.24
90010017	Connecticut	Fairfield	-0.38
90013007	Connecticut	Fairfield	-0.45
90019003	Connecticut	Fairfield	-0.46
90099002	Connecticut	New Haven	-0.43
170310001	Illinois	Cook	-0.08
170314201	Illinois	Cook	-0.09
170317002	Illinois	Cook	-0.11
350130021	New Mexico	Dona Ana	-0.02
350130022	New Mexico	Dona Ana	-0.03
350151005	New Mexico	Eddy	-0.02

<i>Site ID</i>	<i>State</i>	<i>County</i>	<i>Final Rule Case</i>
350250008	New Mexico	Lea	-0.02
480391004	Texas	Brazoria	-0.82
481210034	Texas	Denton	-0.42
481410037	Texas	El Paso	-0.03
481671034	Texas	Galveston	-0.92
482010024	Texas	Harris	-0.68
482010055	Texas	Harris	-0.75
482011034	Texas	Harris	-0.72
482011035	Texas	Harris	-0.70
490110004	Utah	Davis	-0.22
490353006	Utah	Salt Lake	-0.22
490353013	Utah	Salt Lake	-0.15
550590019	Wisconsin	Kenosha	-0.21
551010020	Wisconsin	Racine	-0.22
551170006	Wisconsin	Sheboygan	-0.30

Table 5-3. Ozone Impacts at Violating-Monitor Maintenance-Only Receptors (ppb) in 2023 for the Final Rule Modeled Control Case in 2026.

<i>Site ID</i>	<i>State</i>	<i>County</i>	<i>Final Rule Case</i>
40070010	Arizona	Gila	-0.07
40130019	Arizona	Maricopa	-0.04
40131003	Arizona	Maricopa	-0.05
40131004	Arizona	Maricopa	-0.05
40131010	Arizona	Maricopa	-0.05
40132001	Arizona	Maricopa	-0.04
40132005	Arizona	Maricopa	-0.06
40133002	Arizona	Maricopa	-0.04
40134004	Arizona	Maricopa	-0.05
40134005	Arizona	Maricopa	-0.04
40134008	Arizona	Maricopa	-0.05
40134010	Arizona	Maricopa	-0.06
40137020	Arizona	Maricopa	-0.04
40137021	Arizona	Maricopa	-0.06
40137022	Arizona	Maricopa	-0.05
40137024	Arizona	Maricopa	-0.04
40139702	Arizona	Maricopa	-0.05
40139704	Arizona	Maricopa	-0.06
40139997	Arizona	Maricopa	-0.04

<i>Site ID</i>	<i>State</i>	<i>County</i>	<i>Final Rule Case</i>
40218001	Arizona	Pinal	-0.03
80013001	Colorado	Adams	-0.13
80050002	Colorado	Arapahoe	-0.18
80310002	Colorado	Denver	-0.13
80310026	Colorado	Denver	-0.13
90079007	Connecticut	Middlesex	-0.49
90110124	Connecticut	New London	-0.41
170310032	Illinois	Cook	-0.10
170311601	Illinois	Cook	-0.10
181270024	Indiana	Porter	-0.23
260050003	Michigan	Allegan	-0.39
261210039	Michigan	Muskegon	-0.50
320030043	Nevada	Clark	-0.15
350011012	New Mexico	Bernalillo	-0.04
350130008	New Mexico	Dona Ana	-0.02
361030002	New York	Suffolk	-0.39
390850003	Ohio	Lake	-0.70
480290052	Texas	Bexar	-0.28
480850005	Texas	Collin	-0.48
481130075	Texas	Dallas	-0.45
481211032	Texas	Denton	-0.41
482010051	Texas	Harris	-0.69
482010416	Texas	Harris	-0.73
484390075	Texas	Tarrant	-0.30
484391002	Texas	Tarrant	-0.38
484392003	Texas	Tarrant	-0.38
484393009	Texas	Tarrant	-0.32
490571003	Utah	Weber	-0.27
550590025	Wisconsin	Kenosha	-0.22
550890008	Wisconsin	Ozaukee	-0.24

6. Back Trajectory Analysis

As part of the assessment of interstate transport, the EPA used the HYSPLIT model (Stein, et al., 2017) to provide a “transport climatology” for individual nonattainment and maintenance-only receptors in 2023. This “transport climatology” provides a semi-quantitative approach to identify the predominant transport patterns and interannual variability in transport for days with measured exceedances. In this regard, the information from this analysis provides a qualitative method to corroborate upwind-downwind linkages derived from the air quality contribution modeling. In this

analysis the EPA ran the HYSPLIT model to construct 96-hour back trajectories for days with measured exceedances during 2010 through 2021 at individual receptors. Back trajectories were created for three start times on each exceedance day (8:00 am, 12:00 pm, and 3:00 pm Local Time for each of six vertical elevations (100 m, 250 m, 500 m, 750 m, 1000 m, and 1500 m. Meteorological data from the North American Mesoscale meteorological model (NAM) with 12 km horizontal resolution were used in the HYSPLIT runs. The HYSPLIT outputs were processed to determine the number of trajectory segments that crossed over a particular area.³³ Each HYSPLIT hourly segment was counted individually based on segment intersections. For visualization, the trajectory segment counts were further processed using a 7-element Hanning Function.

Plots showing the back trajectories from each receptor are provided in the following documents which can be found in the docket of this final rule: “Exceedance Day Trajectory Analysis_2010-2021” This file contains (1) composite multi-start time, multi-elevation plots of exceedance day back trajectories for each year individually for each receptor and (2) composite multi-start time, multi-year composite plots of 500 m and 750 m exceedance day back trajectories for each receptor. These two elevations were selected as generally representative of summertime mid-boundary layer transport.

³³ The HYSPLIT segments were processed for a 0.25 degree (approximately 27 km) grid cell. Each grid cell constitutes a particular area.

7. References

- Emery, C., Z. Liu, A. Russell, M. T. Odom, G. Yarwood, and N. Kumar, 2017. Recommendations on Statistics and Benchmarks to Assess Photochemical Model Performance. *J. Air and Waste Management Association*, 67, 582-598.
- Gilliam, R.C. and J.E. Pleim, 2010. Performance Assessment of New Land Surface and Planetary Boundary Layer Physics in the WRF-ARW. *J. Appl. Meteor. Climatol.*, 49, 760–774.
- Henderson, B.H., F. Akhtar, H.O.T. Pye, S.L. Napelenok, W.T. Hutzell, 2014. A Database and Tool for Boundary Conditions for Regional Air Quality Modeling: Description and Evaluations, *Geoscientific Model Development*, 7, 339-360.
- Hong, S-Y, Y. Noh, and J. Dudhia, 2006. A New Vertical Diffusion Package with an Explicit Treatment of Entrainment Processes. *Mon. Wea. Rev.*, 134, 2318–2341.
- Houyoux, M.R., Vukovich, J.M., Coats, C.J., Wheeler, N.J.M., Kasibhatla, P.S., 2000. Emissions Inventory Development and Processing for the Seasonal Model for Regional Air Quality (SMRAQ) project, *Journal of Geophysical Research – Atmospheres*, 105(D7), 9079-9090.
- Iacono, M.J., J.S. Delamere, E.J. Mlawer, M.W. Shephard, S.A Clough, and W.D. Collins, 2008. Radiative Forcing by Long-Lived Greenhouse Gases: Calculations with the AER Radiative Transfer Models, *J. Geophys. Res.*, 113, D13103.
- I. Bey, D.J. Jacob, R.M. Yantosca, J.A. Logan, B.D. Field, A.M. Fiore, Q. Li, H.Y. Liu, L.J. Mickley, M.G. Schultz. Global modeling of tropospheric chemistry with assimilated meteorology: model description and evaluation. *J. Geophys. Res. Atmos.*, 106 (2001), pp. 23073-23095, 10.1029/2001jd000807.
- Kain, J.S., 2004. The Kain-Fritsch Convective Parameterization: An Update, *J. Appl. Meteor.*, 43, 170-181.
- Lyman, S, Trang, T. Inversion structure and winter ozone distribution in the Uintah Basin, Utah, U.S.A. *Atmospheric Environment*. 123 (2015) 156-165.
- Ma, L-M. and Tan Z-M, 2009. Improving the Behavior of Cumulus Parameterization for Tropical Cyclone Prediction: Convective Trigger, *Atmospheric Research*, 92, 190-211.
- Morrison, H.J., A. Curry, and V.I. Khvorostyanov, 2005. A New Double-Moment Microphysics Parameterization for Application in Cloud and Climate Models. Part I: Description, *J. Atmos. Sci.*, 62, 1665–1677.
- Morrison, H. and A. Gettelman, 2008. A New Two-Moment Bulk Stratiform Cloud Microphysics Scheme in the Community Atmosphere Model, version 3 (CAM3). Part I: Description and Numerical Tests, *J. Climate*, 21, 3642-3659.
- Pleim, J.E. and A. Xiu, 2003. Development of a Land-Surface Model. Part II: Data Assimilation, *J. Appl. Meteor.*, 42, 1811–1822

- Pleim, J.E., 2007a. A Combined Local and Nonlocal Closure Model for the Atmospheric Boundary Layer. Part I: Model Description and Testing, *J. Appl. Meteor. Climatol.*, 46, 1383–1395.
- Pleim, J.E., 2007b. A Combined Local and Nonlocal Closure Model for the Atmospheric Boundary Layer. Part II: Application and Evaluation in a Mesoscale Meteorological Model, *J. Appl. Meteor. Climatol.*, 46, 1396–1409.
- Ramboll Environ, 2021. User's Guide Comprehensive Air Quality Model with Extensions version 7.1, www.camx.com. Ramboll Environ International Corporation, Novato, CA.
- Skamarock, W.C., J.B. Klemp, J. Dudhia, et al., 2008. A Description of the Advanced Research WRF Version 3. NCAR Tech. Note NCAR/TN-475+STR. http://www.mmm.ucar.edu/wrf/users/docs/arw_v3.pdf
- Simon, H., K.R. Baker, and S.B. Phillips, 2012. Compilation and Interpretation of Photochemical Model Performance Statistics Published between 2006 and 2012, *Atmospheric Environment*, 61, 124-139.
- Stammer, D., F.J. Wentz, and C.L. Gentemann, 2003. Validation of Microwave Sea Surface Temperature Measurements for Climate Purposes, *J. of Climate*, 16(1), 73-87.
- Stein, A.F., Draxler, R.R, Rolph, G.D., Stunder, B.J.B., Cohen, M.D., and Ngan, F., (2015). NOAA's HYSPLIT atmospheric transport and dispersion modeling system, *Bull. Amer. Meteor. Soc.*, **96**, 2059-2077, <http://dx.doi.org/10.117/BAMS-D-14-0010.1>
- U.S. Environmental Protection Agency, 2018. Modeling Guidance for Demonstrating Attainment of Air Quality Goals for Ozone, PM2.5, and Regional Haze, Research Triangle Park, NC. https://www3.epa.gov/ttn/scram/guidance/guide/O3-PM-RH-Modeling_Guidance-2018.pdf
- Xiu, A., and J.E. Pleim, 2001, Development of a Land Surface Model. Part I: Application in a Meso scale Meteorological Model, *J. Appl. Meteor.*, 40, 192-209.
- Yantosca, B. 2004. GEOS-CHEMv7-01-02 User's Guide, Atmospheric Chemistry Modeling Group, Harvard University, Cambridge, MA.

Appendix A

Model Performance Sensitivity Analysis

As noted in the preamble for this final action, in response to comments the EPA examined the temporal and spatial characteristics of model under prediction in the 2016v2 modeling to investigate the possible causes of under prediction of MDA8 ozone concentrations in different regions of the U.S. The EPA's analysis indicates that the under prediction was most extensive during May and June with less bias during July and August in most regions of the U.S. For example, in the Upper Midwest region model under prediction was larger in May and June compared to July through September. Specifically, the normalized mean bias for days with measured concentrations ≥ 60 ppb improved from a 21.4 percent under prediction for May and June to a 12.6 percent under prediction in the period July through September. As highest by the presentation materials in this Appendix, the seasonal pattern in bias in the Upper Midwest region improves somewhat gradually with time from the middle of May to the latter part of June. In view of the seasonal pattern in bias in the Upper Midwest and in other regions of the U.S., EPA focused its investigation of model performance on model inputs that, by their nature, have the largest temporal variation within the ozone season. These inputs include emissions from biogenic sources and lightning NO_x, and contributions from transport of international anthropogenic emissions and natural sources into the U.S. Both biogenic and lightning NO_x emissions in the U.S. dramatically increase from spring to summer.^{1,2} In contrast, ozone transported into the U.S. from international anthropogenic and natural sources peaks during the period March through

¹ Guenther, A.B., 1997. Seasonal and spatial variations in natural volatile organic compound emissions. *Ecol. Appl.* 7, 34–45. [http://dx.doi.org/10.1890/1051-0761\(1997\)007\[0034:SASVIN\]2.0.CO;2](http://dx.doi.org/10.1890/1051-0761(1997)007[0034:SASVIN]2.0.CO;2).

² Kang D, Mathur R, Pouliot GA, Gilliam RC, Wong DC. Significant ground-level ozone attributed to lightning-induced nitrogen oxides during summertime over the Mountain West States. *NPJ Clim Atmos Sci.* 2020 Jan 30;3:6. doi: 10.1038/s41612-020-0108-2. PMID: 32181370; PMCID: PMC7075249.

June, with lower contributions during July through September.^{3,4} To investigate the impacts of the sources, EPA conducted sensitivity model runs which focused on the effects on model performance of adding NO_x emissions from lightning strikes, updating updated biogenic emissions, and using an alternative approach for quantifying transport of ozone and precursor pollutants into the U.S. from international anthropogenic and natural sources. In the 2016v2 modeling the amount of transport from international anthropogenic and natural sources was based on a simulation of the hemispheric version of the Community Multi-scale Air Quality Model (H-CMAQ) for 2016.⁵ The outputs from this hemispheric modeling were then used to provide boundary conditions for national scale air quality modeling at proposal.⁶ Overall, H-CMAQ tends to under-predict daytime ozone concentrations at rural and remote monitoring sites across the U.S. during the spring of 2016 whereas the predictions from the GEOS-Chem global

³ Jaffe DA, Cooper OR, Fiore AM, Henderson BH, Tonnesen GS, Russell AG, Henze DK, Langford AO, Lin M, Moore T. Scientific assessment of background ozone over the U.S.: Implications for air quality management. *Elementa* (Wash D C). 2018;6(1):56. doi: 10.1525/elementa.309. PMID: 30364819; PMCID: PMC6198683.

⁴ Henderson, B.H., P. Dolwick, C. Jang, A., Eyth, J. Vukovich, R. Mathur, C. Hogrefe, N. Possiel, G. Pouliot, B. Timin, K.W. Appel, 2019. Global Sources of North American Ozone. Presented at the 18th Annual Conference of the UNC Institute for the Environment Community Modeling and Analysis System (CMAS) Center, October 21-23, 2019.

⁵ Mathur, R., Gilliam, R., Bullock, O.R., Roselle, S., Pleim, J., Wong, D., Binkowski, F., and Streets, D.: Extending the applicability of the community multiscale air quality model to 2 hemispheric scales: motivation, challenges, and progress. In: Steyn DG, Trini S (eds) *Air 3 pollution modeling and its applications*, XXI. Springer, Dordrecht, pp 175–179, 2012.

⁶ Boundary conditions are the concentrations of pollutants along the north, east, south, and west boundaries of the air quality modeling domain. Boundary conditions vary in space and time and are typically obtained from predictions of global or hemispheric models. Information on how boundary conditions were developed for the final rule modeling can be found in the AQM TSD.

model⁷ were generally less biased.⁸ During the summer of 2016 both models showed varying degrees of over prediction with GEOS-Chem showing somewhat greater over-prediction, compared to H-CMAQ. In view of those results, EPA examined the impacts of using GEOSChem as an alternative to H-CMAQ for providing boundary conditions for the final rule modeling.

For the lightning NO_x, biogenics, and GEOSChem sensitivity runs, the EPA reran 2016v2 using each of these alternative inputs, individually. Results from these sensitivity runs indicate that each of the three updates provides an improvement in model performance. However, by far the greatest improvement in modeling performance is attributable to the use of GEOSChem. In view of these results the EPA has included lightning NO_x emissions, updated biogenic emissions, and international transport from GEOSChem in the 2016v3 modeling used for this final action. As described in Appendix B, the model has less bias and error regionally and at individual nonattainment/maintenance receptors on high ozone days using these updates.

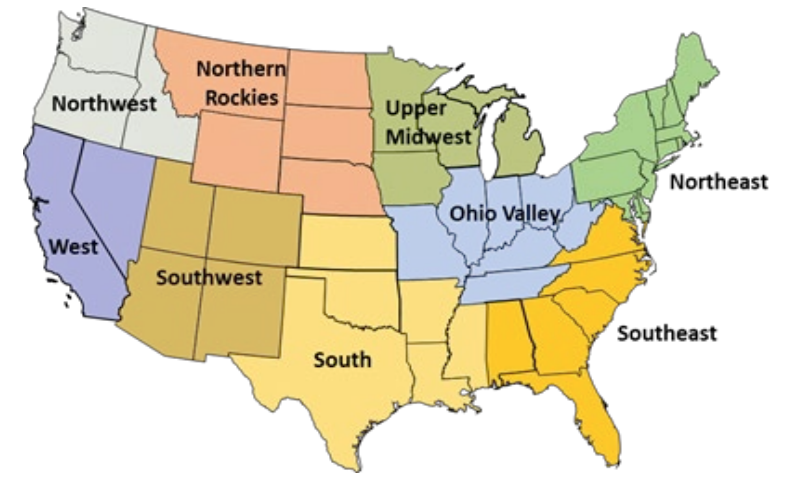
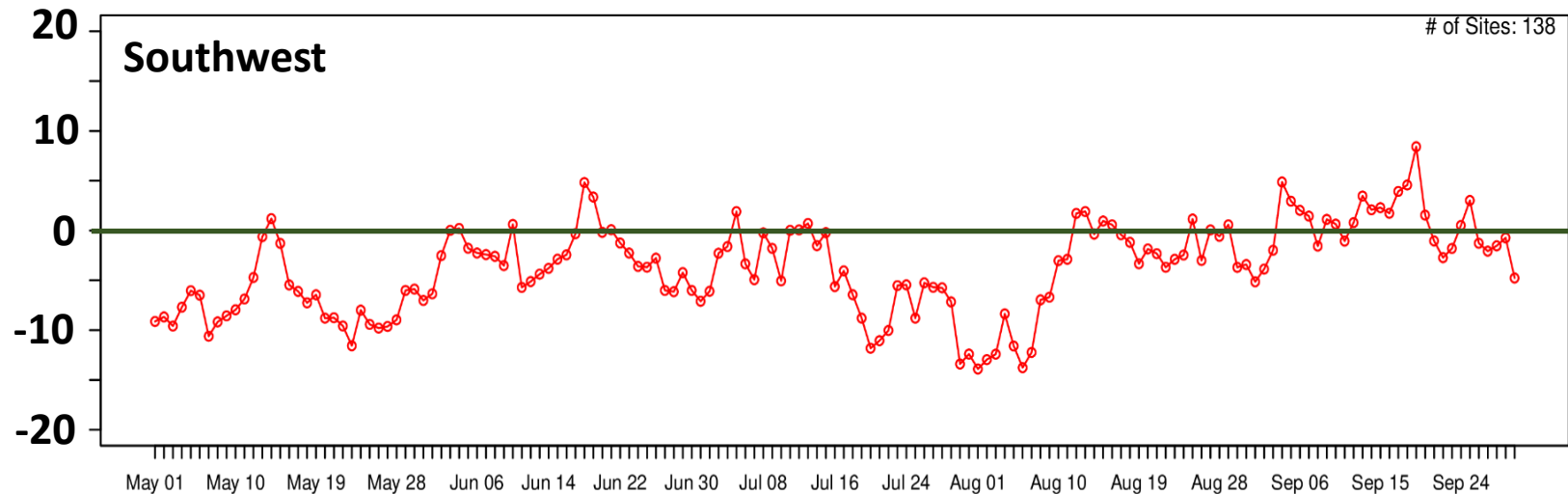
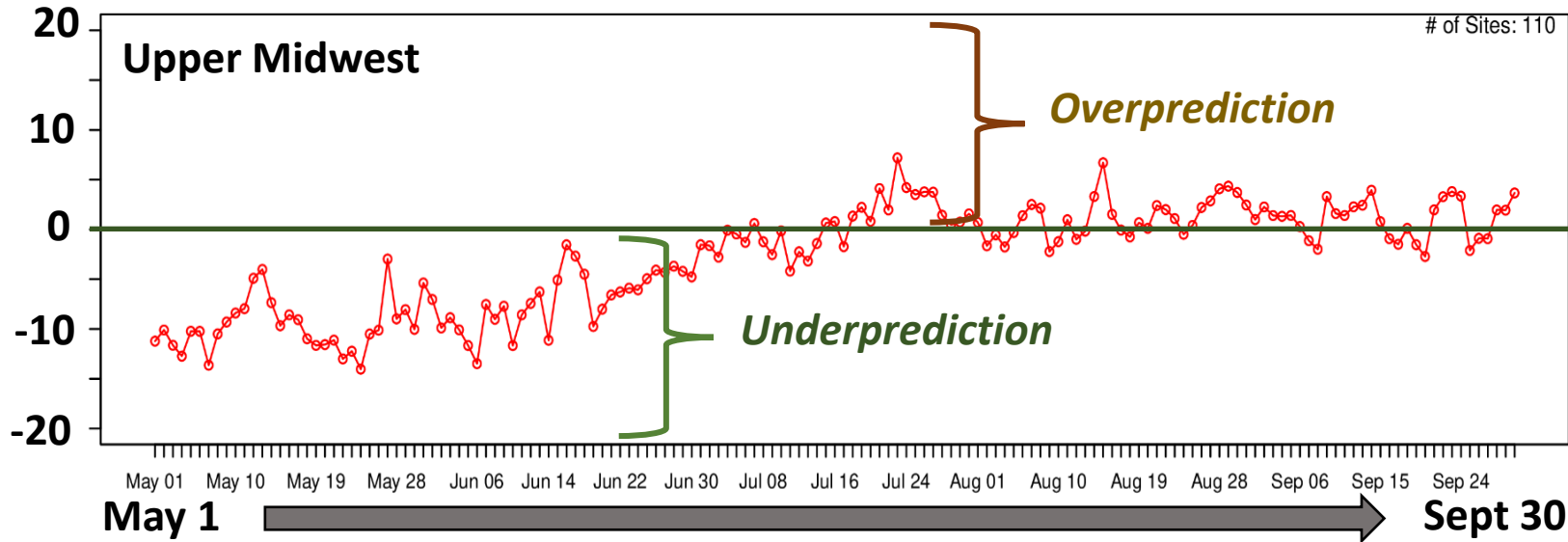
⁷ I. Bey, D.J. Jacob, R.M. Yantosca, J.A. Logan, B.D. Field, A.M. Fiore, Q. Li, H.Y. Liu, L.J. Mickley, M.G. Schultz. Global modeling of tropospheric chemistry with assimilated meteorology: model description and evaluation. *J. Geophys. Res. Atmos.*, 106 (2001), pp. 23073-23095, 10.1029/2001jd000807.

⁸ Henderson, B.H., P. Dolwick, C. Jang, A., Eyth, J. Vukovich, R. Mathur, C. Hogrefe, G. Pouliot, N. Possiel, B. Timin, K.W. Appel, 2022. Meteorological and Emission Sensitivity of Hemispheric Ozone and PM_{2.5}. Presented at the 21st Annual Conference of the UNC Institute for the Environment Community Modeling and Analysis System (CMAS) Center, October 17-19, 2022.

2016 Model Performance Sensitivity Analysis

Bias (ppb) in MDA8 Ozone by Day –

2016v2 modeling generally under predicted measured MDA8 ozone concentrations, particularly in May and June



Modeling Platform Updates Examined to Address Model Performance Concerns

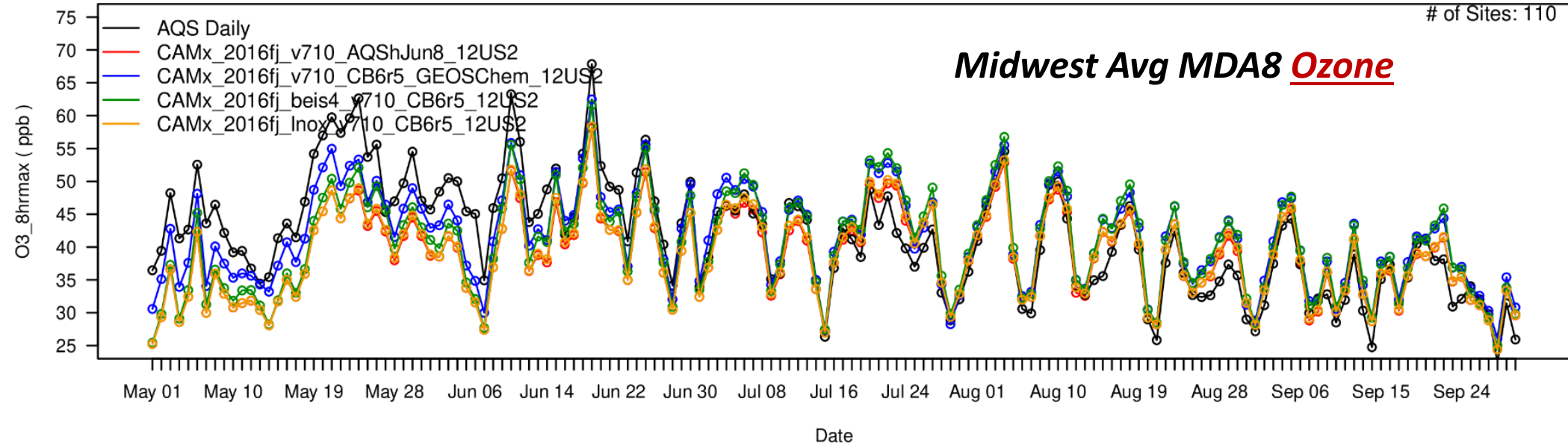
- Initial & Boundary Concentrations: Use GEOSChem rather than Hemispheric CMAQ (H-CMAQ) to provide initial and boundary concentrations for the outer (36 km) modeling domain. (GEOSChem => 36US3 => 12US2 domain)
- Biogenic Emissions: Use a recently released updated version of BEIS + BELD land use (BEIS4/BELD6) which includes state-of-science emissions factors and improved land use data
- Lightning NO_x: Include 3-D NO_x emissions from lightning strikes using a soon-to-be published method developed by ORD.



Sensitivity Model Runs to Explore Impacts of Potential Updates

- Baseline for sensitivities is the 2016fj (i.e., 2016v2 platform) model run
- Model Sensitivity Runs
 - 1) BEIS4/BELD6 Biogenics
 - 2) Include emissions of Lightning NO_x
 - 3) GEOS-Chem + BEIS4/BELD6 + Lightning NO_x
- Results
 - Model performance for MDA8 ozone improved with each of the three updates. The most notable improvements resulted from using GEOS-Chem to provide initial and boundary concentrations

Time Series of Daily Bias in MDA8 Ozone & Bias – May Through September



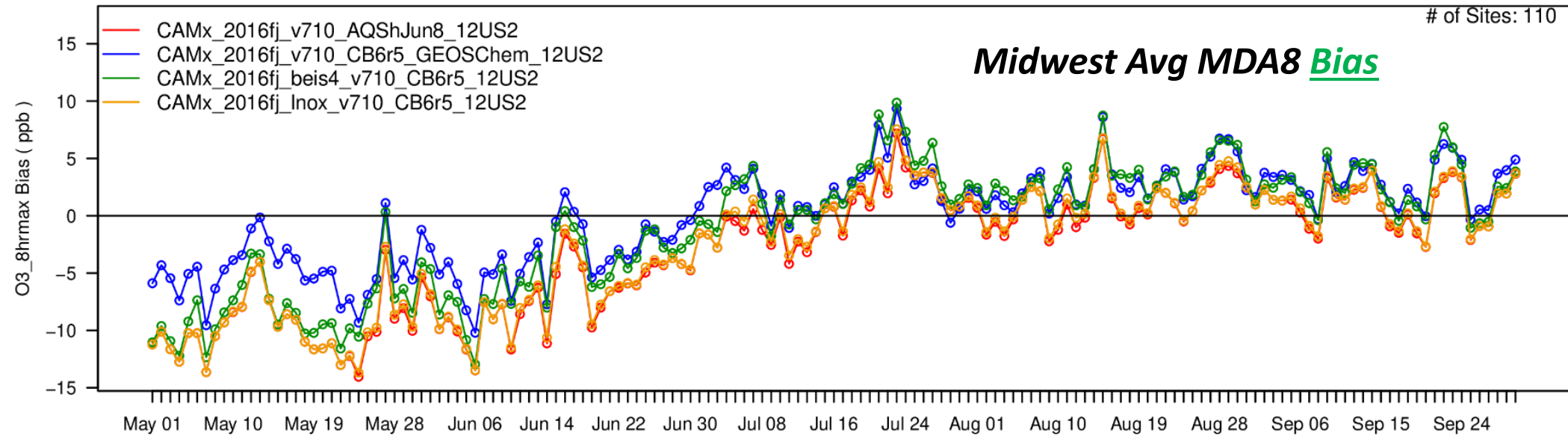
2016 Obs

2016fj Base Model

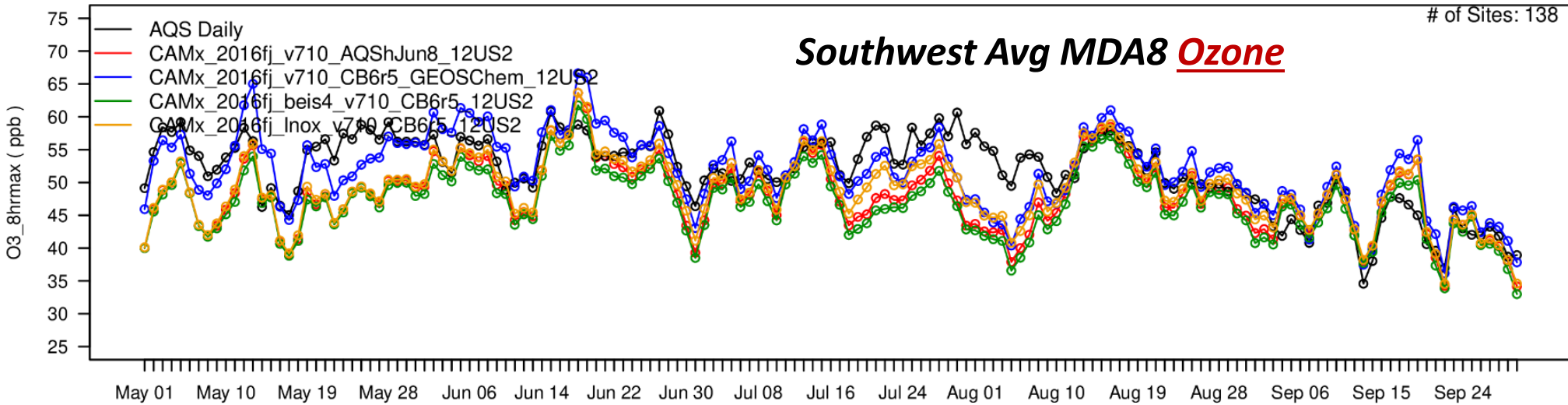
2016fj GEOSChem

2016fj BEIS4/BELD6

2016fj Lightning NOx



Time Series of Daily Bias in MDA8 Ozone & Bias – May Through September



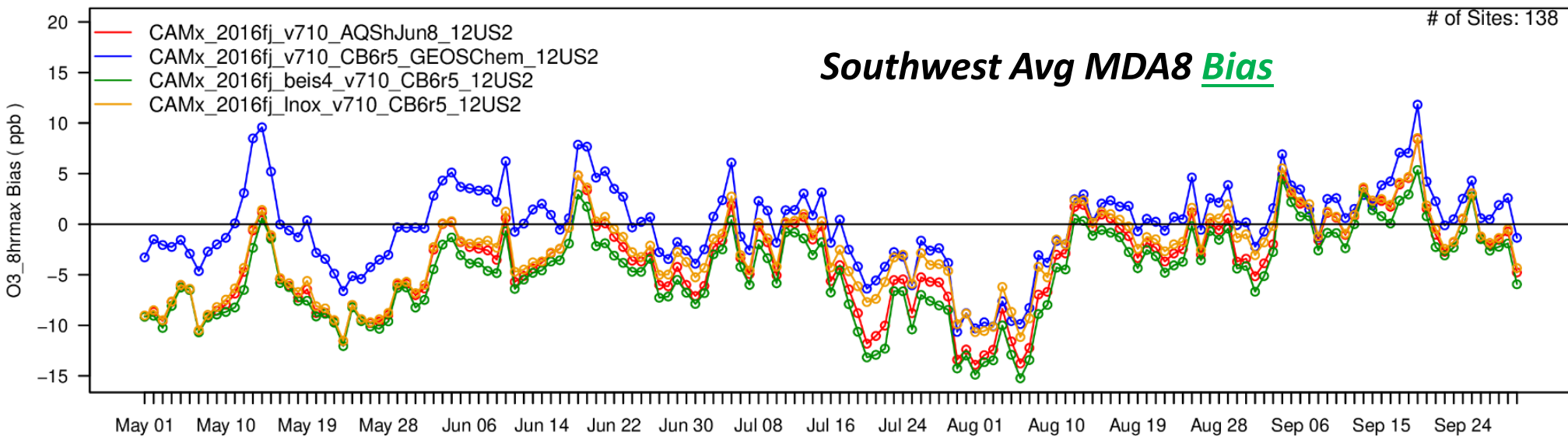
2016 Obs

2016fj Base Model

2016fj GEOSChem

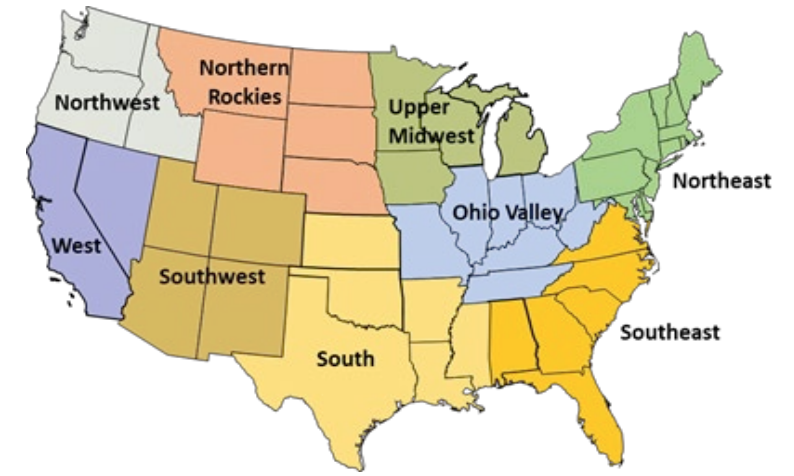
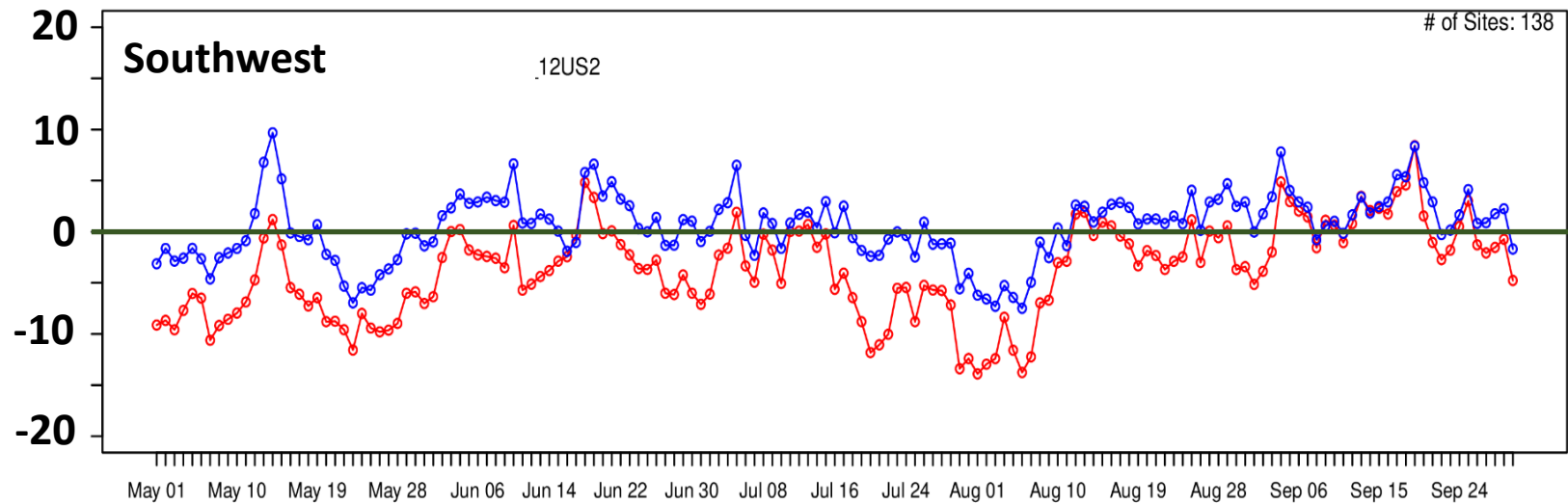
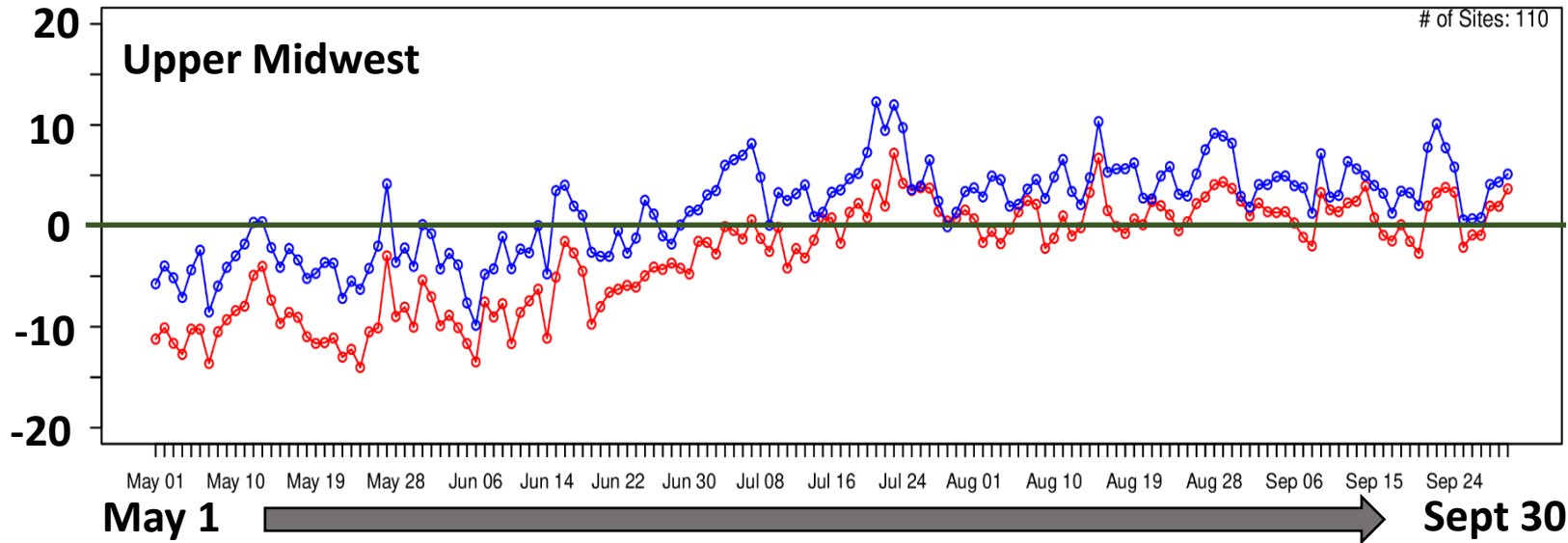
2016fj BEIS4/BELD6

2016fj Lightning NOx



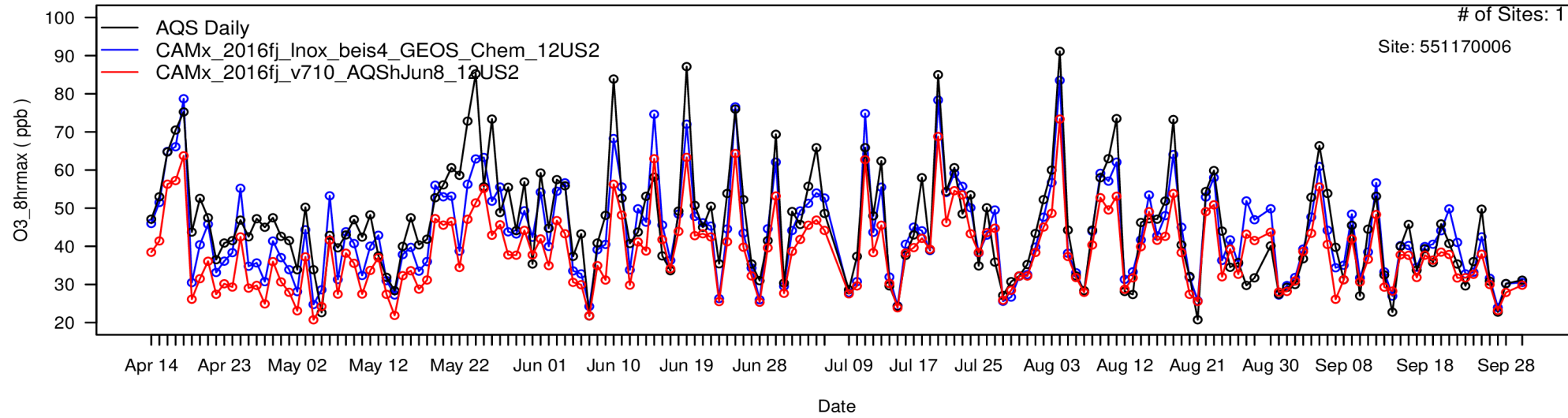
Date

Bias (ppb) in MDA8 Ozone by Day – 2016v2 vs GEOSChem + BEIS + LNOx

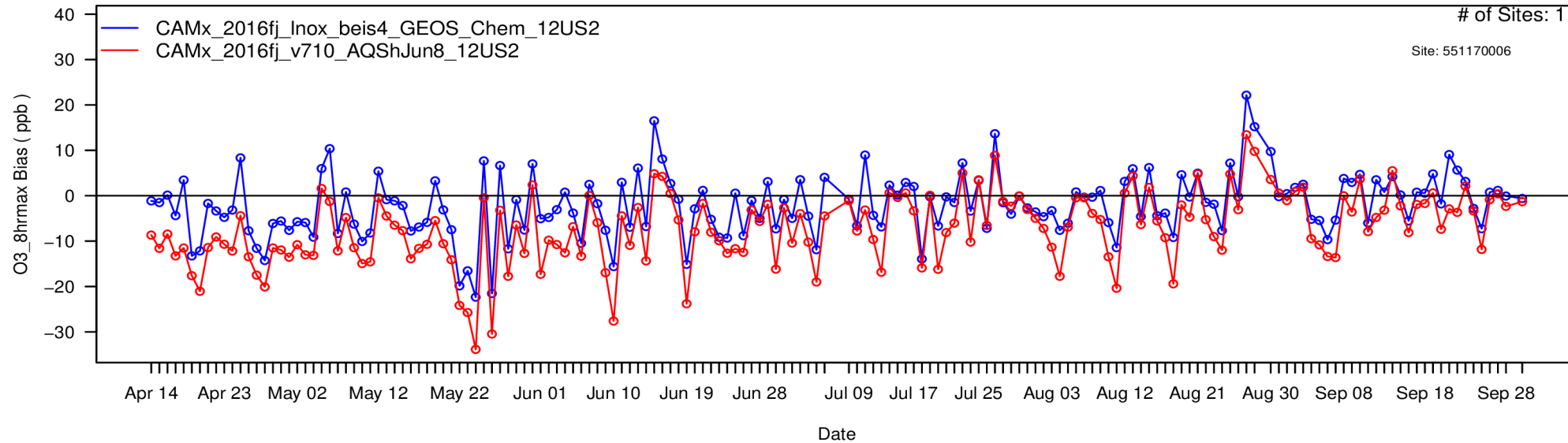


Sheboygan

CAMx_2016fj_Inox_beis4_GEOS_Chem_12US2 O3_8hrmax for AQS_Daily_O3 Site: 551170006 in WI

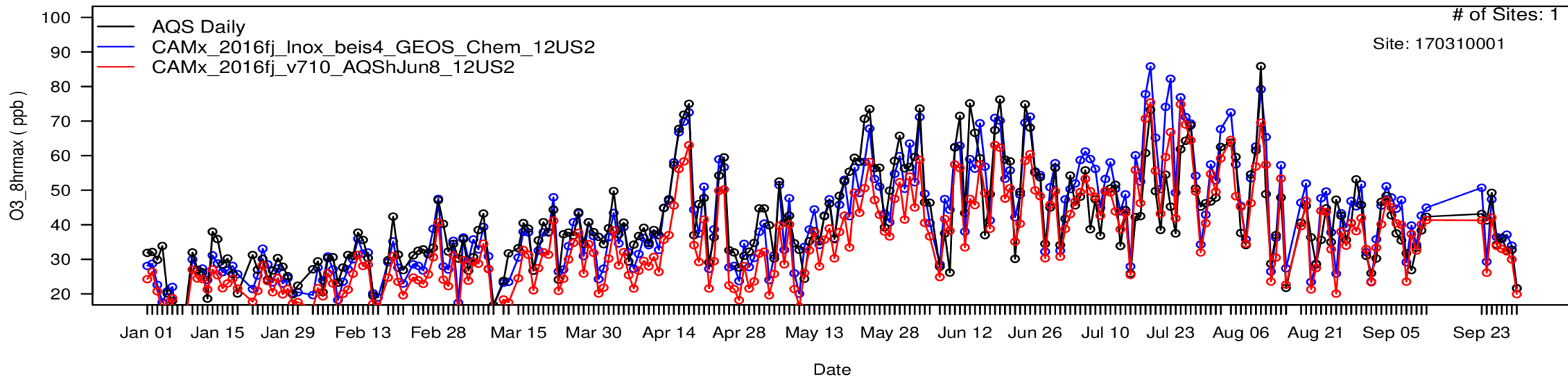


Bias for CAMx_2016fj_Inox_beis4_GEOS_Chem_12US2 O3_8hrmax for AQS_Daily_O3 for 20150501 to 20160930

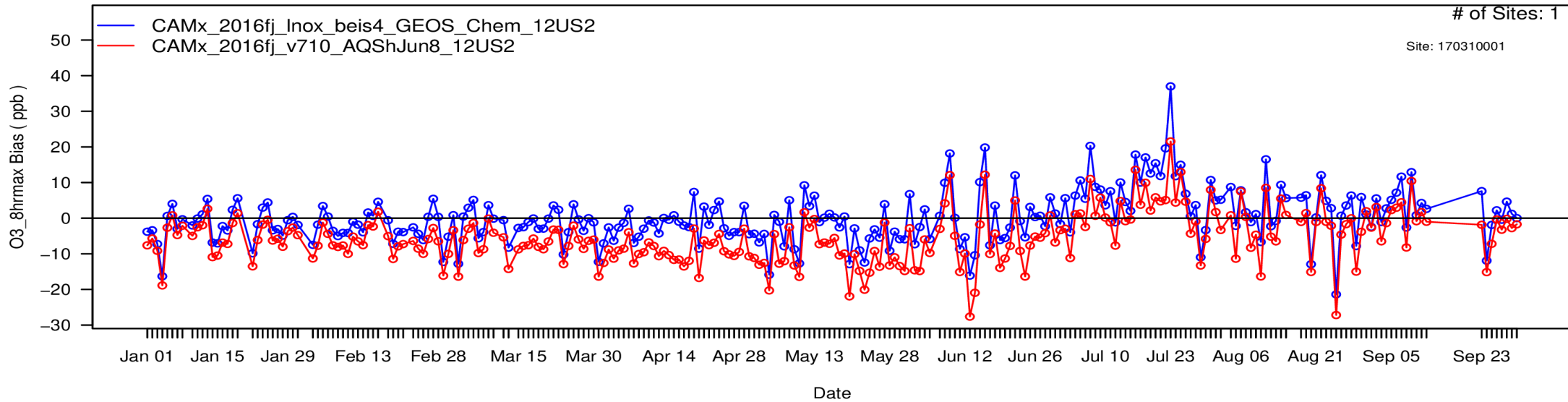


Chicago-Alsip

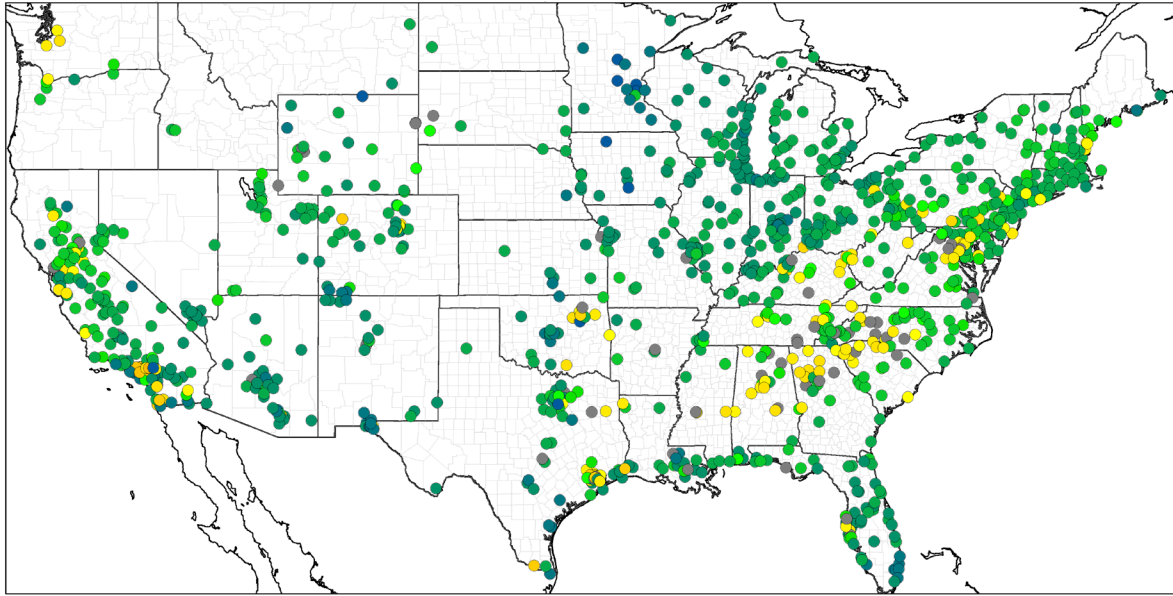
CAMx_2016fj_Inox_beis4_GEOS_Chem_12US2 O3_8hrmax for AQS_Daily_O3 Site: 170310001 in IL



Bias for CAMx_2016fj_Inox_beis4_GEOS_Chem_12US2 O3_8hrmax for AQS_Daily_O3 for 20150501 to 20160930



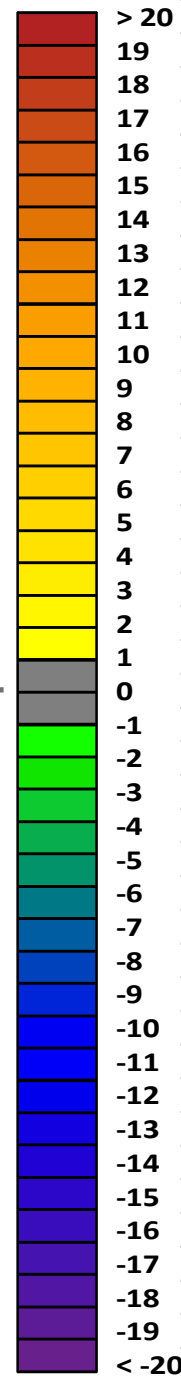
May & June



• AQS Daily

GEOSChem
Greater Bias

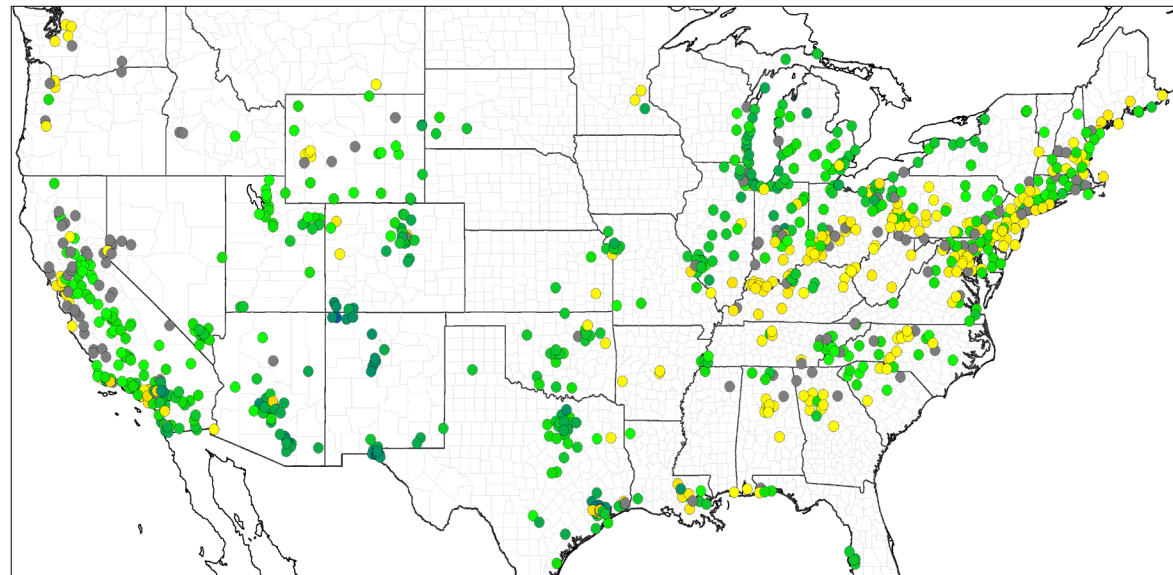
GEOSChem
Less Bias



Change in Bias for MDA8 O3 \geq 60 using GEOS-Chem IC/BCs

Using GEOS-Chem results in less bias at most monitoring sites; the exceptions are mainly at monitors in parts of the Southeast in May and June and in the Southeast, Ohio Valley, and parts of the Northeast in July thru September

July thru September



• AQS Daily

Regional Performance Statistics for Days with Obs MDA8 O3 ≥ 60 ppb

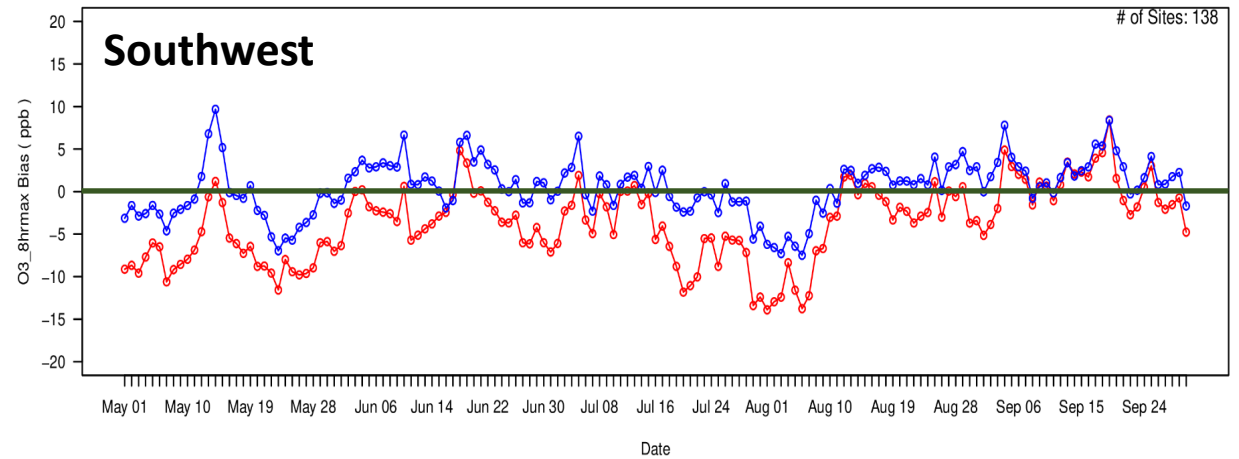
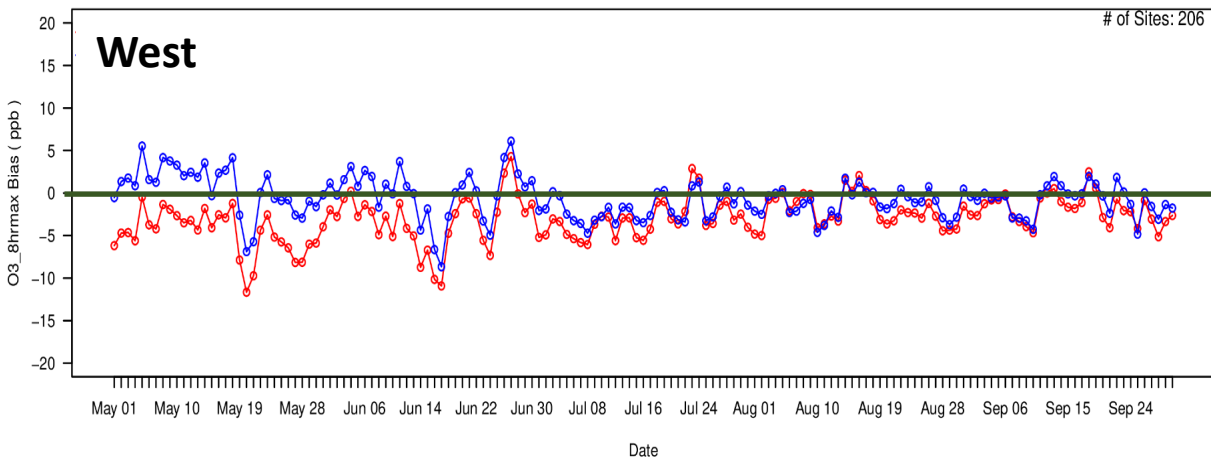
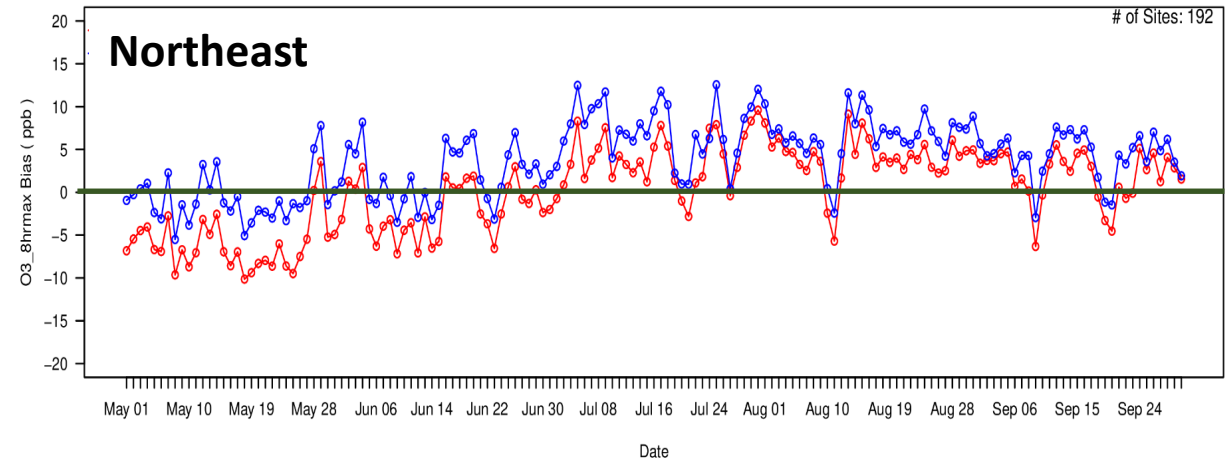
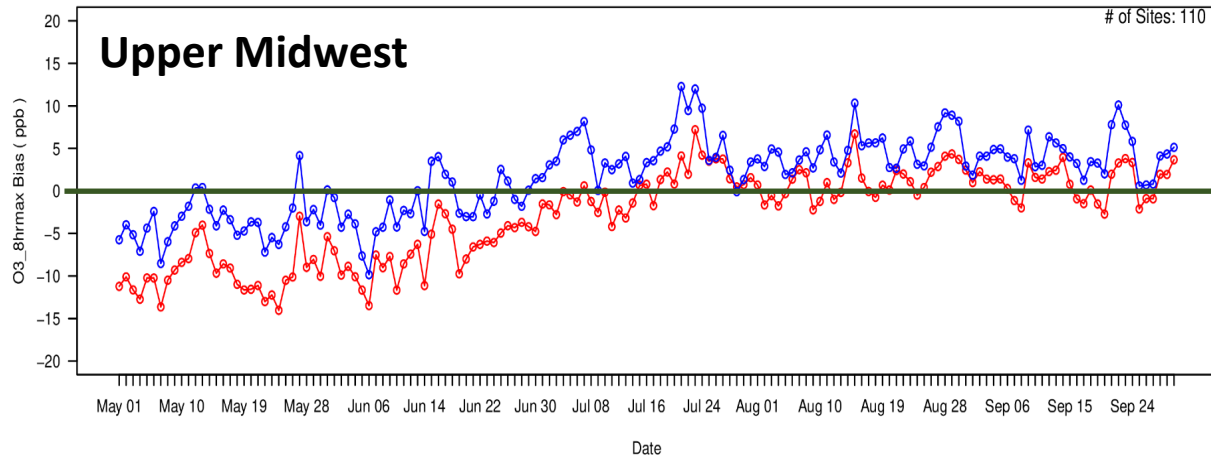
Northeast						South					
	# Sites	Mean Bias (ppb)	Mean Error (ppb)	NMB (%)	NME (%)		# Sites	Mean Bias (ppb)	Mean Error (ppb)	NMB (%)	NME (%)
2016fj	187	-4.2	7.2	-6.2	10.7	2016fj	138	-7.8	9.2	-12.0	14.1
2016fj Update	187	1.5	6.9	2.3	10.3	2016fj Update	138	-1.5	6.6	-2.3	10.1
Ohio Valley						Southwest					
	# Sites	Mean Bias (ppb)	Mean Error (ppb)	NMB (%)	NME (%)		# Sites	Mean Bias (ppb)	Mean Error (ppb)	NMB (%)	NME (%)
2016fj	229	-7.1	8.8	-10.8	13.3	2016fj	137	-8.9	9.8	-13.8	15.2
2016fj Update	229	1.1	6.3	1.6	9.5	2016fj Update	137	-4.4	6.5	-6.9	10.0
Midwest						West					
	# Sites	Mean Bias (ppb)	Mean Error (ppb)	NMB (%)	NME (%)		# Sites	Mean Bias (ppb)	Mean Error (ppb)	NMB (%)	NME (%)
2016fj	108	-12.7	13.0	-19.1	19.5	2016fj	187	-9.7	11.4	-13.8	16.2
2016fj Update	108	-4.9	6.9	-7.4	10.3	2016fj Update	187	-8.1	9.7	-11.6	13.7
Southeast						Northern Rockies					
	# Sites	Mean Bias (ppb)	Mean Error (ppb)	NMB (%)	NME (%)		# Sites	Mean Bias (ppb)	Mean Error (ppb)	NMB (%)	NME (%)
2016fj	182	-2.9	6.1	-4.5	9.4	2016fj	41	-11.9	12.4	-19.0	19.8
2016fj Update	182	2.8	6.4	4.3	9.8	2016fj Update	41	-7.6	7.9	-12.1	12.6

Regional Performance Statistics Including All Days

Northeast						South					
	# Sites	Mean Bias (ppb)	Mean Error (ppb)	NMB (%)	NME (%)		# Sites	Mean Bias (ppb)	Mean Error (ppb)	NMB (%)	NME (%)
2016fj	192	0.2	6.3	0.6	14.3	2016fj	149	0.0	6.6	0.0	16.5
2016fj_Update	192	3.8	6.9	8.7	15.7	2016fj_Update	149	4.8	7.8	12.1	19.5
Ohio Valley						Southwest					
	# Sites	Mean Bias (ppb)	Mean Error (ppb)	NMB (%)	NME (%)		# Sites	Mean Bias (ppb)	Mean Error (ppb)	NMB (%)	NME (%)
2016fj	241	0.4	6.3	1.0	14.1	2016fj	138	-3.7	6.8	-7.1	13.1
2016fj_Update	241	6.0	7.9	13.4	17.6	2016fj_Update	138	0.5	5.6	1.0	10.7
Midwest						West					
	# Sites	Mean Bias (ppb)	Mean Error (ppb)	NMB (%)	NME (%)		# Sites	Mean Bias (ppb)	Mean Error (ppb)	NMB (%)	NME (%)
2016fj	110	-2.9	6.3	-6.9	15.2	2016fj	206	-3.0	7.4	-5.9	14.5
2016fj_Update	110	1.6	5.8	3.9	14.1	2016fj_Update	206	-0.7	6.8	-1.3	13.4
Southeast						Northern Rockies					
	# Sites	Mean Bias (ppb)	Mean Error (ppb)	NMB (%)	NME (%)		# Sites	Mean Bias (ppb)	Mean Error (ppb)	NMB (%)	NME (%)
2016fj	186	1.9	6.1	4.7	14.9	2016fj	58	-3.8	6.1	-8.6	13.7
2016fj_Update	186	5.6	7.7	13.7	18.8	2016fj_Update	58	-0.8	4.9	-1.7	11.1

Appendix

Bias (ppb) in MDA8 Ozone by Day – 2016v2 vs GEOSChem + BEIS + LNOx



Avg Bias (ppb) on Days with Measured MDA8 \geq 60 ppb at 2016v2 Receptor Sites (Part 1)

				May - June Bias (ppb)			July - Sept Bias (ppb)		
Site ID	State	County	Site Name	2016fj Base Case	2016fj GEOSChem BEIS4_LNOx	Bias Diff	2016fj Base Case	2016fj GEOSChem BEIS4_LNOx	Bias Diff
40278011	AZ	Yuma	Supersite	-12.6	-7.3	-5.3	-9.3	-11.7	2.4
80350004	CO	Douglas	Chatfield	-5.7	0.1	-5.6	-7.2	-1.9	-5.4
80590006	CO	Jefferson	Rocky Flats	-6.9	-1.7	-5.2	-7.2	-2.5	-4.7
80590011	CO	Jefferson	NREL	-8.3	-3.1	-5.2	-7.7	-2.8	-4.9
80690011	CO	Larimer	Fort Collins	-10.0	-4.5	-5.5	-11.5	-7.2	-4.3
90010017	CT	Fairfield	Greenwich	1.2	-3.9	2.6	-3.8	-7.4	3.6
90013007	CT	Fairfield	Stratford	-6.1	-1.0	-5.0	-4.0	-0.2	-3.8
90019003	CT	Fairfield	Westport	-7.7	-2.3	-5.4	-3.9	-0.6	-3.3
90099002	CT	New Haven	Madison	-7.0	-2.2	-4.8	-4.5	-0.6	-3.9
170310001	IL	Cook	Alsip	-14.5	-5.5	-9.0	0.2	6.7	6.5
170310032	IL	Cook	South Water Plant	-17.7	-9.3	-8.4	-9.6	-0.7	-8.8
170310076	IL	Cook	Com Ed	-13.6	-5.1	-8.6	-2.4	5.3	2.9
170314201	IL	Cook	Northbrook	-15.2	-6.2	-9.0	-2.5	5.9	3.3
170317002	IL	Cook	Water Plant	-11.4	-2.0	-9.4	-7.7	1.0	-6.6
350130021	NM	Dona Ana	Desert View	-11.5	-6.0	-5.6	-13.4	-7.3	-6.1
350130022	NM	Dona Ana	Santa Teresa	-10.8	-5.0	-5.8	-12.1	-5.6	-6.5
420170012	PA	Bucks	Bristol	-6.4	1.7	-4.7	2.0	10.5	8.5

Avg Bias (ppb) on Days with Measured MDA8 \geq 60 ppb at 2016v2 Receptor Sites (Part 2)

				May - June Bias (ppb)			July - Sept Bias (ppb)		
Site ID	State	County	Site Name	2016fj Base Case	2016fj GEOSChem BEIS4_LNOx	Bias Diff	2016fj Base Case	2016fj GEOSChem BEIS4_LNOx	Bias Diff
480391004	TX	Brazoria	Manvel Croix Park	-6.0	0.2	-5.8	-11.3	-6.3	-5.0
481210034	TX	Denton	Denton	-7.2	0.1	-7.1	-9.4	-3.2	-6.2
481410037	TX	El Paso	UTEP	-12.7	-7.3	-5.4	-18.5	-11.8	-6.8
481671034	TX	Galveston	Galveston	-16.4	-10.3	-6.1	-16.0	-12.0	-4.0
482010024	TX	Harris	Houston Aldine	-1.5	5.1	3.6	-6.7	-0.4	-6.3
482010047	TX	Harris	Lang	2.8	9.7	6.9	-6.1	-0.3	-5.8
482010055	TX	Harris	Houston Bayland Park	-8.0	-2.3	-5.7	-1.2	3.9	2.7
482010416	TX	Harris	Park Place	-2.4	3.9	1.5	-1.6	3.6	2.0
482011034	TX	Harris	Houston East	-2.7	4.4	1.7	-16.9	-10.2	-6.7
482011035	TX	Harris	Clinton	1.3	9.0	7.7	2.6	9.0	6.4
490110004	UT	Davis	Bountiful Viewmont	-13.7	-9.3	-4.4	-8.3	-5.3	-3.0
490353006	UT	Salt Lake	Hawthorne	-18.7	-15.7	-3.0	-8.6	-6.0	-2.5
490353013	UT	Salt Lake	Herriman	-14.1	-8.9	-5.2	-9.8	-6.9	-2.8
490450004	UT	Tooele	Erda	-12.5	-7.4	-5.1	-8.9	-6.3	-2.6
490571003	UT	Weber	Harrisville	-12.8	-8.0	-4.9	-10.0	-7.3	-2.7
550590019	WI	Kenosha	Chiwaukee	-21.3	-12.5	-8.8	-11.3	-4.1	-7.3
550590025	WI	Kenosha	Kenosha - Water Tower	-15.6	-6.3	-9.3	-8.8	-0.3	-8.6
551010020	WI	Racine	Racine - Payne And Dolan	-18.5	-9.3	-9.3	-13.4	-4.8	-8.6
551170006	WI	Sheboygan	Sheboygan - Kohler Andrae	-22.9	-13.2	-9.8	-14.0	-5.5	-8.5

Appendix B

Model Performance Evaluation for 2016v3 Base Year CAMx Simulation

I. Introduction

An operational model evaluation was conducted for the 2016v3 base year CAMx v7.10 simulation performed for the 12 km U.S. modeling domain. The purpose of this evaluation is to examine the ability of the 2016 air quality modeling platform to represent the magnitude and spatial and temporal variability of measured (i.e., observed) maximum daily average (i.e., MDA8) ozone concentrations within the modeling domain. The evaluation presented here is based on model simulations using the 2016v3 emissions platform (i.e., scenario name 2016gf). As part of this evaluation, we compare model performance for the 2016v3 platform to model performance for the 2016v2 platform that used for the proposed disapproval actions.

The model evaluation for ozone focuses on comparing 8-hour daily maximum (i.e., MDA8) ozone concentrations to the corresponding observed data at monitoring sites in the EPA Air Quality System (AQS). The locations of the ozone monitoring sites in this network are shown in Figure B-1.

This evaluation includes statistical measures and graphical displays of model performance based upon model-predicted versus observed concentrations. The evaluation focusses on model predicted and observed MDA8 ozone concentrations that were paired in space and time. Model performance statistics were calculated for several spatial scales and temporal periods. Statistics were calculated for individual monitoring sites and in aggregate for monitoring sites within each of the nine climate regions of the 12 km U.S. modeling domain. The regions include the Northeast, Ohio Valley, (Upper) Midwest, Southeast, South, Southwest, Northern Rockies, Northwest and West^{1,2}, which are defined based upon the states contained within the

¹ The nine climate regions are defined by States where: Northeast includes CT, DE, ME, MA, MD, NH, NJ, NY, PA, RI, and VT; Ohio Valley includes IL, IN, KY, MO, OH, TN, and WV; Midwest includes IA, MI, MN, and WI; Southeast includes AL, FL, GA, NC, SC, and VA; South includes AR, KS, LA, MS, OK, and TX; Southwest includes AZ, CO, NM, and UT; Northern Rockies includes MT, NE, ND, SD, WY; Northwest includes ID, OR, and WA; and West includes CA and NV.

² Note most monitoring sites in the West region are located in California (see Figures B-1 and B-2), therefore the statistics for the West region will be mostly representative of model performance in California ozone.

National Oceanic and Atmospheric Administration (NOAA) climate regions (Figure B-2)³ as defined in Karl and Koss (1984).

II. Methodology

Model performance statistics were created for the period May through September (i.e., seasonal) and for individual months during this time period. Statistics were created using data on all days with valid observed data during this period as well as for the subset of days with observed MDA8 concentrations ≥ 60 ppb.⁴ The aggregate statistics by climate region and for the monitor plus modeled 2023 receptors are presented in this appendix. Model performance statistics for MDA8 ozone at individual monitoring sites nationwide based on days with observed values ≥ 60 ppb can be found in the docket in the file named “2016v3 CAMx Ozone Model Performance Statistics by Site”.

In addition to the above performance statistics, we prepared several graphical presentations of model performance for MDA8 ozone. These graphical presentations include:

- (1) maps that show the mean bias and error as well as normalized mean bias and error calculated for MDA8 ≥ 60 ppb for May through September at individual monitoring sites;
- (2) maps that show the change in bias and error in the 2016v3 modeling compared to the 2016v2 modeling;
- (2) bar and whisker plots that show the distribution of the predicted and observed MDA8 ozone concentrations by month (May through September) and by region; and
- (3) time series plots (May through September) of observed and predicted MDA8 ozone concentrations for each region and for a selected set of monitoring sites that are projected to be nonattainment or maintenance-only receptors in 2023.

The Atmospheric Model Evaluation Tool (AMET) was used to calculate the model performance statistics used in this document (Gilliam et al., 2005). For this evaluation we have selected the mean bias, mean error, normalized mean bias, and normalized mean error to

³ NOAA, National Centers for Environmental Information scientists have identified nine climatically consistent regions within the contiguous U.S., <http://www.ncdc.noaa.gov/monitoring-references/maps/us-climate-regions.php>.

⁴ We limited the data to those observed and predicted pairs with observations that are ≥ 60 ppb in order to focus on concentrations at the upper portion of the distribution of values.

characterize model performance, statistics which are consistent with the recommendations in Simon et al. (2012) and EPA's photochemical modeling guidance (U.S. EPA, 2018).

Mean bias (MB) is the average of the difference (predicted – observed) divided by the total number of replicates (n). Mean bias is given in units of ppb and is defined as:

$$MB = \frac{1}{n} \sum_1^n (P - O) , \text{ where } P = \text{predicted and } O = \text{observed concentrations}$$

Mean error (ME) calculates the absolute value of the difference (predicted - observed) divided by the total number of replicates (n). Mean error is given in units of ppb and is defined as:

$$ME = \frac{1}{n} \sum_1^n |P - O|$$

Normalized mean bias (NMB) is the average the difference (predicted - observed) over the sum of observed values. NMB is a useful model performance indicator because it avoids over inflating the observed range of values, especially at low concentrations. Normalized mean bias is given in percentage units and is defined as:

$$NMB = \frac{\sum_1^n (P-O)}{\sum_1^n (O)} * 100$$

Normalized mean error (NME) is the absolute value of the difference (predicted - observed) over the sum of observed values. Normalized mean error is given in percentage units and is defined as:

$$NME = \frac{\sum_1^n |P-O|}{\sum_1^n (O)} * 100$$

III. Overview of Findings

As described in more detail below, the model performance statistics indicate that the MDA8 ozone concentrations predicted by the 2016v2 CAMx modeling platform closely reflect the corresponding MDA8 observed ozone concentrations in each region of the 12 km U.S. modeling domain. The acceptability of model performance was judged by considering the 2016v2 CAMx performance results in light of the range of performance found in recent regional ozone model applications (Emery et al., 2017; NRC, 2002; Phillips et al., 2007; Simon et al.,

2012; U.S. EPA, 2005; U.S. EPA, 2009; U.S. EPA, 2010).⁵ These other modeling studies represent a wide range of modeling analyses that cover various models, model configurations, domains, years and/or episodes, chemical mechanisms, and aerosol modules. In particular, Emery et.al. extend the results of Simon et.al., to include performance results from a few more recent photochemical model applications. The results in the former paper indicate that about a third of the top performing past applications have normalized mean bias and a normalized mean error statistics for MDA8 ozone of less than ± 5 percent and less 15 percent, respectively. In addition, two-thirds of past applications have normalized mean bias less than ± 15 percent and normalized mean error less than 25 percent. These “benchmarks” are not intended to represent “rigid pass/fail tests” but rather as “simple references to the range of recent historical performance” that can be used to understand where the performance results of a particular application “fall in the spectrum of past published results.”

Overall, the ozone model performance results for the 2016v2 CAMx simulation are in large part within the range found in other recent peer-reviewed and regulatory applications. The model performance results, as described in this document, demonstrate that the predictions from the 2016v2 modeling platform correspond closely to observed concentrations in terms of the magnitude, temporal fluctuations, and geographic differences for MDA8 ozone concentrations.

⁵ Christopher Emery, Zhen Liu, Armistead G. Russell, M. Talat Odman, Greg Yarwood & Naresh Kumar (2017) Recommendations on statistics and benchmarks to assess photochemical model performance, *Journal of the Air & Waste Management Association*, 67:5, 582-598, DOI: 10.1080/10962247.2016.1265027
National Research Council (NRC), 2002. Estimating the Public Health Benefits of Proposed Air Pollution Regulations, Washington, DC: National Academies Press.
U.S. Environmental Protection Agency; Technical Support Document for the Final Clean Air Interstate Rule: Air Quality Modeling; Office of Air Quality Planning and Standards; RTP, NC; March 2005 (CAIR Docket OAR-2005-0053-2149).
U.S. Environmental Protection Agency, Proposal to Designate an Emissions Control Area for Nitrogen Oxides, Sulfur Oxides, and Particulate Matter: Technical Support Document. EPA-420-R-007, 329pp., 2009. (<http://www.epa.gov/otaq/regs/nonroad/marine/ci/420r09007.pdf>)
Phillips, S., K. Wang, C. Jang, N. Possiel, M. Strum, T. Fox, 2007. Evaluation of 2002 Multi-pollutant Platform: Air Toxics, Ozone, and Particulate Matter, 7th Annual CMAS Conference, Chapel Hill, NC, October 6-8, 2008. (<http://www.cmascenter.org/conference/2008/agenda.cfm>).
U.S. Environmental Protection Agency, 2010, Renewable Fuel Standard Program (RFS2) Regulatory Impact Analysis. EPA-420-R-10-006. February 2010. Sections 3.4.2.1.2 and 3.4.3.3. Docket EPA-HQ-OAR-2009-0472-11332. (<http://www.epa.gov/oms/renewablefuels/420r10006.pdf>)
Simon, H., Baker, K.R., and Phillips, S. (2012) Compilation and interpretation of photochemical model performance statistics published between 2006 and 2012. *Atmospheric Environment* **61**, 124-139.

IV. Analysis of Model Performance Statistics and Graphics

The MDA8 ozone model performance bias and error statistics for the period May-September for each climate region are provided in Table B-1. The statistics shown in this table were calculated using all data pairs for May-September. Seasonal statistics for each region based on the subset of days with observed MDA8 ozone ≥ 60 ppb are presented in Table B-2. Seasonal statistics at each receptor on days with observed MDA8 ozone ≥ 60 ppb are presented in Table B-3 for the 2016v3 and 2016v2 modeling.

Spatial plots of the mean bias and error as well as the normalized mean bias and error at individual monitors nationwide are shown in Figures B-3 through B-8. Time series plots of observed and predicted MDA8 ozone during the period May through September for each region and for selected 2023 nonattainment and/or maintenance sites in 2023 are provided in Figures B-9 and B-10, respectively.

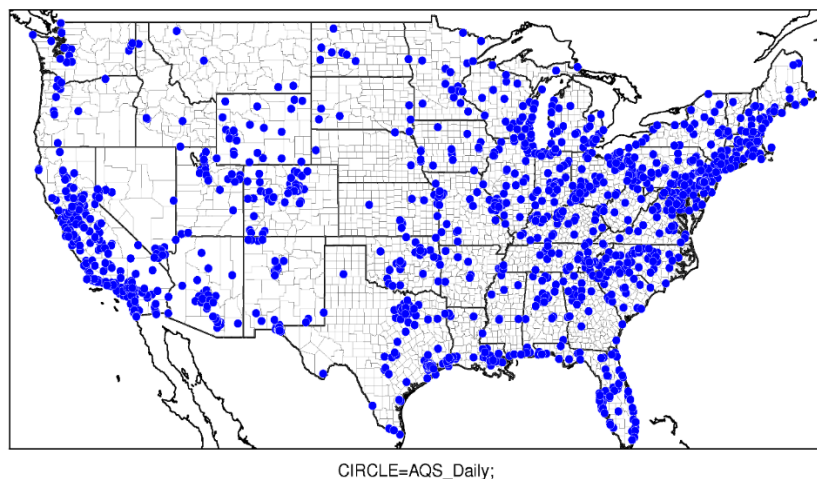


Figure B-1. Location of ozone monitoring sites.

U.S. Climate Regions

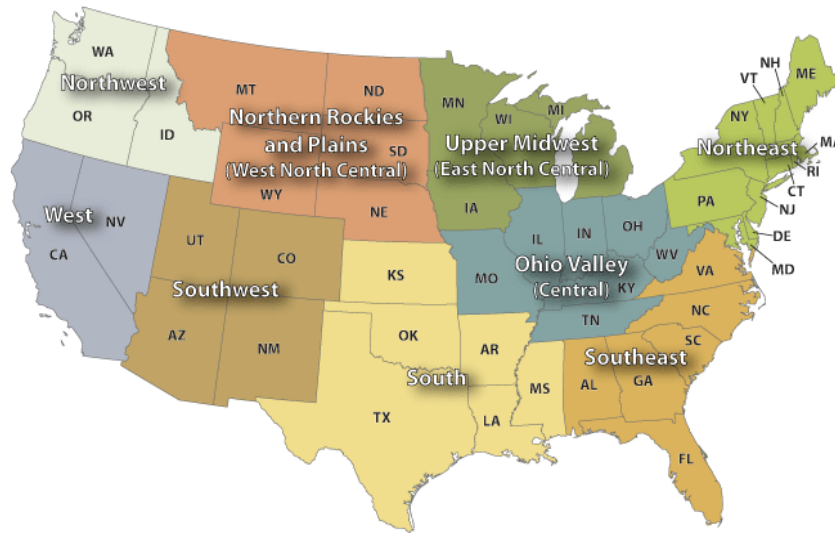


Figure B-2. NOAA climate regions (source: <http://www.ncdc.noaa.gov/monitoring-references/maps/us-climate-regions.php#references>)

A. Seasonal and Monthly Performance

1. Model Performance Statistics by Region

The model performance statistics provided in Table B-1 show that regional mean tends to overpredict in most regions on average for all days during the period May through September in each region. Normalized mean bias is less than ± 5 percent in the Midwest, Southwest, Northern Rockies, Northwest, and West. In the other four regions, normalized mean bias is between 5 and 15 percent. Normalized mean error is less than 15 percent in the Midwest, Southwest, Northern Rockies, and West and between 15 and 20 percent in the other regions.

The model performance statistics for days with observed MDA8 ozone ≥ 60 ppb provided in Table B-2 indicates that, on average, the model is relatively unbiased in all regions. The seasonal mean bias for MDA8 ozone ≥ 60 ppb is within ± 5 ppb in six of the regions and within ± 10 ppb in the other three regions. The mean error is less than 10 ppb in all regions. Normalized mean bias is within 10 percent for all regions, except for the West where the normalized mean bias is -11.5 percent. The normalized mean error is less than 15 percent in each region.

The model performance statistic for individual receptors in Table B-3 indicates improved performance in the 2016v3 modeling compared to the 2016v2 modeling. The 2016v3 modeling has significantly less bias and error on days with observed MDA8 ozone ≥ 60 compared to the

2016v2 modeling at all receptors, except for the Greenwich and Houston/Clinton. The normalized mean bias and normalized mean error statistics are within the performance benchmarks identified above.

2. Spatial Variability in Model Performance

Figures B-3 through B-6 show the spatial variability in bias and error for MDA8 ozone on days with observed concentrations ≥ 60 ppb. Mean bias, as seen in Figure B-3, is within ± 5 ppb at many sites nationwide. The 2016v3 modeling tends to overpredict MDA8 concentrations on days ≥ 60 ppb in parts of the Southeast, Ohio Valley, and mid-Atlantic states. Biases within the range of ± 5 ppb or between -5 and -10 ppb are noted at monitoring sites elsewhere across the U.S. Figure B-4 provides a comparison of the mean bias in the 2016v3 modeling to the mean bias in the 2016v2 modeling. The figure indicates that model performance for days ≥ 60 ppb is improved at most monitoring sites nationwide, the exceptions are some of the monitoring sites in the Southeast and mid-Atlantic states. As is evident from Figure B-5, the mean error is mainly less than 10 ppb nationwide. The comparison of mean error between the 2016v3 modeling and the 2016v2 modeling, as shown in Figure B-6, shows improved performance in terms of model error with the 2016v3 modeling.

The normalized mean error on days > 60 ppb, as shown in Figure B-7, indicates that model performance using this statistic is within the range of the performance benchmark offered by Emery et al (i.e., ± 15 %) at nearly all monitoring sites. The normalized mean bias and mean bias statistics suggest a tendency for some over prediction by the model in portions of the South, Southeast, and Northeast regions. As indicated in Figure B-8, normalized mean error is less than the 25 percent benchmark at nearly all monitoring sites nationwide.

B. Observed and Predicted Temporal Patterns

In addition to the above analysis of overall model performance, we also examine how well the 2016v3 modeling platform replicates day to day fluctuations in observed MDA8 ozone concentrations for the period May through September in each region and for selected 2023 nonattainment and/or maintenance receptors.

Time series of regional average MDA8 ozone concentrations for the Northeast, Midwest, Ohio Valley, South, Southeast, Southwest, and West regions are provided in Figure B-9. The plots show that the modeled concentrations closely track the corresponding observed values in terms of day-to-day fluctuations and the general magnitude of concentrations. Comparing the

plots for these seven regions reveals that there are large differences in the day-to-day variability among the regions in both observations and predictions. For example, the degree of temporal variability in MDA8 ozone concentrations in the Northeast, Midwest, and Ohio Valley is much greater than in the Southwest and West. As is evident from Figure B-9, the modeling platform captures regional differences in the degree of temporal variability in MDA8 ozone concentrations. The model performs equally as well in eastern and western regions in terms of replicating the relative magnitude of concentrations and day-to-day variability that are characteristic of observed MDA8 ozone concentrations in each region.

The time series for selected receptors indicate that, again, the modeling platform generally replicates the day-to-day variability in ozone during this time period at these sites.⁶ That is, days with high modeled concentrations are generally also days with high measured concentrations and, conversely, days with low modeled concentrations are also days with low measured concentrations in most cases. Although there is a tendency for over prediction, particularly on days with low measured ozone concentrations, the model predictions, as illustrated by these receptors, captures the day-to-day variability in the observations, and also generally the timing and relative magnitude of multi-day high ozone episodes. In this regard, the model captures the geographic differences in the timing, duration, and general magnitude of ozone episodes in different parts of the U.S.

At the Stratford and Madison receptors in Coastal Connecticut, the model closely replicates both the day-to-day variability and magnitude of the observed MDA8 ozone concentrations on most days. At the Chicago-Northbrook and Chicago-Evanston receptors, the model closely tracks the day-to-day variability during the entire 5-month period. At both receptors, the modeled concentrations are similar to the corresponding measured. At the Kenosha-Chiwaukee and Sheboygan monitors the model captures the high ozone episodes, but under predicts peak MDA8 ozone concentrations of several of the days with the highest concentrations, particularly at the Sheboygan receptor. At the Dallas/Denton, Houston, and Brazoria receptors the temporal pattern in the observed values appears to be rather “chaotic”, compared to the temporal pattern at other receptors in the eastern U.S. The model predictions have a temporal pattern that is similar to the observed concentrations, but with a tendency for

⁶ The extent to which the day-to-day variability in model-predicted MDA8 ozone matches the corresponding observations values at the receptors selected for Figure B-9 is generally representative of most other receptors within the same areas.

overprediction. In contrast to receptors in the East, the observed concentrations at receptors in the West have much less temporal variability. This difference between the observed concentrations in the East versus the West is well simulated by the model. Although the model appears to capture most of the days with high ozone at the receptors in Denver, there is a tendency for the model to under predict on the peak days at receptors in Salt Lake City.

C. Conclusions

In summary, the ozone model performance statistics for the CAMx 2016v3 (2016gf) simulation are within or close to the ranges found in other recent peer-reviewed applications (e.g., Simon et al, 2012 and Emory et al, 2017). As described in this appendix, the predictions from the 2016v3 modeling platform generally correspond closely to observed concentrations in terms of the magnitude, temporal fluctuations, and geographic differences for MDA8 ozone concentrations. Thus, the model performance results demonstrate the scientific credibility of our 2016v3 modeling platform. These results provide confidence in the ability of the modeling platform to provide a reasonable projection of expected future year ozone concentrations and contributions.

Table B-1. Performance statistics for MDA8 ozone by Region for the period May through September (all days) based on 2016v3 modeling.

Climate Region	Number of Site-Days	MB (ppb)	ME (ppb)	NMB (%)	NME (%)
Northeast	27,724	4.0	7.0	9.0	15.9
Ohio Valley	33,762	6.4	8.2	14.3	18.4
Midwest	16,279	1.9	6.0	4.5	14.6
Southeast	26,490	6.1	8.1	15.0	19.7
South	21,437	5.5	8.2	13.8	20.5
Southwest	19,926	2.0	5.9	3.8	11.4
Northern Rockies	8,471	-0.3	5.0	-0.6	11.3
Northwest	4,012	1.1	5.9	3.0	15.9
West	29,930	-0.5	6.9	-0.9	13.5

Table B-2. Performance statistics for MDA8 ozone ≥ 60 ppb by Region for the period May through September based on 2016v3 modeling.

Climate Region	Number of Site-Days	MB (ppb)	ME (ppb)	NMB (%)	NME (%)
Northeast	2,997	1.7	7.0	2.5	10.4
Ohio Valley	3,211	1.5	6.4	2.3	9.8
Midwest	1,134	-4.6	6.8	-7.0	10.2
Southeast	1,447	3.3	6.6	5.1	10.2
South	993	-0.9	6.6	-1.3	10.1
Southwest	3,359	-3.2	5.9	-4.9	9.1
Northern Rockies	215	-6.0	7.1	-9.6	11.3
Northwest	84	-6.7	9.7	-10.3	14.9
West	8,279	-8.1	9.6	-11.5	13.6

Table B-3. Performance statistics for MDA8 ozone ≥ 60 ppb for monitor plus modeled receptors for the period May through September for the 2016v2 and 2016v3 modeling.

Site ID	State	Receptor	Mean Bias		Mean Error		Normalized Mean Bias		Normalized Mean Error	
			2016 v2	2016 v3	2016 v2	2016 v3	2016 v2	2016 v3	2016 v2	2016 v3
40278011	AZ	Yuma Supersite	-12	-8	13	9	-19	-11	20	13
80350004	CO	Denver Chatfield	-7	0	8	5	-10	0	12	7
80590006	CO	Denver Rocky Flats	-7	-1	8	5	-11	-2	12	8
80590011	CO	Denver NREL	-8	-2	9	5	-12	-3	13	8
80690011	CO	Fort Collins	-11	-5	11	6	-17	-8	17	9
90010017	CT	Greenwich	-3	-7	9	9	-4	-11	12	12
90013007	CT	Stratford	-5	-1	9	9	-6	-1	12	12
90019003	CT	Westport	-5	-1	9	8	-7	-2	12	11
90099002	CT	Madison	-5	-1	7	6	-8	-2	10	9
170310001	IL	Chicago Alsip	-8	0	11	7	-12	0	16	11
170314201	IL	Chicago Northbrook	-12	-3	13	7	-17	-4	18	11
170317002	IL	Chicago Water Plant	-10	-1	10	7	-15	-1	15	10
350130021	NM	Las Cruces Desert View	-12	-5	13	7	-19	-8	20	11
350130022	NM	Las Cruces Santa Teresa	-11	-4	12	6	-18	-6	19	10
350151005	NM	Carlsbad	-12	-5	13	7	-19	-8	20	11
350250008	NM	Hobbs	-13	-7	13	7	-21	-11	21	11
480391004	TX	Brazoria	-8	-3	9	5	-13	-4	13	8

Site ID	State	Receptor	Mean Bias		Mean Error		Normalized Mean Bias		Normalized Mean Error	
			2016 v2	2016 v3	2016 v2	2016 v3	2016 v2	2016 v3	2016 v2	2016 v3
481210034	TX	Denton	-8	-1	9	5	-12	-1	13	7
481410037	TX	El Paso UTEP	-15	-8	16	9	-23	-11	24	14
481671034	TX	Galveston	-16	-10	16	11	-24	-15	24	17
482010024	TX	Houston Aldine	-4	3	9	10	-7	4	13	15
482010055	TX	Houston Bayland Park	-6	0	7	5	-9	0	11	8
482011034	TX	Houston East	-7	1	10	7	-10	1	16	11
482011035	TX	Houston Clinton	2	9	6	9	3	15	10	15
490110004	UT	SLC Bountiful Viewmont	-10	-5	10	6	-15	-8	15	10
490353006	UT	SLC Hawthorne	-10	-5	11	8	-14	-8	16	11
490353013	UT	SLC Herriman	-11	-6	11	7	-17	-9	17	11
550590019	WI	Kenosha Chiwaukee	-17	-9	18	12	-24	-13	25	17
551010020	WI	Racine	-16	-8	17	11	-23	-11	24	15
551170006	WI	Sheboygan Kohler Andre	-18	-8	18	10	-25	-12	25	13

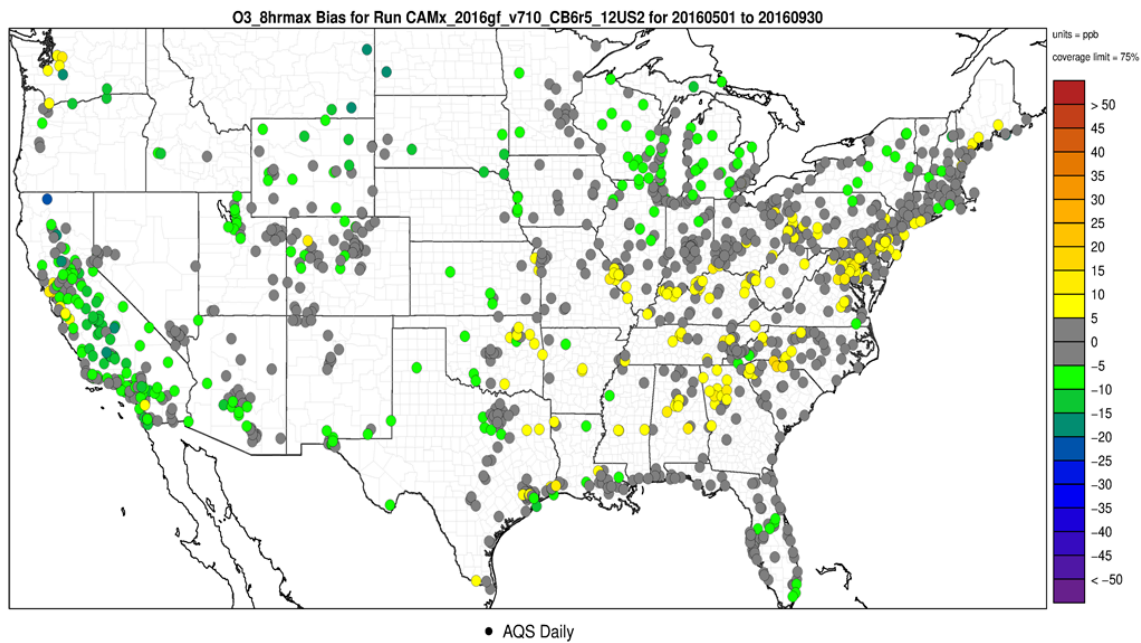


Figure B-3. Mean Bias (ppb) of MDA8 ozone for days with observed values ≥ 60 ppb over the period May-September.

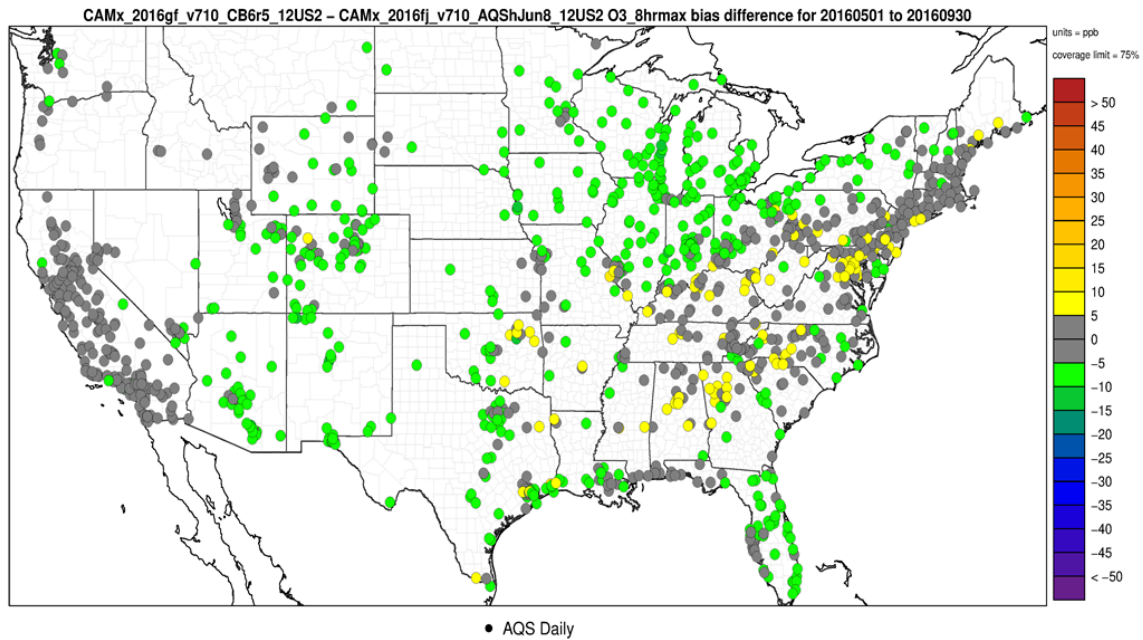


Figure B-4. Difference in Mean Bias (ppb) (2016v3 Bias – 2016v2 Bias) of MDA8 ozone for days with observed values ≥ 60 ppb over the period May-September.

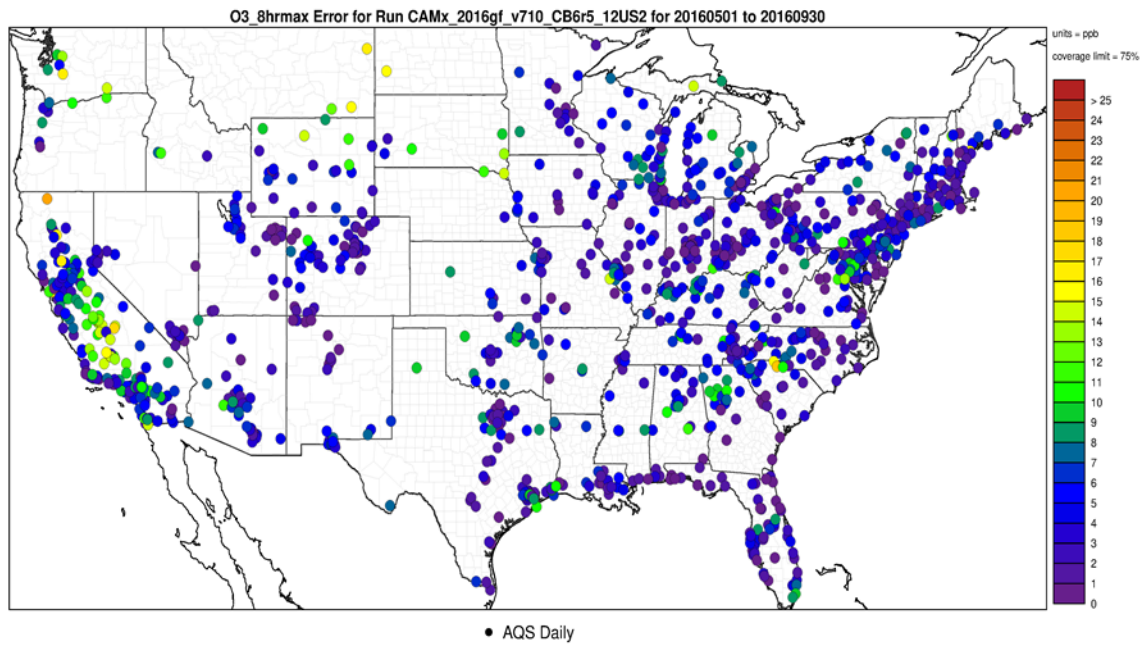


Figure B-5. Mean Error (ppb) of MDA8 ozone ≥ 60 ppb over the period May-September 2016, paired in time and space.

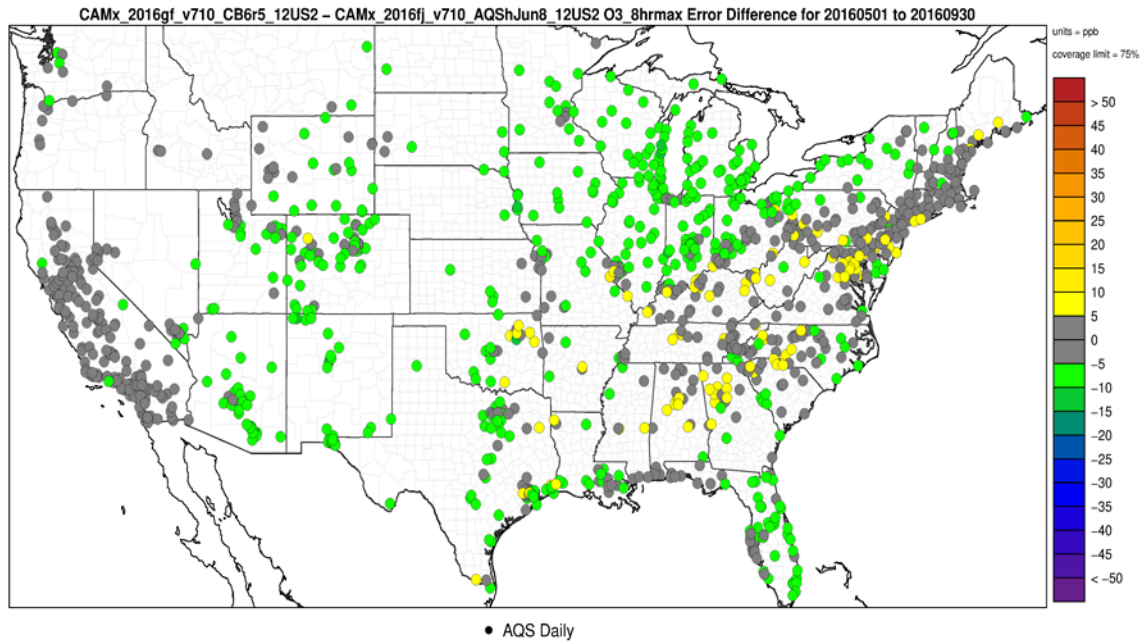


Figure B-6. Difference in Mean Error (2016v3 Error – 2016v2 Error) of MDA8 ozone (ppb) for days with observed values ≥ 60 ppb over the period May-September.

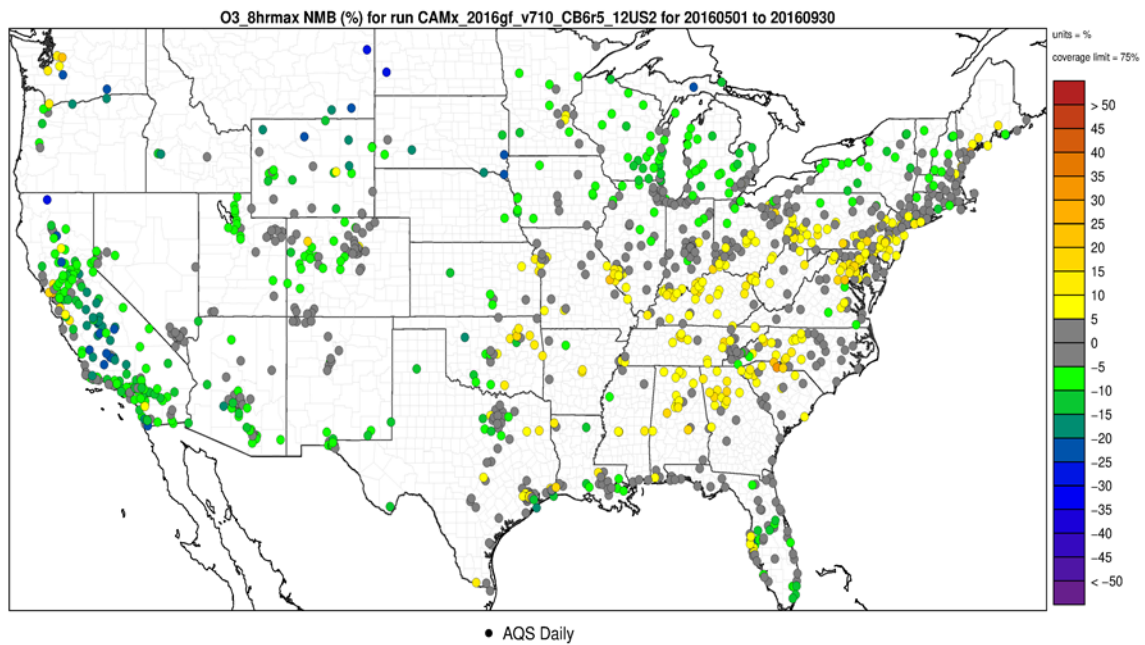


Figure B-7. Normalized Mean Bias (ppb) of MDA8 ozone for days with observed ozone ≥ 60 ppb over the period May-September.

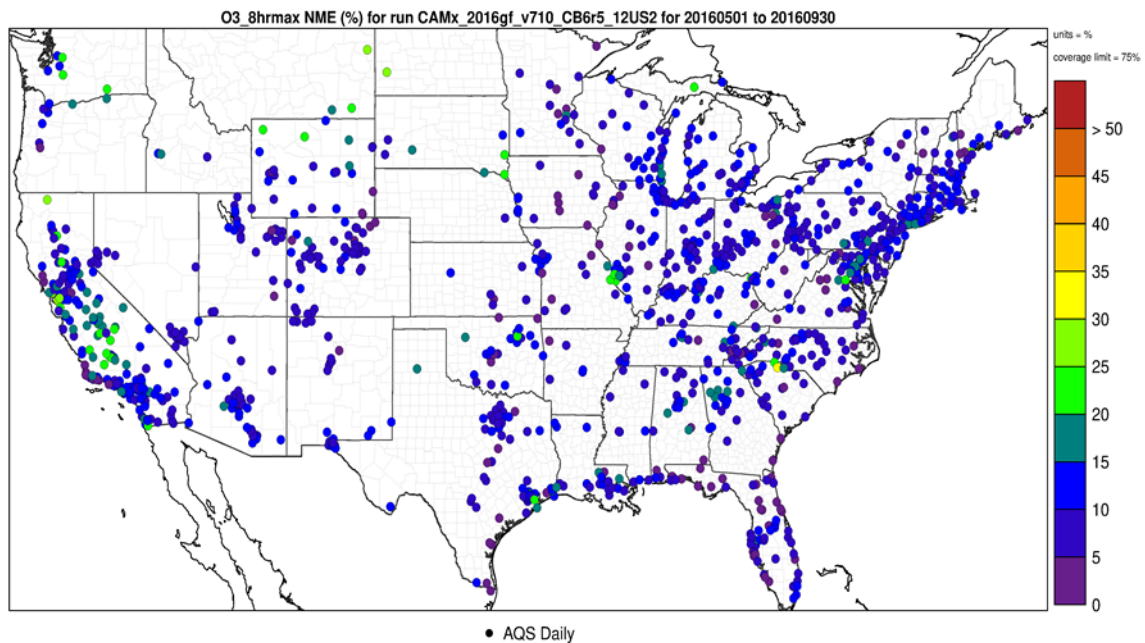


Figure B-8. Normalized Mean Error (ppb) of MDA8 ozone for days with observed ozone ≥ 60 ppb over the period May-September.

Figure B-9. Time series of observed and predicted regional average MDA8 ozone concentrations for the period May through September 2016.

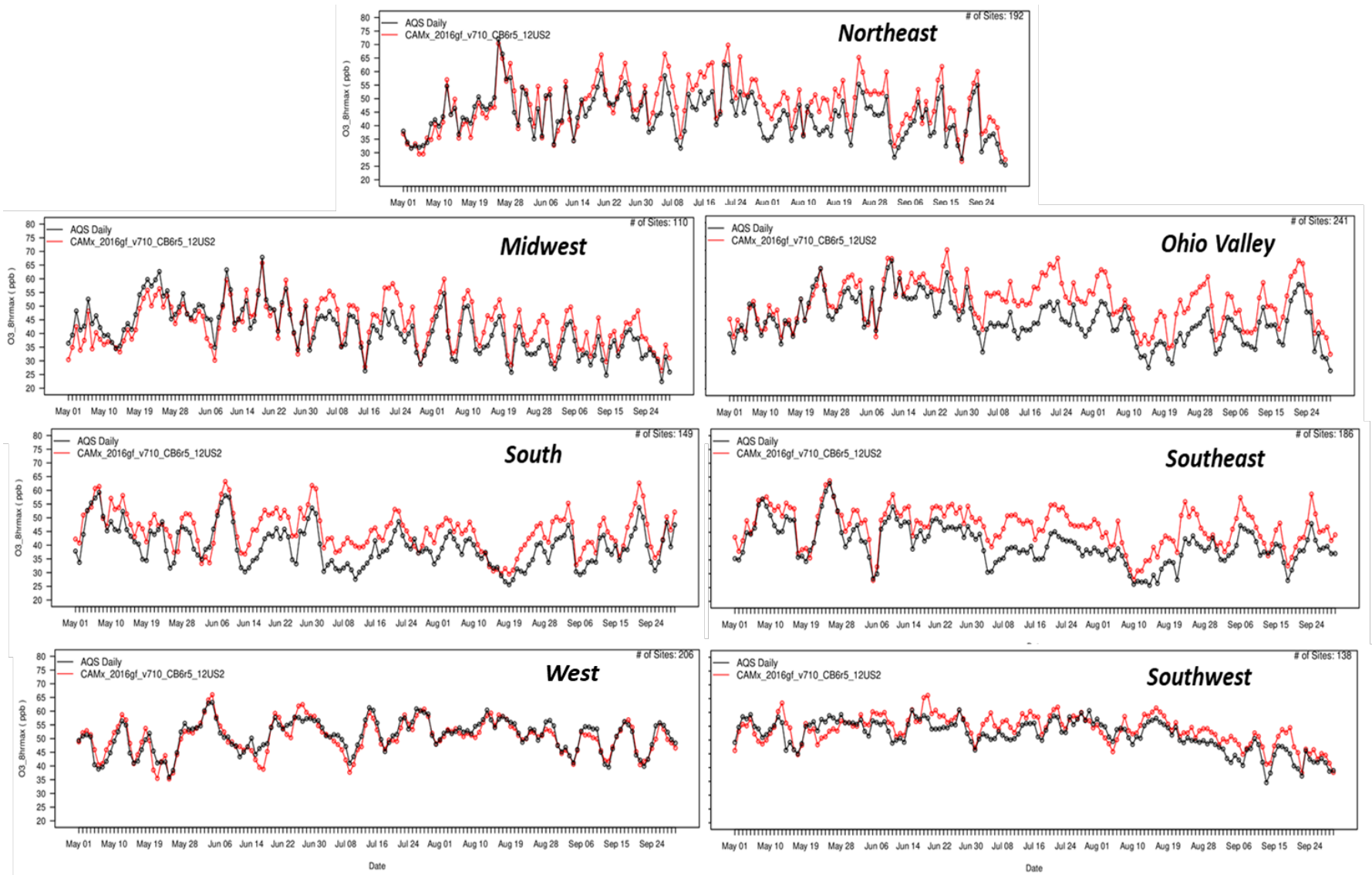
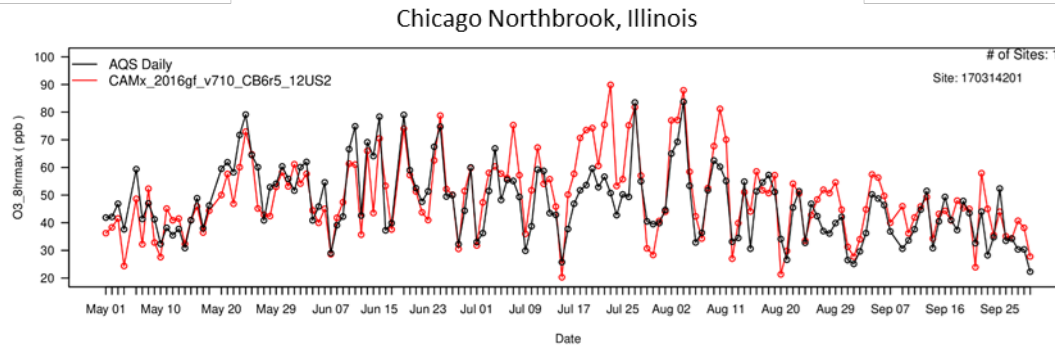
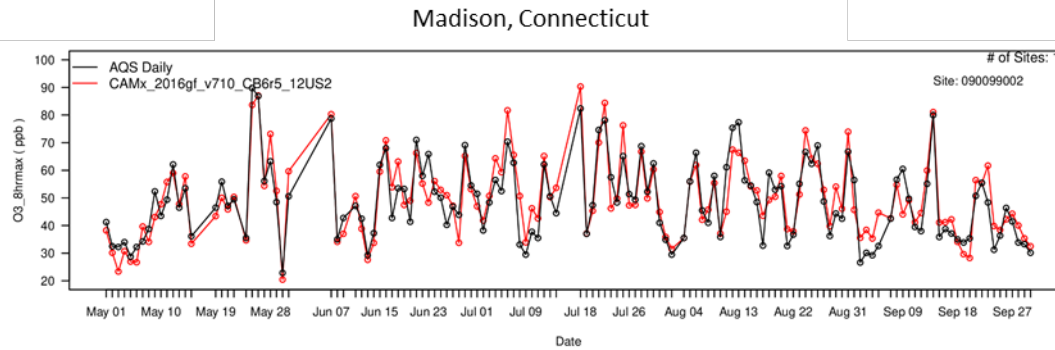
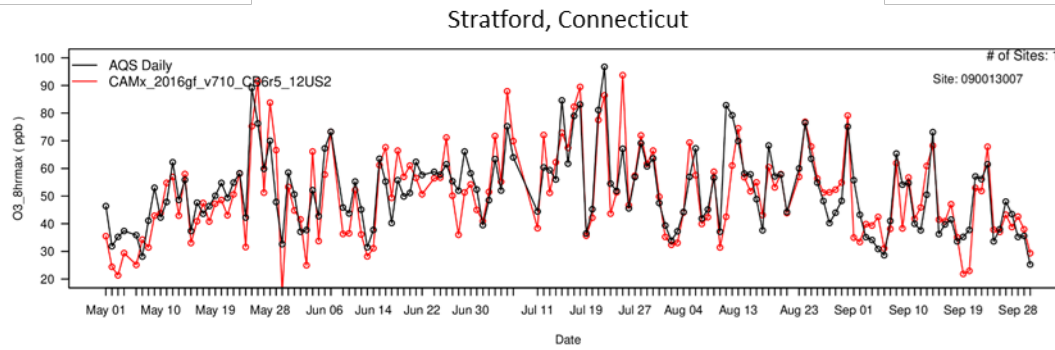
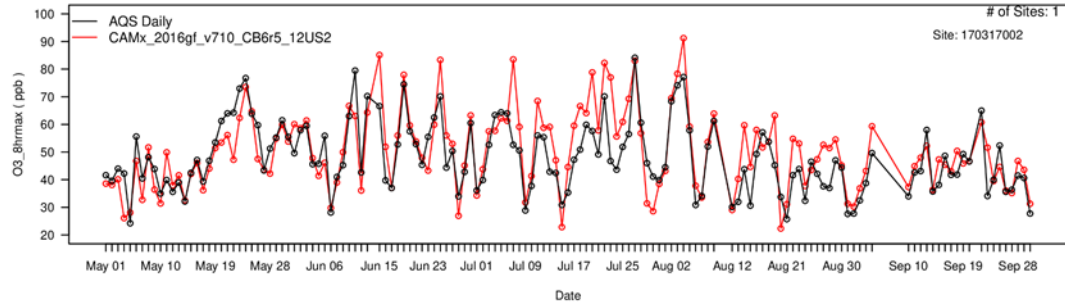


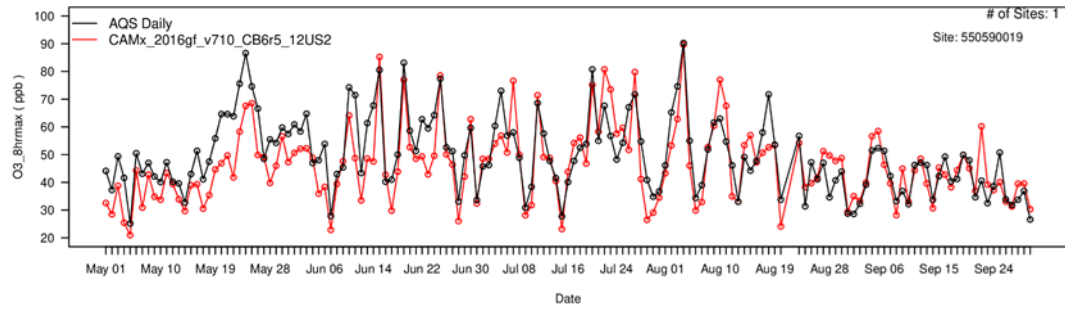
Figure B-10. Observed and model predicted MDA8 ozone concentrations by day for the period May 1 through September at selected nonattainment/maintenance receptors in 2023 (ppb).



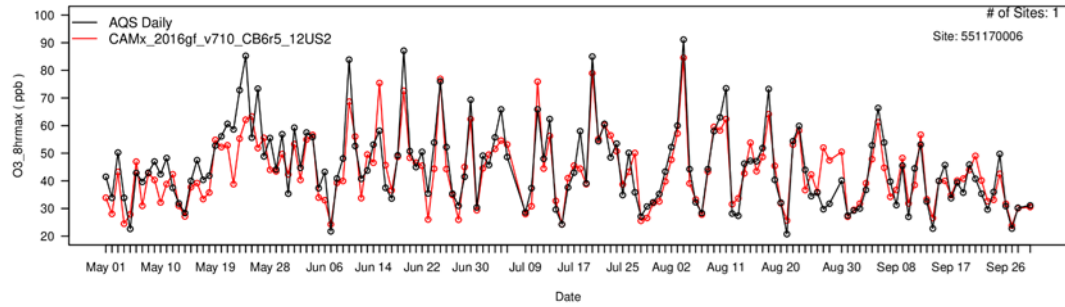
Chicago Evanston, Illinois



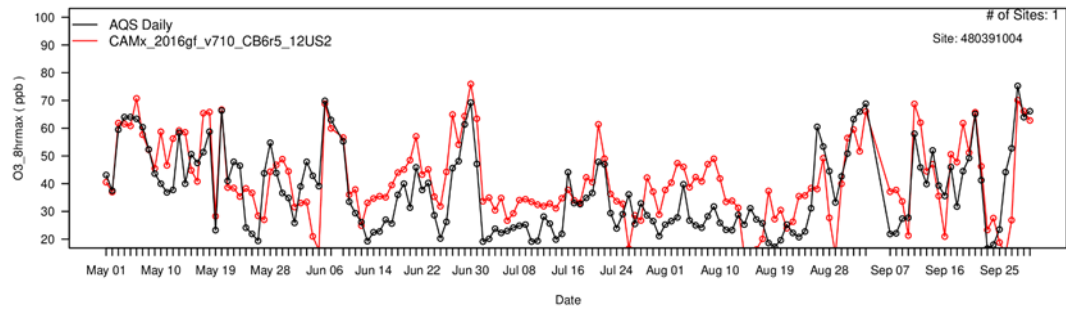
Kenosha Chiwaukee Prairie, Wisconsin



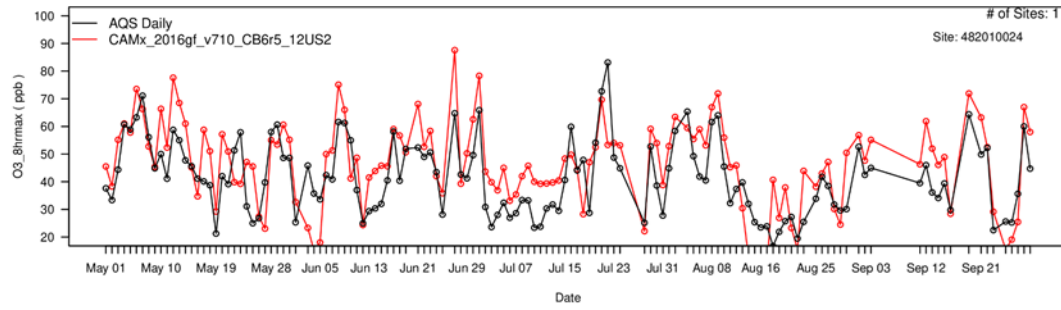
Sheboygan, Wisconsin



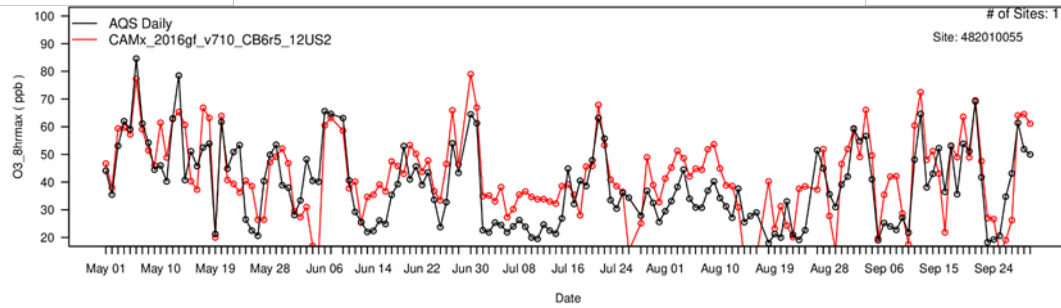
Dallas Denton Airport, Texas



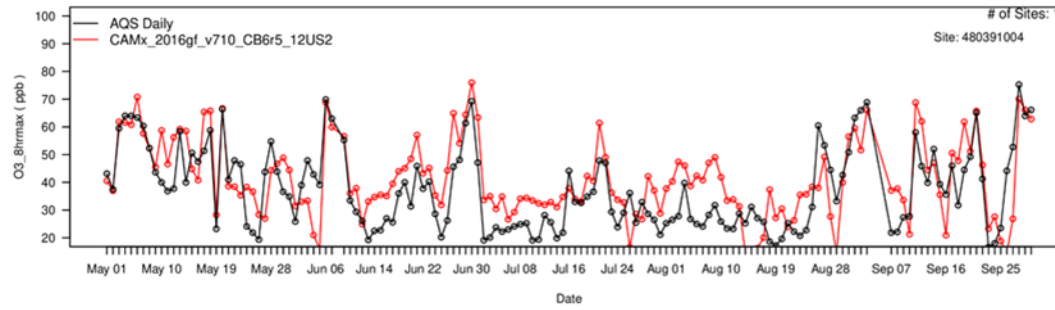
Houston Aldine, Texas



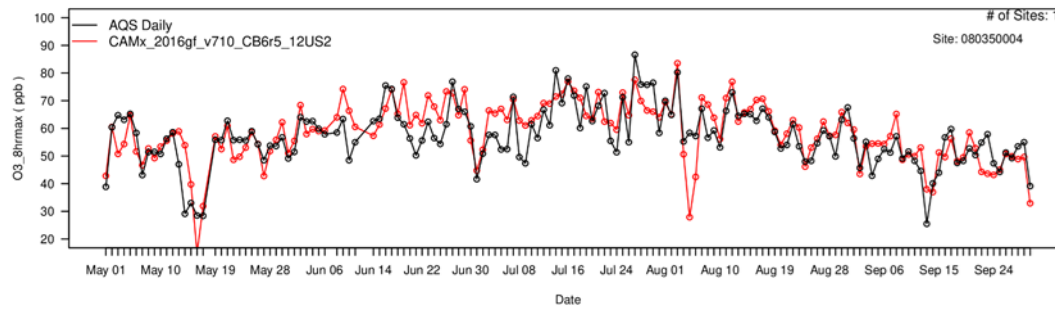
Houston Bayland Park, Texas



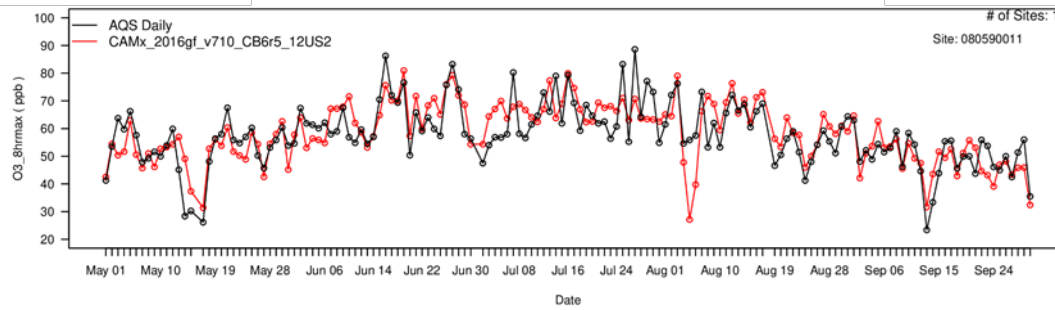
Brazoria, Texas



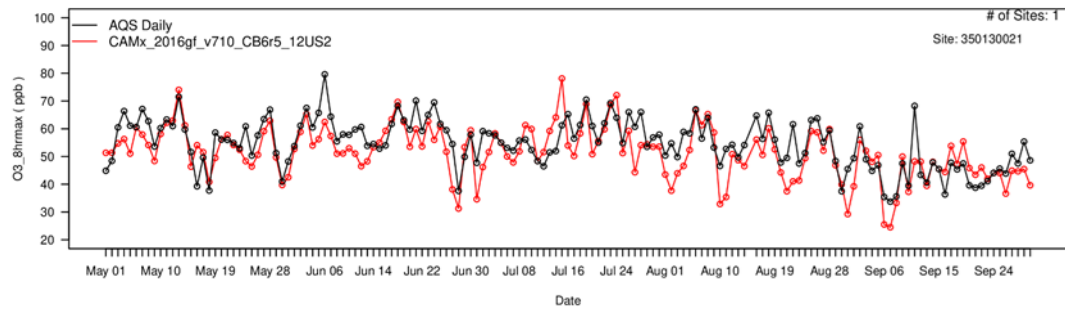
Denver Chatfield, Colorado



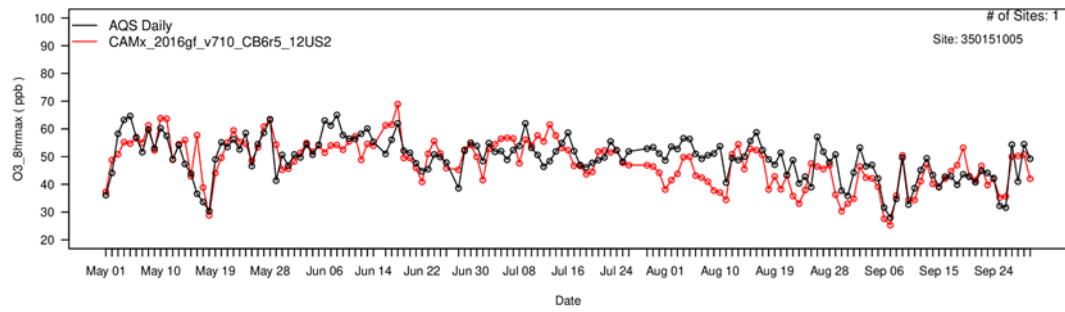
Denver NREL, Colorado



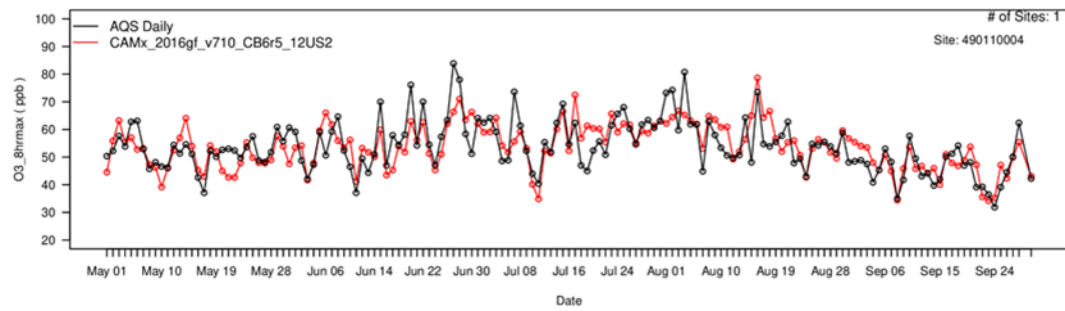
Las Cruces Desert View, New Mexico



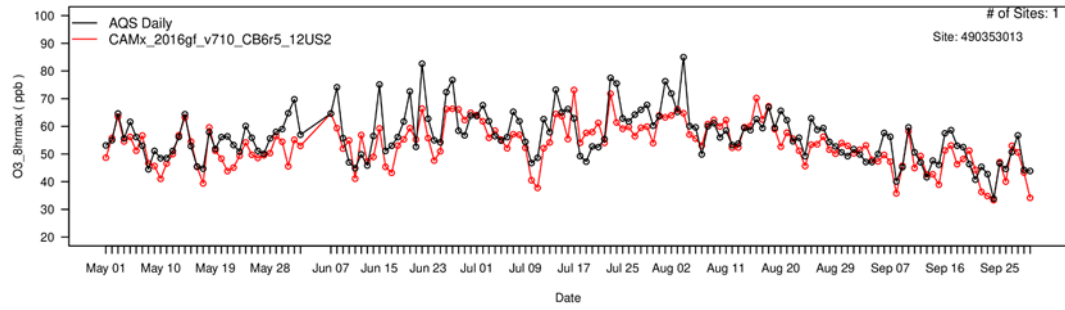
Eddy County, New Mexico



Salt Lake City Bountiful Viewmont, Utah



Salt Lake City Herriman, Utah



Appendix C
Ozone Contributions to
Nonattainment & Maintenance-Only
Receptors in 2023 & 2026

The tables in this appendix provide projected design values and contribution metric data from each state and the other source tags to nonattainment and maintenance-only in 2023 and 2026. Highlighted values denote contributions greater than or equal to the 1 percent of the NAAQS screening threshold. The contributions and design values are in units of ppb. Contributions to individual monitoring sites is provided in the file: “Final GNP O3 DVs_Contributions” which can be found in the docket for this final rule.

Design Values and Contributions for Monitoring plus Modeled Receptors in 2026 – Part 1

					Contributions																												
Site ID	ST	County	2026 Avg	2026 Max	AL	AZ	AR	CA	CO	CT	DE	DC	FL	GA	ID	IL	IN	IA	KS	KY	LA	ME	MD	MA	MI	MN	MS	MO	MT	NE	NV	NH	NJ
40278011	AZ	Yuma	69.9	71.5	0.00	2.67	0.00	6.16	0.02	0.00	0.00	0.00	0.00	0.00	0.01	0.00	0.00	0.00	0.00	0.00	0.00	0.00	0.00	0.00	0.00	0.00	0.00	0.00	0.00	0.14	0.00	0.00	
60650016	CA	Riverside	71.4	72.4	0.00	0.10	0.00	26.78	0.01	0.00	0.00	0.00	0.00	0.00	0.00	0.00	0.00	0.00	0.00	0.00	0.00	0.00	0.00	0.00	0.00	0.00	0.00	0.00	0.00	0.14	0.00	0.00	
60651016	CA	Riverside	90.0	91.2	0.00	0.34	0.00	34.03	0.02	0.00	0.00	0.00	0.00	0.00	0.00	0.00	0.00	0.00	0.00	0.00	0.00	0.00	0.00	0.00	0.00	0.00	0.00	0.00	0.00	0.09	0.00	0.00	
80590006	CO	Jefferson	72.0	72.6	0.00	0.44	0.00	1.40	16.51	0.00	0.00	0.00	0.00	0.00	0.10	0.00	0.00	0.00	0.04	0.00	0.00	0.00	0.00	0.00	0.00	0.00	0.00	0.01	0.04	0.37	0.00	0.00	
80590011	CO	Jefferson	72.4	73.0	0.00	0.40	0.00	1.27	17.15	0.00	0.00	0.00	0.00	0.00	0.11	0.00	0.00	0.00	0.03	0.00	0.00	0.00	0.00	0.00	0.00	0.00	0.00	0.01	0.06	0.38	0.00	0.00	
80690011	CO	Larimer	70.0	71.2	0.00	0.71	0.00	0.88	13.53	0.00	0.00	0.00	0.00	0.00	0.12	0.00	0.00	0.00	0.15	0.00	0.00	0.00	0.00	0.00	0.00	0.00	0.00	0.02	0.09	0.25	0.00	0.00	
90013007	CT	Fairfield	70.9	71.7	0.09	0.01	0.15	0.03	0.05	3.71	0.41	0.02	0.05	0.13	0.02	0.67	1.08	0.14	0.09	0.76	0.23	0.01	0.92	0.31	1.32	0.16	0.09	0.31	0.07	0.07	0.01	0.09	7.04
90019003	CT	Fairfield	71.3	71.5	0.08	0.01	0.14	0.03	0.04	2.42	0.43	0.03	0.05	0.13	0.02	0.63	1.06	0.14	0.09	0.79	0.23	0.00	1.06	0.06	1.39	0.15	0.08	0.29	0.06	0.06	0.01	0.01	8.10
350130021	NM	Dona Ana	69.9	71.2	0.01	0.82	0.00	0.30	0.14	0.00	0.00	0.00	0.04	0.01	0.02	0.00	0.00	0.00	0.06	0.00	0.02	0.00	0.00	0.00	0.00	0.01	0.00	0.00	0.01	0.04	0.00	0.00	
350130022	NM	Dona Ana	69.0	71.6	0.00	0.82	0.00	0.31	0.17	0.00	0.00	0.00	0.04	0.01	0.02	0.00	0.00	0.00	0.05	0.00	0.01	0.00	0.00	0.00	0.00	0.00	0.01	0.00	0.00	0.01	0.04	0.00	0.00
350151005	NM	Eddy	69.1	73.4	0.00	1.06	0.02	0.62	0.17	0.00	0.00	0.00	0.00	0.00	0.03	0.00	0.00	0.00	0.09	0.00	0.03	0.00	0.00	0.00	0.00	0.00	0.00	0.06	0.07	0.07	0.00	0.00	
350250008	NM	Lea	69.2	71.6	0.00	1.34	0.00	0.70	0.08	0.00	0.00	0.00	0.00	0.00	0.01	0.00	0.00	0.00	0.01	0.00	0.00	0.00	0.00	0.00	0.00	0.00	0.00	0.01	0.09	0.00	0.00	0.00	
480391004	TX	Brazoria	69.1	71.2	0.25	0.00	1.16	0.01	0.05	0.00	0.00	0.00	0.09	0.09	0.01	0.06	0.06	0.23	0.34	0.08	5.03	0.00	0.00	0.00	0.00	0.13	0.48	0.58	0.04	0.19	0.00	0.00	0.00
481671034	TX	Galveston	70.2	71.4	0.69	0.04	0.88	0.04	0.13	0.00	0.00	0.00	0.17	0.16	0.01	0.14	0.34	0.19	0.42	0.37	9.37	0.00	0.00	0.00	0.17	0.19	1.15	0.42	0.04	0.18	0.01	0.00	0.00
482010024	TX	Harris	73.9	75.5	0.20	0.00	0.53	0.00	0.01	0.00	0.00	0.00	0.46	0.04	0.00	0.01	0.01	0.14	0.14	0.01	4.57	0.00	0.00	0.00	0.00	0.09	0.29	0.22	0.01	0.09	0.00	0.00	0.00
490110004	UT	Davis	69.9	72.1	0.00	0.24	0.00	2.42	0.03	0.00	0.00	0.00	0.00	0.00	0.36	0.00	0.00	0.00	0.00	0.00	0.00	0.00	0.00	0.00	0.00	0.00	0.00	0.00	0.00	0.00	0.83	0.00	0.00
490353006	UT	Salt Lake	70.5	72.1	0.00	0.21	0.00	2.63	0.03	0.00	0.00	0.00	0.00	0.00	0.33	0.00	0.00	0.00	0.00	0.00	0.00	0.00	0.00	0.00	0.00	0.00	0.00	0.00	0.00	0.90	0.00	0.00	
490353013	UT	Salt Lake	71.9	72.3	0.00	0.21	0.00	2.16	0.04	0.00	0.00	0.00	0.00	0.00	0.27	0.00	0.00	0.00	0.00	0.00	0.00	0.00	0.00	0.00	0.00	0.02	0.00	0.00	0.00	0.67	0.00	0.00	
551170006	WI	Sheboygan	70.8	71.7	0.01	0.02	0.58	0.04	0.05	0.01	0.00	0.00	0.01	0.00	0.02	13.57	8.53	0.62	0.36	0.42	0.33	0.00	0.05	0.01	1.47	0.32	0.09	1.68	0.06	0.16	0.01	0.00	0.04

Design Values and Contributions for Monitoring plus Modeled Receptors in 2026 – Part 2

					Contributions																										
Site ID	ST	County	2026 Avg	2026 Max	NM	NY	NC	ND	OH	OK	OR	PA	RI	SC	SD	TN	TX	UT	VT	VA	WA	WV	WI	WY	TRIBAL	Canada & Mexico	Offshore	Fires	Initial & Boundary	Biogenic	Lightning NOx
40278011	AZ	Yuma	69.9	71.5	0.11	0.00	0.00	0.00	0.00	0.00	0.08	0.00	0.00	0.00	0.00	0.00	0.02	0.12	0.00	0.00	0.02	0.00	0.00	0.00	0.01	9.46	0.53	3.12	44.47	2.31	0.55
60650016	CA	Riverside	71.4	72.4	0.04	0.00	0.00	0.00	0.00	0.00	0.16	0.00	0.00	0.00	0.00	0.00	0.01	0.05	0.00	0.00	0.07	0.00	0.00	0.00	0.00	2.33	2.03	2.93	33.29	3.19	0.19
60651016	CA	Riverside	90.0	91.2	0.11	0.00	0.00	0.00	0.00	0.00	0.14	0.00	0.00	0.00	0.00	0.00	0.04	0.04	0.00	0.00	0.04	0.00	0.00	0.00	0.01	2.46	1.57	2.88	44.08	3.41	0.62
80590006	CO	Jefferson	72.0	72.6	0.35	0.00	0.00	0.00	0.00	0.03	0.09	0.00	0.00	0.00	0.00	0.00	0.20	0.97	0.00	0.00	0.04	0.00	0.00	0.40	0.13	0.60	0.06	1.22	44.08	3.46	1.34
80590011	CO	Jefferson	72.4	73.0	0.28	0.00	0.00	0.00	0.00	0.02	0.10	0.00	0.00	0.00	0.00	0.00	0.10	1.05	0.00	0.00	0.04	0.00	0.00	0.40	0.14	0.55	0.06	1.25	44.52	3.29	1.05
80690011	CO	Larimer	70.0	71.2	0.46	0.00	0.00	0.01	0.00	0.05	0.08	0.00	0.00	0.00	0.00	0.00	0.31	0.81	0.00	0.00	0.04	0.00	0.00	0.59	0.17	0.93	0.08	1.25	41.95	4.25	3.16
90013007	CT	Fairfield	70.9	71.7	0.04	12.34	0.42	0.11	1.93	0.12	0.02	4.94	0.03	0.15	0.04	0.23	0.48	0.02	0.02	1.10	0.04	1.34	0.18	0.07	0.00	2.20	0.69	0.31	19.31	5.73	0.73
90019003	CT	Fairfield	71.3	71.5	0.04	12.65	0.40	0.09	1.95	0.13	0.02	5.47	0.00	0.14	0.03	0.24	0.48	0.02	0.01	1.09	0.04	1.36	0.17	0.07	0.00	2.18	0.65	0.34	19.41	5.73	0.74
350130021	NM	Dona Ana	69.9	71.2	2.70	0.00	0.00	0.00	0.00	0.14	0.01	0.00	0.00	0.00	0.00	0.00	4.34	0.14	0.00	0.00	0.01	0.00	0.00	0.05	0.04	13.43	0.12	0.86	39.30	2.63	4.50
350130022	NM	Dona Ana	69.0	71.6	2.68	0.00	0.00	0.01	0.00	0.13	0.01	0.00	0.00	0.00	0.00	0.00	3.23	0.13	0.00	0.00	0.00	0.00	0.00	0.05	0.05	12.98	0.12	0.82	40.21	2.68	4.27
350151005	NM	Eddy	69.1	73.4	6.32	0.00	0.00	0.00	0.00	0.24	0.05	0.00	0.00	0.00	0.01	0.00	1.81	0.04	0.00	0.00	0.05	0.00	0.00	0.13	0.02	3.42	0.18	1.08	50.16	2.33	0.85
350250008	NM	Lea	69.2	71.6	9.95	0.00	0.00	0.01	0.00	0.01	0.02	0.00	0.00	0.00	0.00	0.00	2.10	0.07	0.00	0.00	0.01	0.00	0.00	0.04	0.02	3.80	0.15	0.62	45.82	2.25	1.97
480391004	TX	Brazoria	69.1	71.2	0.03	0.00	0.02	0.11	0.02	0.57	0.00	0.00	0.00	0.01	0.04	0.18	28.35	0.01	0.00	0.01	0.02	0.00	0.01	0.04	0.00	0.33	1.39	0.65	21.73	5.90	0.54
481671034	TX	Galveston	70.2	71.4	0.12	0.01	0.03	0.15	0.29	0.74	0.00	0.02	0.00	0.07	0.04	0.54	18.71	0.04	0.00	0.01	0.01	0.03	0.07	0.09	0.00	0.40	5.72	0.78	19.47	6.85	0.63
482010024	TX	Harris	73.9	75.5	0.03	0.00	0.01	0.03	0.00	0.19	0.00	0.00	0.00	0.00	0.02	0.05	30.50	0.00	0.00	0.00	0.00	0.00	0.01	0.01	0.00	0.13	2.93	0.88	27.03	4.08	0.97
490110004	UT	Davis	69.9	72.1	0.07	0.00	0.00	0.00	0.00	0.00	0.41	0.00	0.00	0.00	0.00	0.00	0.04	7.21	0.00	0.00	0.14	0.00	0.00	0.06	0.01	0.63	0.11	2.86	50.51	3.48	0.36
490353006	UT	Salt Lake	70.5	72.1	0.08	0.00	0.00	0.00	0.00	0.00	0.41	0.00	0.00	0.00	0.00	0.00	0.06	7.54	0.00	0.00	0.14	0.00	0.00	0.05	0.01	0.45	0.11	3.30	49.84	3.71	0.59
490353013	UT	Salt Lake	71.9	72.3	0.07	0.00	0.00	0.01	0.00	0.01	0.26	0.00	0.00	0.00	0.00	0.00	0.04	6.43	0.00	0.00	0.10	0.00	0.00	0.23	0.01	0.63	0.11	2.52	54.67	2.95	0.32
551170006	WI	Sheboygan	70.8	71.7	0.05	0.25	0.02	0.17	1.46	0.58	0.01	0.42	0.00	0.00	0.04	0.14	0.95	0.02	0.00	0.07	0.03	0.16	6.48	0.07	0.00	1.29	0.09	0.27	17.37	11.25	0.84

This page is intentionally left blank

Appendix D
Upwind State Collective Contribution
in 2023

This appendix provides the 2023 average and maximum design values, the “home state” contribution, the total “collective” contribution from all upwind states, the total upwind contribution expressed as a percent of total ozone (i.e., the 2023 average design value), and the total upwind contribution expressed as a percent of the total U.S. anthropogenic contribution at each monitoring site with projected 2023 average design values that exceed the 2015 NAAQS and each violating monitor maintenance-only receptor. The design value and contribution data are in units of ppb.

Table D-1. Upwind contribution summary data at monitoring sites that are projected to have maximum design values that exceed the NAAQS in 2015, based on air quality modeling.

Site ID	State	County	2023gf Avg DV	2023gf Max DV	Home State	Upwind Total	Anthro Total	Upwind % of Avg DV	Upwind % of Total Anthro
40278011	AZ	Yuma	70.4	72.1	2.98	6.97	9.95	9.9%	70.1%
60170010	CA	El Dorado	75.3	77.7	27.04	1.17	28.21	1.6%	4.2%
60170020	CA	El Dorado	73.3	75.0	30.95	1.61	32.55	2.2%	4.9%
60190007	CA	Fresno	80.4	82.2	31.79	1.60	33.39	2.0%	4.8%
60190011	CA	Fresno	83.3	84.2	33.02	1.64	34.66	2.0%	4.7%
60190242	CA	Fresno	78.4	80.0	28.40	1.57	29.97	2.0%	5.2%
60194001	CA	Fresno	83.2	84.7	31.75	1.39	33.14	1.7%	4.2%
60195001	CA	Fresno	83.8	86.6	33.35	1.52	34.86	1.8%	4.4%
60250005	CA	Imperial	76.4	76.7	7.05	0.62	7.67	0.8%	8.1%
60251003	CA	Imperial	74.8	74.8	9.54	0.77	10.31	1.0%	7.5%
60290007	CA	Kern	82.2	83.4	28.80	1.22	30.02	1.5%	4.1%
60290008	CA	Kern	77.8	79.7	22.47	1.07	23.55	1.4%	4.6%
60290011	CA	Kern	77.9	79.5	15.58	0.93	16.50	1.2%	5.6%
60290014	CA	Kern	81.0	82.9	27.84	1.24	29.08	1.5%	4.3%
60290232	CA	Kern	74.8	77.3	26.63	0.94	27.57	1.3%	3.4%
60292012	CA	Kern	83.5	84.2	30.20	1.17	31.38	1.4%	3.7%
60295002	CA	Kern	81.7	83.3	27.19	1.25	28.44	1.5%	4.4%
60296001	CA	Kern	75.9	76.2	23.76	1.23	24.99	1.6%	4.9%
60311004	CA	Kings	76.7	77.4	25.40	1.00	26.40	1.3%	3.8%
60370002	CA	Los Angeles	91.2	95.7	43.25	0.71	43.97	0.8%	1.6%
60370016	CA	Los Angeles	96.7	99.6	45.86	0.75	46.62	0.8%	1.6%
60371103	CA	Los Angeles	70.5	71.5	32.83	0.78	33.62	1.1%	2.3%
60371201	CA	Los Angeles	83.1	85.6	34.27	1.07	35.34	1.3%	3.0%
60371602	CA	Los Angeles	75.9	76.2	36.50	0.84	37.34	1.1%	2.2%
60371701	CA	Los Angeles	88.1	91.0	43.25	0.55	43.80	0.6%	1.3%
60372005	CA	Los Angeles	81.7	83.0	38.01	0.88	38.88	1.1%	2.3%
60376012	CA	Los Angeles	91.3	93.2	40.12	1.04	41.15	1.1%	2.5%
60379033	CA	Los Angeles	79.4	81.0	24.98	1.02	26.00	1.3%	3.9%

Site ID	State	County	2023gf Avg DV	2023gf Max DV	Home State	Upwind Total	Anthro Total	Upwind % of Avg DV	Upwind % of Total Anthro
60390004	CA	Madera	74.7	77.2	27.06	1.49	28.55	2.0%	5.2%
60392010	CA	Madera	76.4	77.6	27.77	1.60	29.38	2.1%	5.5%
60430003	CA	Mariposa	72.1	75.0	9.74	0.87	10.61	1.2%	8.2%
60470003	CA	Merced	73.9	75.1	26.82	1.39	28.20	1.9%	4.9%
60570005	CA	Nevada	76.5	79.8	25.61	1.68	27.30	2.2%	6.2%
60592022	CA	Orange	72.5	72.7	30.36	0.51	30.87	0.7%	1.6%
60595001	CA	Orange	74.7	75.4	34.58	0.76	35.34	1.0%	2.1%
60610003	CA	Placer	75.9	78.6	32.04	1.67	33.71	2.2%	4.9%
60610004	CA	Placer	70.8	75.9	24.11	1.66	25.76	2.3%	6.4%
60610006	CA	Placer	72.5	73.4	34.24	1.61	35.85	2.2%	4.5%
60650008	CA	Riverside	71.4	73.8	14.66	0.92	15.58	1.3%	5.9%
60650012	CA	Riverside	87.1	89.6	35.52	1.20	36.72	1.4%	3.3%
60650016	CA	Riverside	72.2	73.1	27.46	0.73	28.19	1.0%	2.6%
60651016	CA	Riverside	91.0	92.2	35.27	1.01	36.28	1.1%	2.8%
60652002	CA	Riverside	76.1	78.3	14.23	0.87	15.10	1.1%	5.7%
60655001	CA	Riverside	80.5	82.6	24.52	1.14	25.66	1.4%	4.4%
60656001	CA	Riverside	84.6	85.2	37.50	0.79	38.30	0.9%	2.1%
60658001	CA	Riverside	91.3	92.6	46.25	0.73	46.98	0.8%	1.6%
60658005	CA	Riverside	89.7	92.6	45.44	0.72	46.16	0.8%	1.6%
60659001	CA	Riverside	81.4	83.5	34.10	0.82	34.92	1.0%	2.3%
60670002	CA	Sacramento	71.6	71.9	33.03	1.61	34.64	2.3%	4.7%
60670012	CA	Sacramento	73.4	74.0	31.62	1.23	32.86	1.7%	3.7%
60675003	CA	Sacramento	70.0	71.5	29.31	1.24	30.55	1.8%	4.0%
60710001	CA	San Bernardino	74.8	75.8	15.04	0.90	15.94	1.2%	5.6%
60710005	CA	San Bernardino	103.1	104.6	42.93	1.45	44.38	1.4%	3.3%
60710012	CA	San Bernardino	88.0	90.8	28.36	0.79	29.15	0.9%	2.7%
60710306	CA	San Bernardino	78.6	80.5	27.89	1.27	29.17	1.6%	4.4%
60711004	CA	San Bernardino	100.2	103.4	48.82	0.82	49.64	0.8%	1.7%
60711234	CA	San Bernardino	70.0	73.5	9.53	0.82	10.35	1.2%	7.9%
60712002	CA	San Bernardino	92.2	93.5	45.54	1.14	46.68	1.2%	2.4%
60714001	CA	San Bernardino	83.9	84.6	35.59	1.43	37.02	1.7%	3.8%
60714003	CA	San Bernardino	97.4	100.3	48.34	1.00	49.34	1.0%	2.0%
60719002	CA	San Bernardino	78.9	80.5	18.89	1.11	20.00	1.4%	5.6%
60719004	CA	San Bernardino	101.8	104.0	50.52	1.05	51.57	1.0%	2.0%
60731006	CA	San Diego	77.7	78.7	26.32	0.88	27.20	1.1%	3.2%
60773005	CA	San Joaquin	69.6	71.1	28.18	1.32	29.50	1.9%	4.5%
60990005	CA	Stanislaus	74.7	75.6	30.91	1.62	32.53	2.2%	5.0%
60990006	CA	Stanislaus	76.5	76.8	30.35	1.45	31.80	1.9%	4.5%
61070006	CA	Tulare	78.6	79.8	18.15	1.16	19.31	1.5%	6.0%
61070009	CA	Tulare	82.2	82.2	26.25	1.50	27.75	1.8%	5.4%

Site ID	State	County	2023gf Avg DV	2023gf Max DV	Home State	Upwind Total	Anthro Total	Upwind % of Avg DV	Upwind % of Total Anthro
61072002	CA	Tulare	75.6	77.7	28.93	1.22	30.15	1.6%	4.0%
61072010	CA	Tulare	77.0	78.8	27.49	1.11	28.60	1.4%	3.9%
61090005	CA	Tuolumne	73.4	75.5	19.84	1.45	21.29	2.0%	6.8%
80350004	CO	Douglas	71.3	71.9	15.68	5.68	21.36	8.0%	26.6%
80590006	CO	Jefferson	72.8	73.5	16.83	5.11	21.93	7.0%	23.3%
80590011	CO	Jefferson	73.5	74.1	17.55	4.90	22.45	6.7%	21.8%
80690011	CO	Larimer	70.9	72.1	14.00	5.22	19.22	7.4%	27.2%
90010017	CT	Fairfield	71.6	72.2	4.60	39.87	44.47	55.7%	89.7%
90013007	CT	Fairfield	72.9	73.8	3.94	40.05	44.00	54.9%	91.0%
90019003	CT	Fairfield	73.3	73.6	2.52	41.80	44.33	57.0%	94.3%
90099002	CT	New Haven	70.5	72.6	3.85	36.84	40.69	52.2%	90.5%
170310001	IL	Cook	68.2	71.9	18.81	17.66	36.47	25.9%	48.4%
170314201	IL	Cook	68.0	71.5	23.47	15.88	39.35	23.4%	40.4%
170317002	IL	Cook	68.5	71.3	20.58	18.85	39.43	27.5%	47.8%
350130021	NM	Dona Ana	70.8	72.1	2.88	6.98	9.86	9.9%	70.8%
350130022	NM	Dona Ana	69.7	72.4	2.89	5.83	8.72	8.4%	66.8%
350151005	NM	Eddy	69.7	74.1	6.52	5.20	11.72	7.5%	44.3%
350250008	NM	Lea	69.8	72.2	10.23	5.05	15.28	7.2%	33.0%
480391004	TX	Brazoria	70.4	72.5	29.22	10.79	40.01	15.3%	27.0%
481210034	TX	Denton	69.8	71.6	28.72	11.00	39.72	15.8%	27.7%
481410037	TX	El Paso	69.8	71.4	3.17	4.23	7.40	6.1%	57.1%
481671034	TX	Galveston	71.5	72.8	19.31	18.47	37.79	25.8%	48.9%
482010024	TX	Harris	75.1	76.7	31.24	7.82	39.06	10.4%	20.0%
482010055	TX	Harris	70.9	71.9	28.74	11.24	39.98	15.9%	28.1%
482011034	TX	Harris	70.1	71.3	28.34	9.91	38.25	14.1%	25.9%
482011035	TX	Harris	67.8	71.3	27.41	9.59	36.99	14.1%	25.9%
490110004	UT	Davis	72.0	74.2	8.73	5.08	13.81	7.1%	36.8%
490353006	UT	Salt Lake	72.6	74.2	9.15	5.42	14.58	7.5%	37.2%
490353013	UT	Salt Lake	73.3	73.8	7.50	4.55	12.05	6.2%	37.8%
550590019	WI	Kenosha	70.8	71.7	5.51	36.92	42.43	52.1%	87.0%
551010020	WI	Racine	69.7	71.5	7.99	34.08	42.07	48.9%	81.0%
551170006	WI	Sheboygan	72.7	73.6	7.23	34.76	41.99	47.8%	82.8%

Table D-2. Upwind contribution summary data at violating monitor receptors.

Site ID	State	County	2023gf Avg DV	2023gf Max DV	Home State	Upwind Total	Anthro Total	Upwind % of Avg DV	Upwind % of Total Anthro
40070010	AZ	Gila	67.9	69.5	7.66	3.19	10.85	4.7%	29.4%
40130019	AZ	Maricopa	69.8	70.0	15.33	3.43	18.76	4.9%	18.3%
40131003	AZ	Maricopa	70.1	70.7	13.83	4.16	17.99	5.9%	23.1%
40131004	AZ	Maricopa	70.2	70.8	14.57	2.81	17.38	4.0%	16.2%
40131010	AZ	Maricopa	68.3	69.2	13.90	4.25	18.15	6.2%	23.4%
40132001	AZ	Maricopa	63.8	64.1	12.84	2.96	15.80	4.6%	18.7%
40132005	AZ	Maricopa	69.6	70.5	13.82	3.02	16.84	4.3%	17.9%
40133002	AZ	Maricopa	65.8	65.8	13.60	2.67	16.27	4.1%	16.4%
40134004	AZ	Maricopa	65.7	66.6	11.02	4.26	15.28	6.5%	27.9%
40134005	AZ	Maricopa	62.3	62.3	12.29	3.70	15.99	5.9%	23.1%
40134008	AZ	Maricopa	65.6	66.5	13.07	2.76	15.83	4.2%	17.5%
40134010	AZ	Maricopa	63.8	66.9	12.32	3.06	15.38	4.8%	19.9%
40137020	AZ	Maricopa	67.0	67.0	14.42	2.68	17.10	4.0%	15.7%
40137021	AZ	Maricopa	69.8	70.1	14.25	3.47	17.73	5.0%	19.6%
40137022	AZ	Maricopa	68.2	69.1	13.92	3.39	17.32	5.0%	19.6%
40137024	AZ	Maricopa	67.0	67.9	14.42	2.68	17.10	4.0%	15.7%
40139702	AZ	Maricopa	66.9	68.1	12.53	3.48	16.01	5.2%	21.7%
40139704	AZ	Maricopa	65.3	66.2	12.21	3.15	15.36	4.8%	20.5%
40139997	AZ	Maricopa	70.5	70.5	14.57	2.86	17.43	4.1%	16.4%
40218001	AZ	Pinal	67.8	69.0	9.81	3.44	13.25	5.1%	25.9%
60430006	CA	Mariposa	69.2	70.1	17.92	1.39	19.31	2.0%	7.2%
61112002	CA	Ventura	69.6	70.2	27.04	0.86	27.90	1.2%	3.1%
80013001	CO	Adams	63.0	63.0	13.95	4.00	17.95	6.4%	22.3%
80050002	CO	Arapahoe	68.0	68.0	14.73	5.63	20.36	8.3%	27.7%
80310002	CO	Denver	63.6	64.8	14.08	4.04	18.12	6.4%	22.3%
80310026	CO	Denver	64.5	64.8	14.28	4.10	18.38	6.4%	22.3%
90079007	CT	Middlesex	68.7	69.0	5.39	35.86	41.26	52.2%	86.9%
90110124	CT	New London	65.5	67.0	6.76	32.20	38.96	49.2%	82.6%
170310032	IL	Cook	67.3	69.8	17.28	19.99	37.27	29.7%	53.6%
170311601	IL	Cook	63.8	64.5	17.08	16.26	33.35	25.5%	48.8%
181270024	IN	Porter	63.4	64.6	15.38	19.39	34.77	30.6%	55.8%
260050003	MI	Allegan	66.2	67.4	2.03	34.52	36.55	52.1%	94.4%
261210039	MI	Muskegon	67.5	68.4	1.98	38.91	40.89	57.6%	95.2%
320030043	NV	Clark	68.4	69.4	9.06	8.54	17.60	12.5%	48.5%
350011012	NM	Bernalillo	63.8	66.0	6.58	3.86	10.44	6.1%	37.0%
350130008	NM	Dona Ana	65.6	66.3	1.69	6.22	7.91	9.5%	78.6%
361030002	NY	Suffolk	66.2	68.0	12.56	26.44	39.00	39.9%	67.8%
390850003	OH	Lake	64.3	64.6	18.67	17.65	36.31	27.4%	48.6%
480290052	TX	Bexar	67.1	67.8	18.42	3.11	21.53	4.6%	14.4%

Site ID	State	County	2023gf Avg DV	2023gf Max DV	Home State	Upwind Total	Anthro Total	Upwind % of Avg DV	Upwind % of Total Anthro
480850005	TX	Collin	65.4	66.0	27.06	9.75	36.81	14.9%	26.5%
481130075	TX	Dallas	65.3	66.5	21.71	12.54	34.26	19.2%	36.6%
481211032	TX	Denton	65.9	67.7	23.86	11.65	35.51	17.7%	32.8%
482010051	TX	Harris	65.3	66.3	26.47	10.35	36.82	15.9%	28.1%
482010416	TX	Harris	68.8	70.4	28.64	10.38	39.02	15.1%	26.6%
484390075	TX	Tarrant	63.8	64.7	24.97	9.78	34.75	15.3%	28.1%
484391002	TX	Tarrant	64.1	65.7	24.06	10.92	34.98	17.0%	31.2%
484392003	TX	Tarrant	65.2	65.9	24.84	10.67	35.51	16.4%	30.0%
484393009	TX	Tarrant	67.5	68.1	27.70	10.08	37.78	14.9%	26.7%
490571003	UT	Weber	69.3	70.3	8.27	5.58	13.85	8.1%	40.3%
550590025	WI	Kenosha	67.6	70.7	5.38	31.77	37.15	47.0%	85.5%
550890008	WI	Ozaukee	65.2	65.8	8.22	27.37	35.59	42.0%	76.9%

Appendix E
Upwind Linkages for
Individual Receptors in 2023 & 2026

Upwind states linked to monitored plus modeled receptors in 2023.

Site ID	State	County	Receptor	Upwind States Linked to Individual Monitor Plus Modeled										
				Receptors in 2023										
40278011	AZ	Yuma	Yuma	CA										
60650016	CA	Riverside	Temecula	CA										
60651016	CA	Riverside	Morongo	CA										
80350004	CO	Douglas	Chatfield	CA	UT									
80590006	CO	Jefferson	Rocky Flats	CA	UT									
80590011	CO	Jefferson	NREL	CA	UT									
80690011	CO	Larimer	Fort Collins	AZ	CA	UT								
90010017	CT	Fairfield	Greenwich	IN	MD	MI	NJ	NY	OH	PA	WV			
90013007	CT	Fairfield	Stratford	IL	IN	KY	MD	MI	NJ	NY	OH	PA	VA	WV
90019003	CT	Fairfield	Westport	IN	KY	MD	MI	NJ	NY	OH	PA	VA	WV	
90099002	CT	New Haven	Madison	IL	IN	KY	MD	MI	NJ	NY	OH	PA	VA	WV
170310001	IL	Cook	Alsip	IN	IA	MI	MN	TX	WI					
170314201	IL	Cook	Northbrook	IN	MI	OH	TX	WI						
170317002	IL	Cook	Evanston	IN	MI	MO	OH	TX	WI					
350130021	NM	Dona Ana	Las Cruces Desert View	AZ	TX									
350130022	NM	Dona Ana	Las Cruces Santa	AZ	TX									
350151005	NM	Eddy	BLM	AZ	TX									
350250008	NM	Lea	Hobbs	AZ	CA	TX								
480391004	TX	Brazoria	Manvel Croix Park	AR	LA									
481210034	TX	Denton	Denton Airport	AR	LA	MS	OK							
481410037	TX	El Paso	UTEP	AZ	NM									
481671034	TX	Galveston	Galveston	AL	AR	LA	MS	OK						
482010024	TX	Harris	Houston Aldine	LA										
482010055	TX	Harris	Houston Bayland Park	AR	LA	MS								
482011034	TX	Harris	Houston East	AR	LA									
482011035	TX	Harris	Houston Clinton	AR	LA									
490110004	UT	Davis	Bountiful Viewmont	CA	NV									
490353006	UT	Salt Lake	Hawthorne	CA	NV									
490353013	UT	Salt Lake	Herriman	CA	NV									
550590019	WI	Kenosha	Chiwaukee Prairie	IA	IL	IN	MI	MO	OH	TX				
551010020	WI	Racine	Racine	IL	IN	MI	MO	OH	TX					
551170006	WI	Sheboygan	Sheboygan Kohler	IL	IN	MI	MO	OH	TX					

Upwind states linked to violating monitor receptors in 2023.

Site ID	State	County	Receptor	Upwind States Linked to Individual Violating Monitor Receptors in 2023											
				CA											
40070010	AZ	Gila	Tonto National Monument	CA											
40130019	AZ	Maricopa	West Phoenix	CA											
40131003	AZ	Maricopa	Mesa	CA											
40131004	AZ	Maricopa	North Phoenix	CA											
40131010	AZ	Maricopa	Falcon Field	CA											
40132001	AZ	Maricopa	Glendale	CA											
40132005	AZ	Maricopa	Pinnacle Peak	CA											
40133002	AZ	Maricopa	Central Phoenix	CA											
40134004	AZ	Maricopa	West Chandler	CA											
40134005	AZ	Maricopa	Tempe	CA											
40134008	AZ	Maricopa	Cave Creek	CA											
40134010	AZ	Maricopa	Dysart	CA											
40137020	AZ	Maricopa	Senior Center	CA											
40137021	AZ	Maricopa	Red Mountain	CA											
40137022	AZ	Maricopa	Lehi	CA											
40137024	AZ	Maricopa	High School	CA											
40139702	AZ	Maricopa	Tonto National Forest	CA											
40139704	AZ	Maricopa	Fountain Hills	CA											
40139997	AZ	Maricopa	JLG Supersite	CA											
40218001	AZ	Pinal	Queen Valley	CA											
80013001	CO	Adams	Welby	CA	UT										
80050002	CO	Arapahoe	Highland Reservoir	CA	UT										
80310002	CO	Denver	Denver Camp	CA	UT										
80310026	CO	Denver	La Casa	CA	UT										
90079007	CT	Middlesex	Middlesex	IN	KY	MD	MI	NJ	NY	OH	PA	VA	WV		

Site ID	State	County	Receptor	Upwind States Linked to Individual Violating Monitor Receptors in 2023									
				IN	MD	MI	NJ	NY	OH	PA	VA	WV	
90110124	CT	New London	Fort Griswold Park	IN	MD	MI	NJ	NY	OH	PA	VA	WV	
170310032	IL	Cook	South Water Plant	IN	IA	MI	OH	OK	TX	WI			
170311601	IL	Cook	Cook County Trailer	IN	MI	OH	TX	WI					
181270024	IN	Porter	Ogden Dunes	IL	MI	OH	TX	WI					
260050003	MI	Allegan	Holland	IL	IN	IA	KS	MO	OH	OK	TX	WI	
261210039	MI	Muskegon	Muskegon	AR	IL	IN	KY	MO	OH	OK	TX	WI	
320030043	NV	Clark	Paul Meyer	AZ	CA								
350011012	NM	Bernalillo	Foothills	AZ	TX								
350130008	NM	Dona Ana	La Union	AZ	TX								
361030002	NY	Suffolk	Babylon	IN	KY	MD	MI	NJ	OH	PA	VA	WV	
390850003	OH	Lake	Eastlake	IL	IN	KY	MI	PA	TX	WV			
480290052	TX	Bexar	Camp Bullis	LA									
480850005	TX	Collin	Frisco	LA	MS	TN							
481130075	TX	Dallas	Dallas North	AR	LA	MS	OK	TN					
481211032	TX	Denton	Pilot Point	AL	AR	LA	MS	MO	TN				
482010051	TX	Harris	Houston Croquet	LA	MS								
482010416	TX	Harris	Park Place	AR	LA	MS							
484390075	TX	Tarrant	Eagle Mountain Lake	AR	LA	MS	OK	TN					
484391002	TX	Tarrant	Fort Worth Northwest	AR	LA	OK							
484392003	TX	Tarrant	Keller	AR	LA	MS	OK	TN					
484393009	TX	Tarrant	Grapevine	LA	MS	OK							
490571003	UT	Weber	Harrisville	CA	NV								
550590025	WI	Kenosha	Kenosha Water Tower	IL	IN	IA	MO	TX					
550890008	WI	Ozaukee	Grafton	IL	IN	MI	MO	OH	TX				

Upwind states linked to monitored plus modeled receptors in 2026.

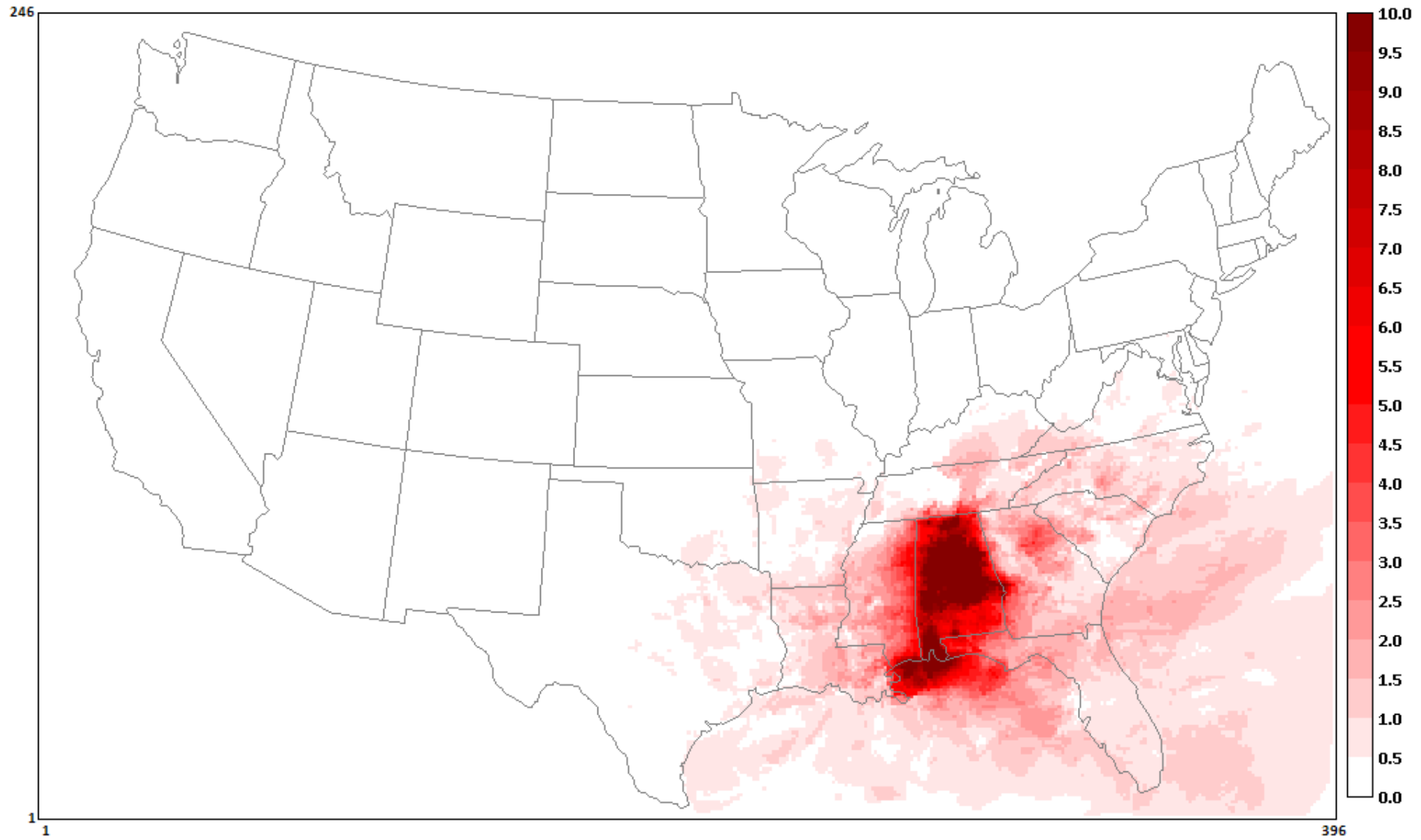
Site ID	State	County	Receptor	Upwind States Linked to Individual Receptors in 2026										
40278011	AZ	Yuma	Yuma	CA										
60650016	CA	Riverside	Temecula (Pechanga)	CA										
60651016	CA	Riverside	Morongo	CA										
80590006	CO	Jefferson	Rocky Flats	CA	UT									
80590011	CO	Jefferson	NREL	CA	UT									
80690011	CO	Larimer	Ft Collins	AZ	CA	UT								
90013007	CT	Fairfield	Stratford	IN	KY	MD	MI	NJ	NY	OH	PA	VA	WV	
90019003	CT	Fairfield	Westport	IN	KY	MD	MI	NJ	NY	OH	PA	VA	WV	
350130021	NM	Dona Ana	Las Cruces Desert View	AZ	TX									
350130022	NM	Dona Ana	Las Cruces Santa Teresa	AZ	TX									
350151005	NM	Eddy	Carlsbad BLM	AZ	TX									
350250008	NM	Lea	Hobbs	AZ	CA	TX								
480391004	TX	Brazoria	Manvel Croix Park	AR	LA									
481671034	TX	Galveston	Galveston	AR	LA	MS	OK							
482010024	TX	Harris	Houston Aldine	LA										
490110004	UT	Davis	Bountiful Viewmont	CA	NV									
490353006	UT	Salt Lake	Hawthorne	CA	NV									
490353013	UT	Salt Lake	Herriman	CA										
551170006	WI	Sheboygan	Sheboygan Kohler Andrae	IL	IN	MI	MO	OH	TX					

Appendix F

Spatial Fields of Top 10-Day Average Contributions from Emissions in Upwind States in 2023

This appendix contains maps showing the spatial distribution of top 10-day average contributions in 2023 from individual upwind states covered by this final rule. The maps illustrate the transport patterns that carry ozone formed from emissions in each state to both nearby and far distant downwind areas. Note that the average contribution data shown on the maps do not conform to the average contribution metric values calculated in Step 2 of the four-step transport framework. The data shown on the maps are based on averaging the model-predicted contributions without applying the criterion of a minimum of five days with model-predicted ozone concentrations greater than or equal to 60 ppb and without applying the average modeled contributions in a relative manner via the Relative Contribution Factor (RCF) to projected design values. In this regard, the data on these maps should not be viewed as equivalent to the average contribution metric.

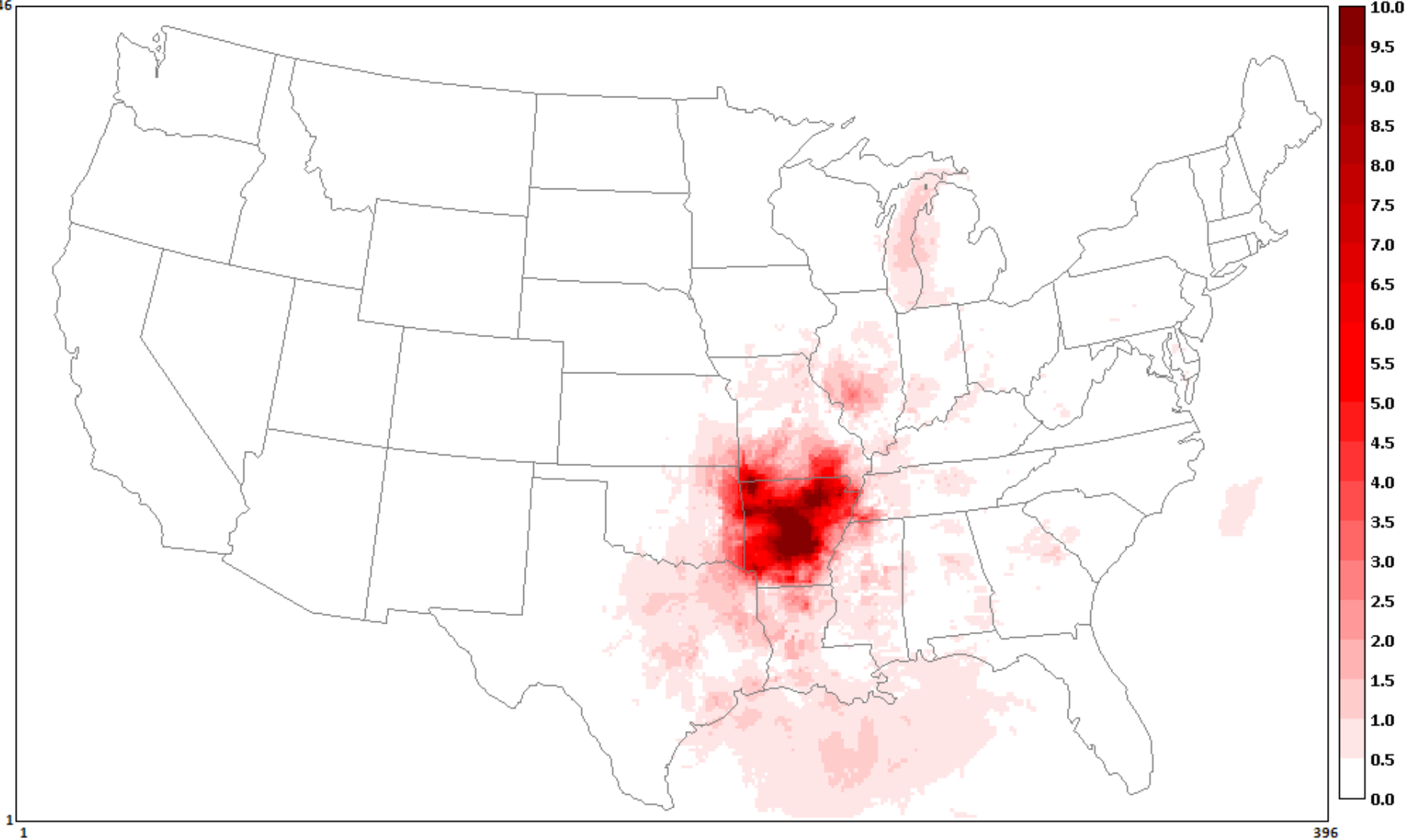
Alabama



data = [11]2023gf_ussa_apca.tagged.O3NV.12U52.camx.O3_8hrmax_LST.5-9.top10avg.ioapi

Arkansas

246

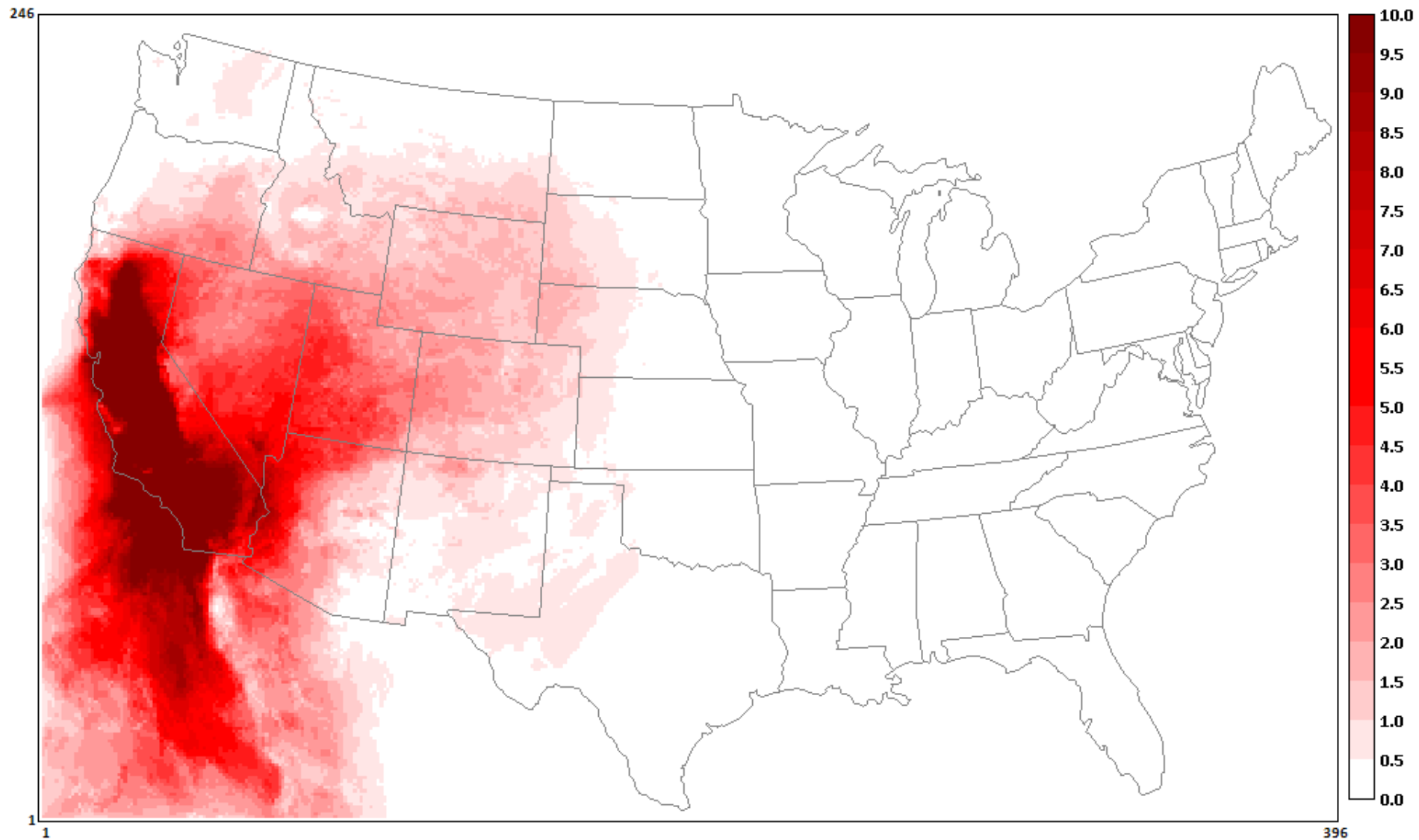


1

396

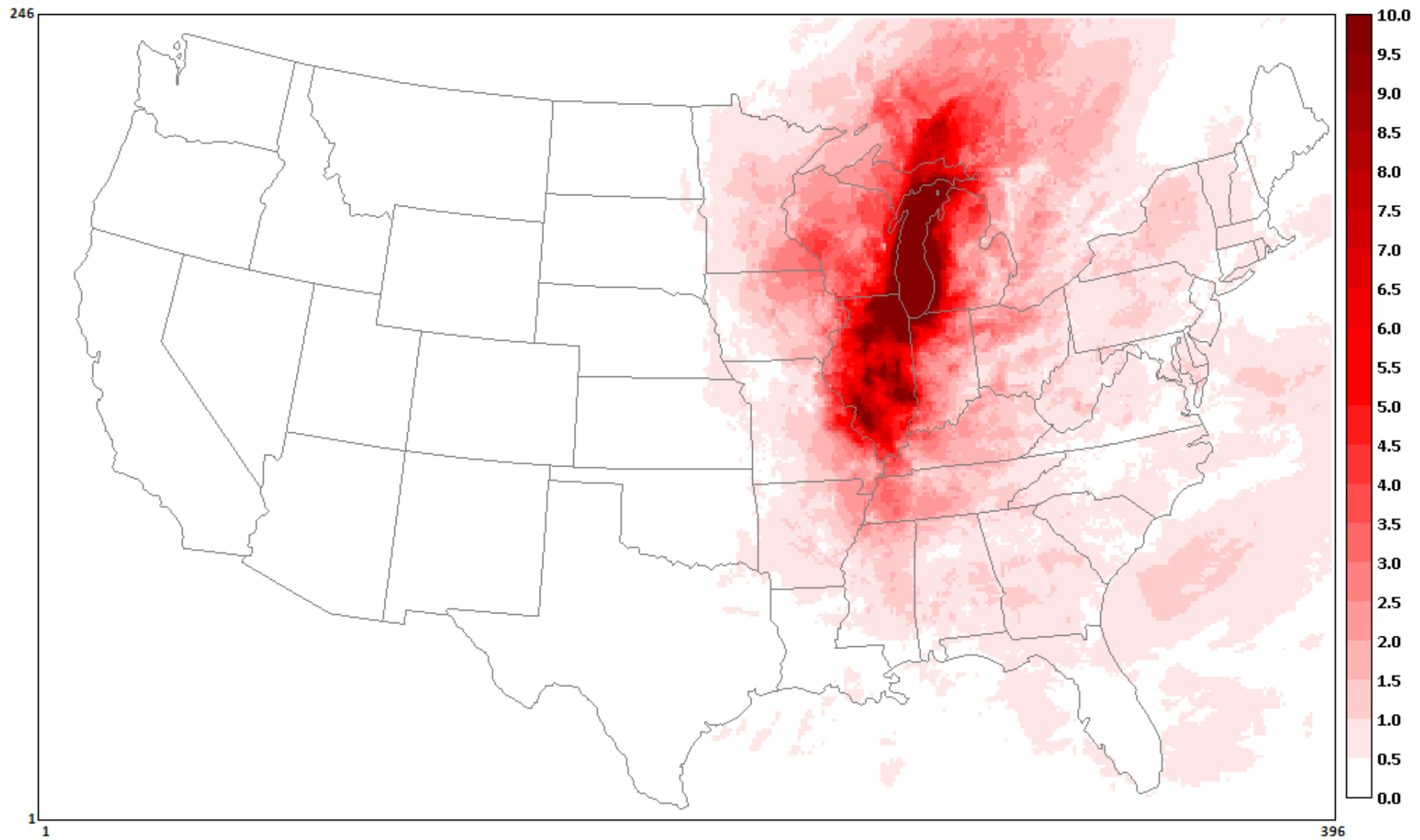
data = [11]2023gf_ussa_apca.tagged.O3NV.12US2.camx.O3_8hrmax_LST.5-9.top10avg.ioapi

California



data = [11]2023gf_ussa_apca.tagged.O3NV.12US2.camx.O3_8hrmax_LST.5-9.top10avg.ioapi

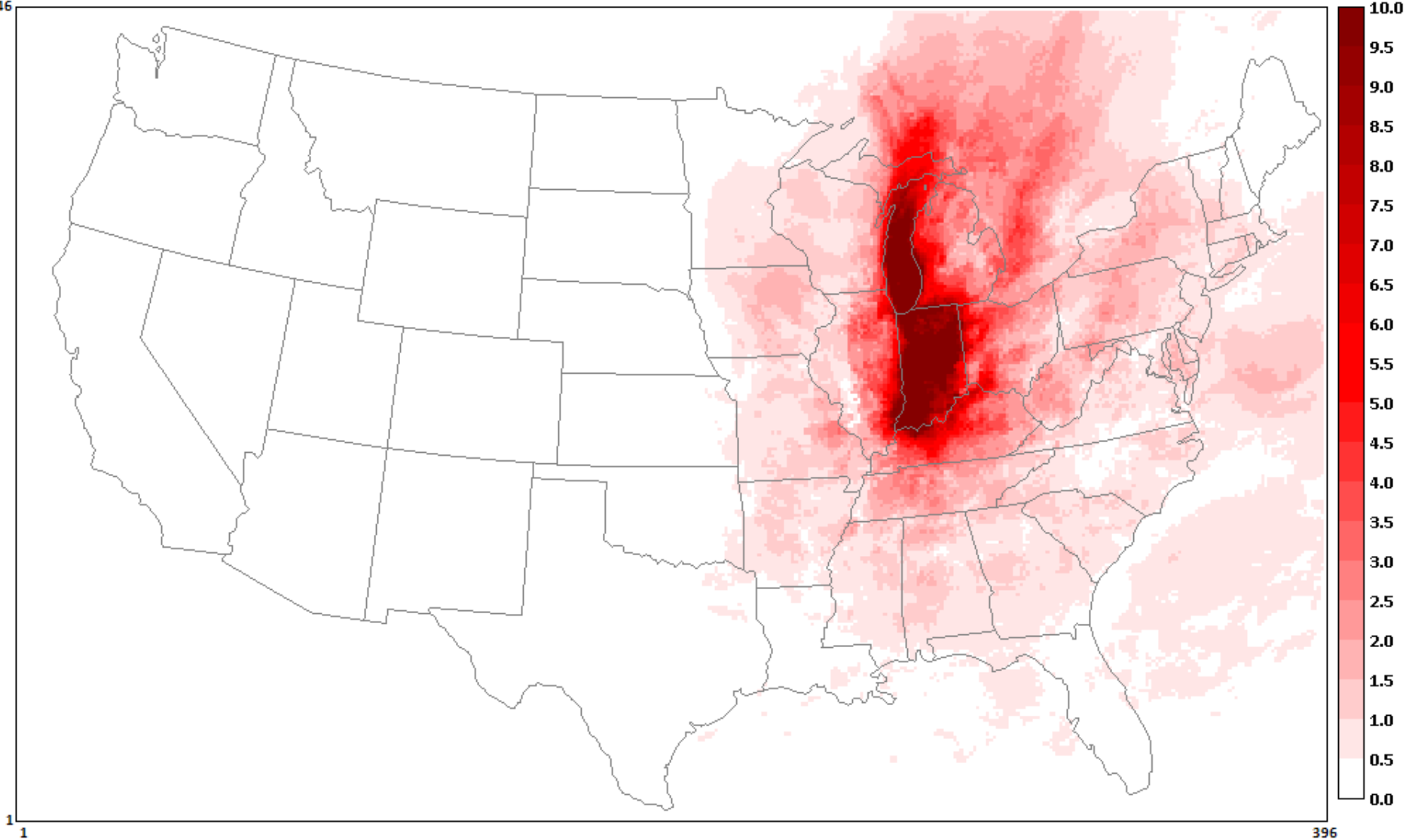
Illinois



data = [11]2023gf_ussa_apca.tagged.O3NV.12U52.camx.O3_8hrmax_LST.5-9.top10avg.ioapi

Indiana

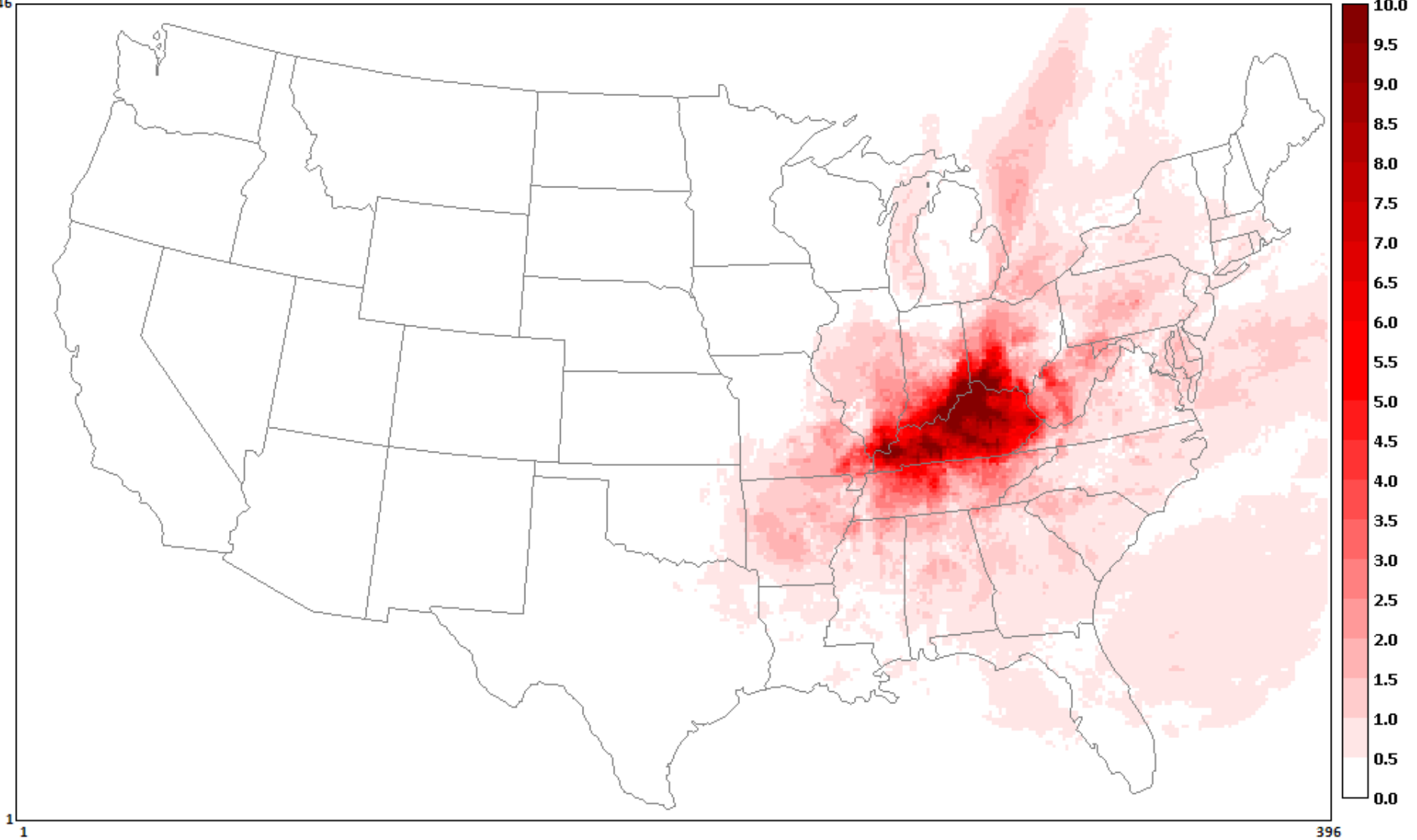
246



data = [11]2023gf_ussa_apca.tagged.O3NV.12US2.camx.O3_8hrmax_LST.5-9.top10avg.ioapi

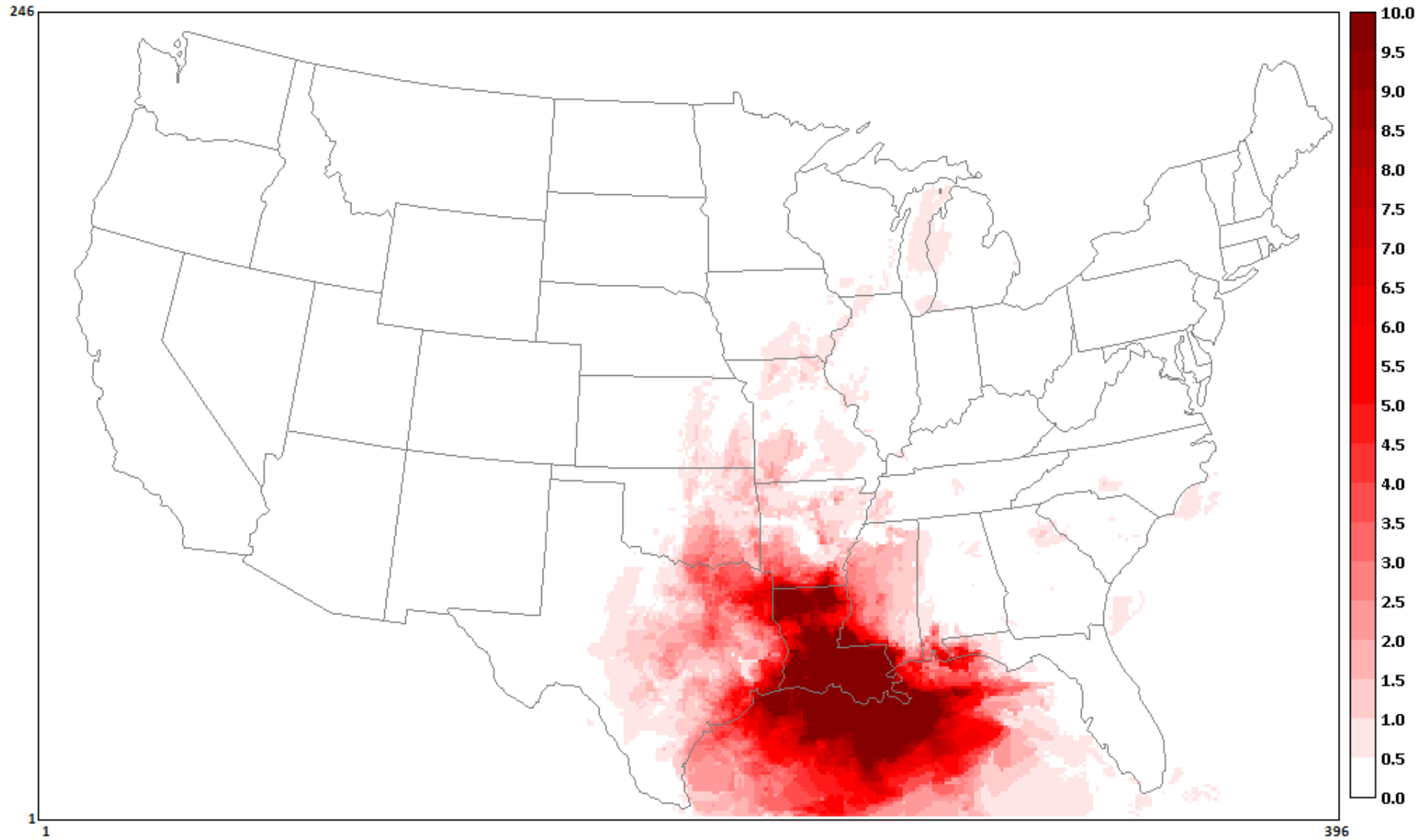
Kentucky

246



data = [11]2023gf_ussa_apca.tagged.O3NV.12US2.camx.O3_8hrmax_LST.5-9.top10avg.ioapi

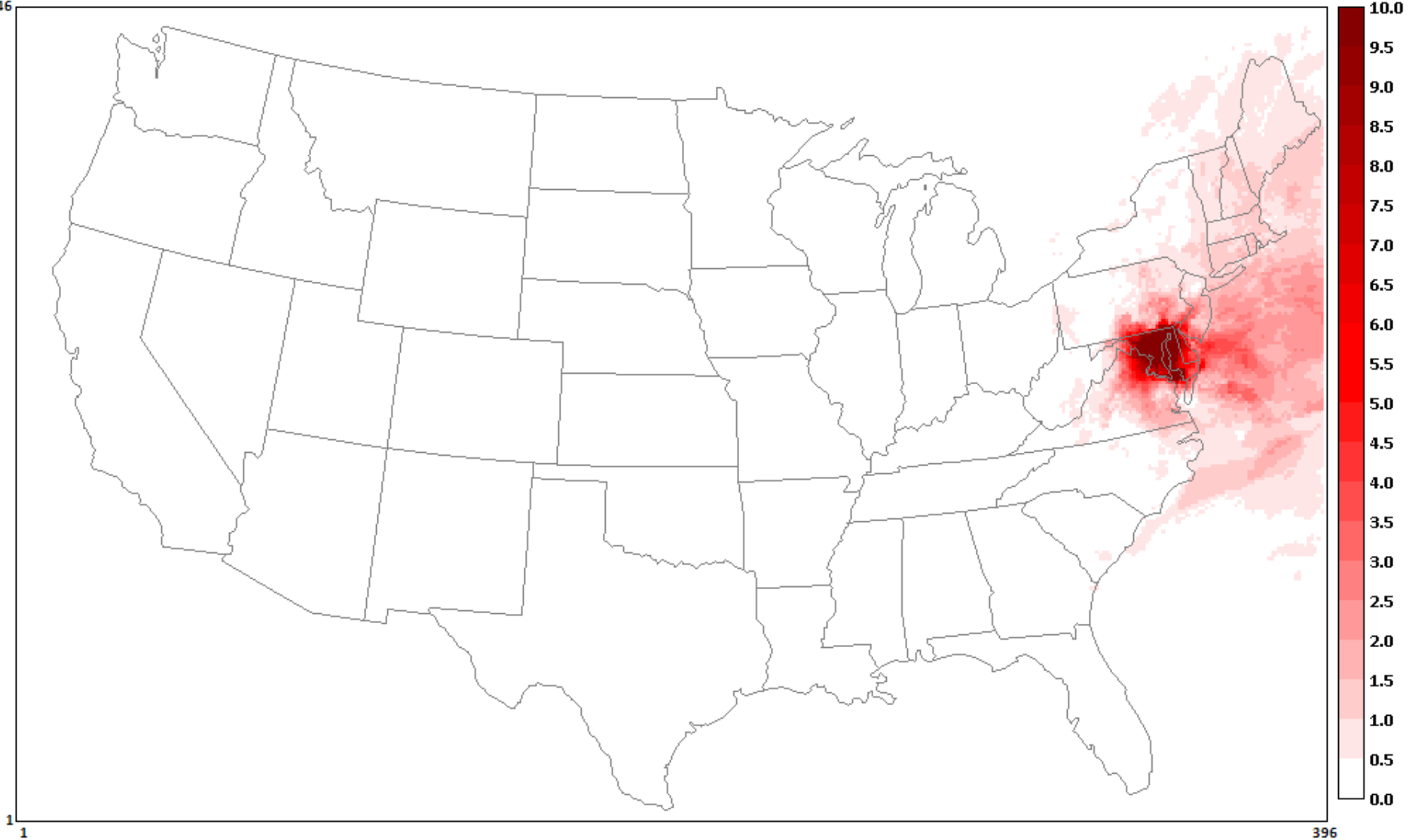
Louisiana



data = [11]2023gf_ussa_apca.tagged.O3NV.12U52.camx.O3_8hrmax_LST.5-9.top10avg.ioapi

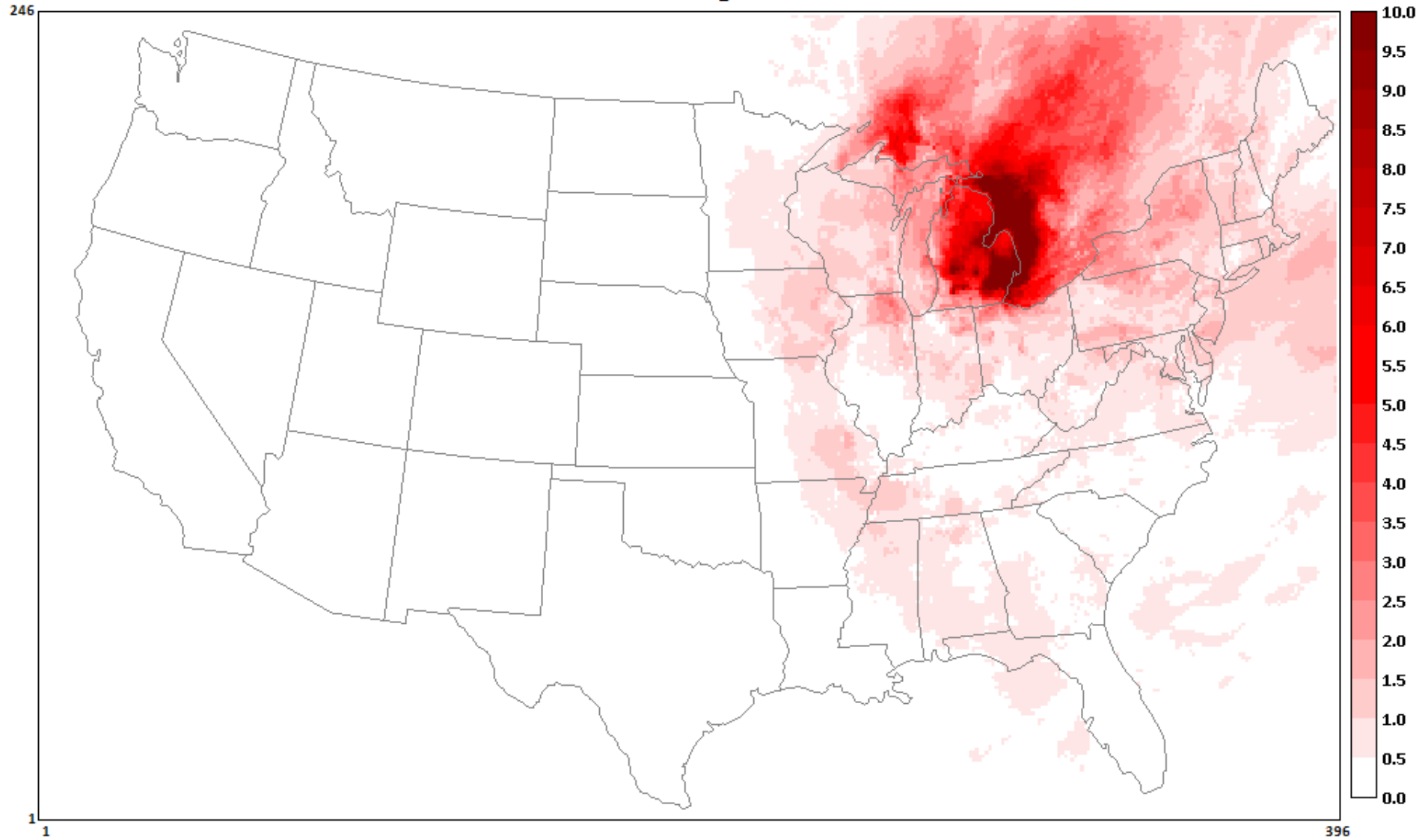
Maryland

246



data = [11]2023gf_ussa_apca.tagged.O3NV.12US2.camx.O3_8hrmax_LST.5-9.top10avg.ioapi

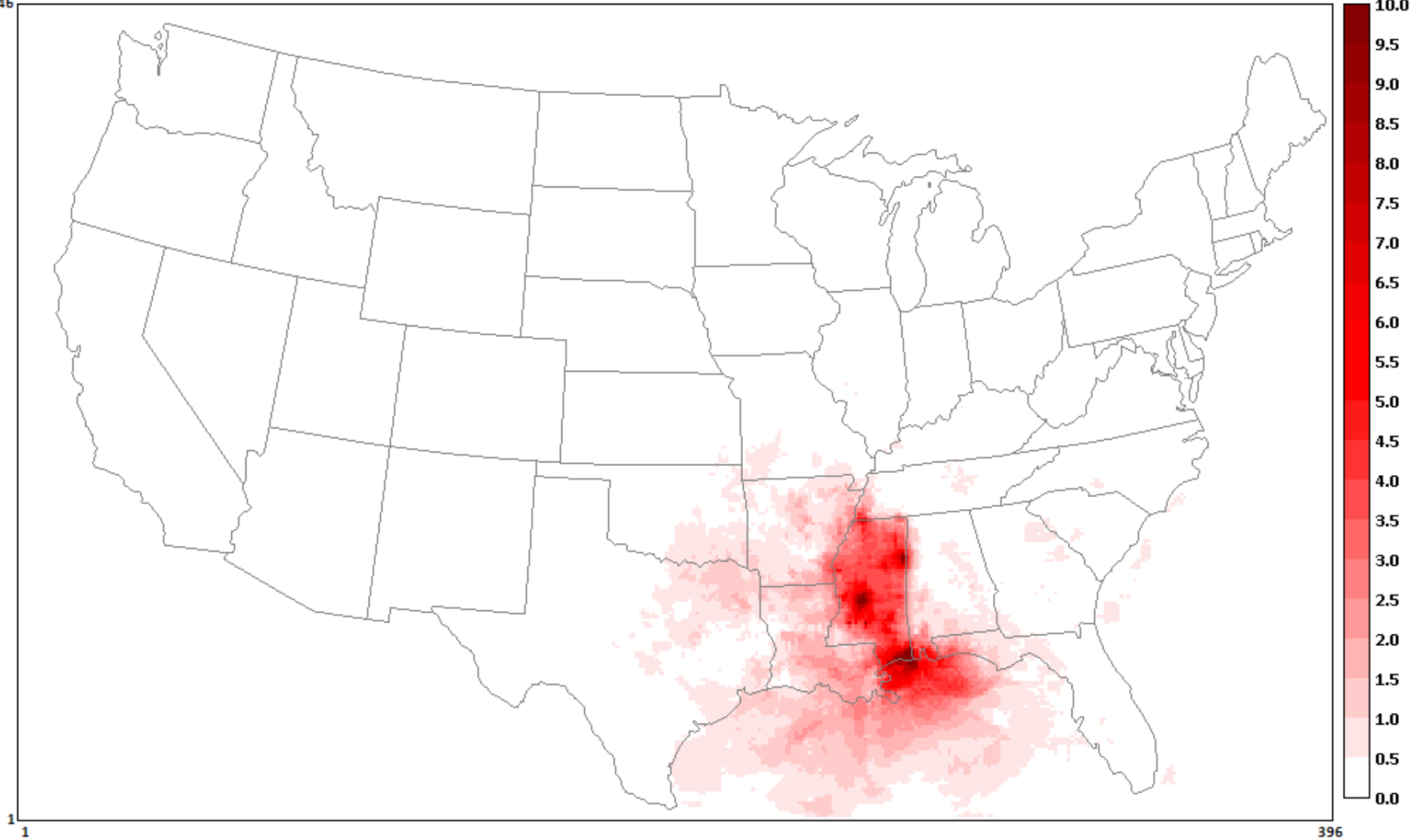
Michigan



data = [11]2023gf_ussa_apca.tagged.O3NV.12US2.camx.O3_8hrmax_LST.5-9.top10avg.ioapi

Mississippi

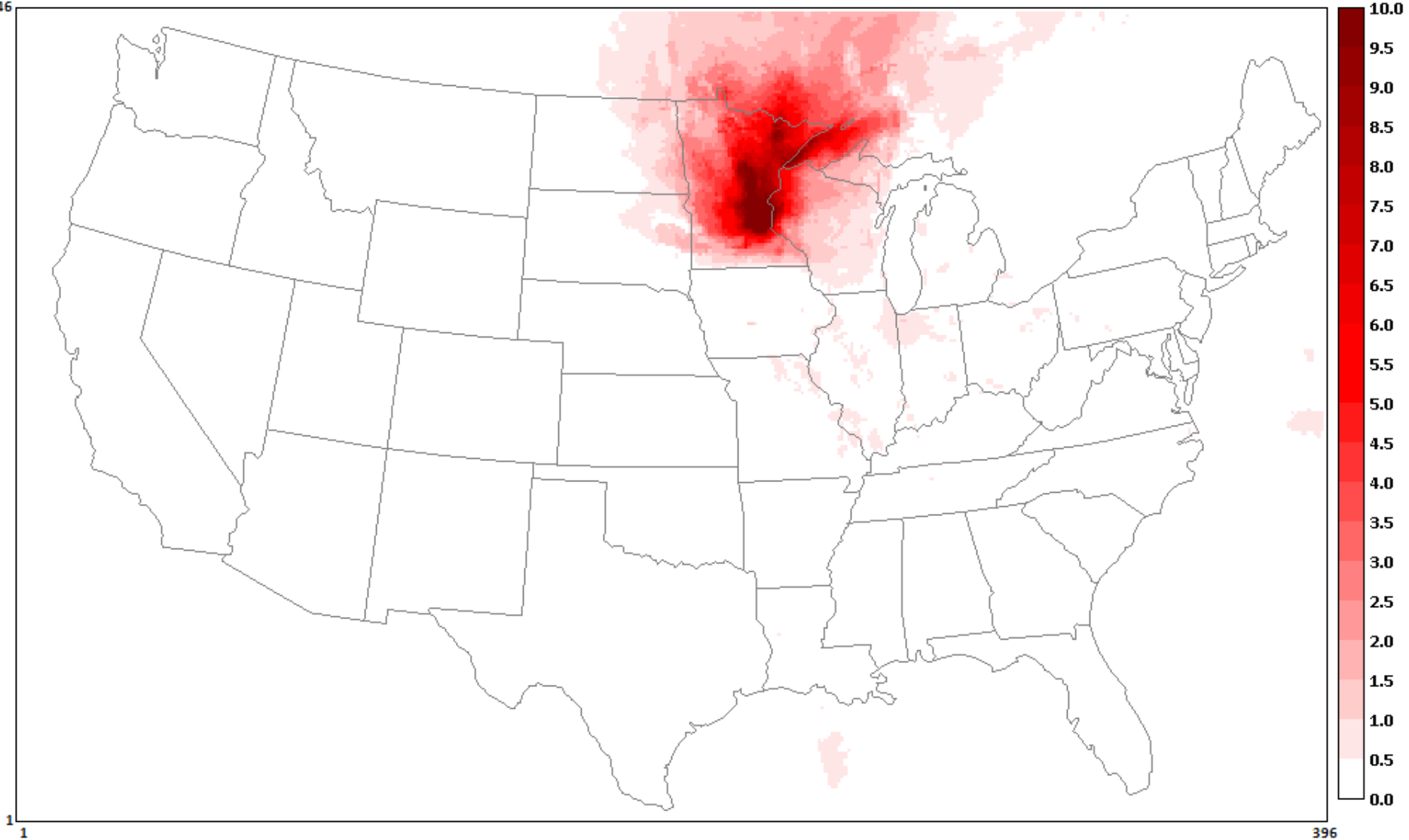
246



data = [11]2023gf_ussa_apca.tagged.O3NV.12US2.camx.O3_8hrmax_LST.5-9.top10avg.ioapi

Minnesota

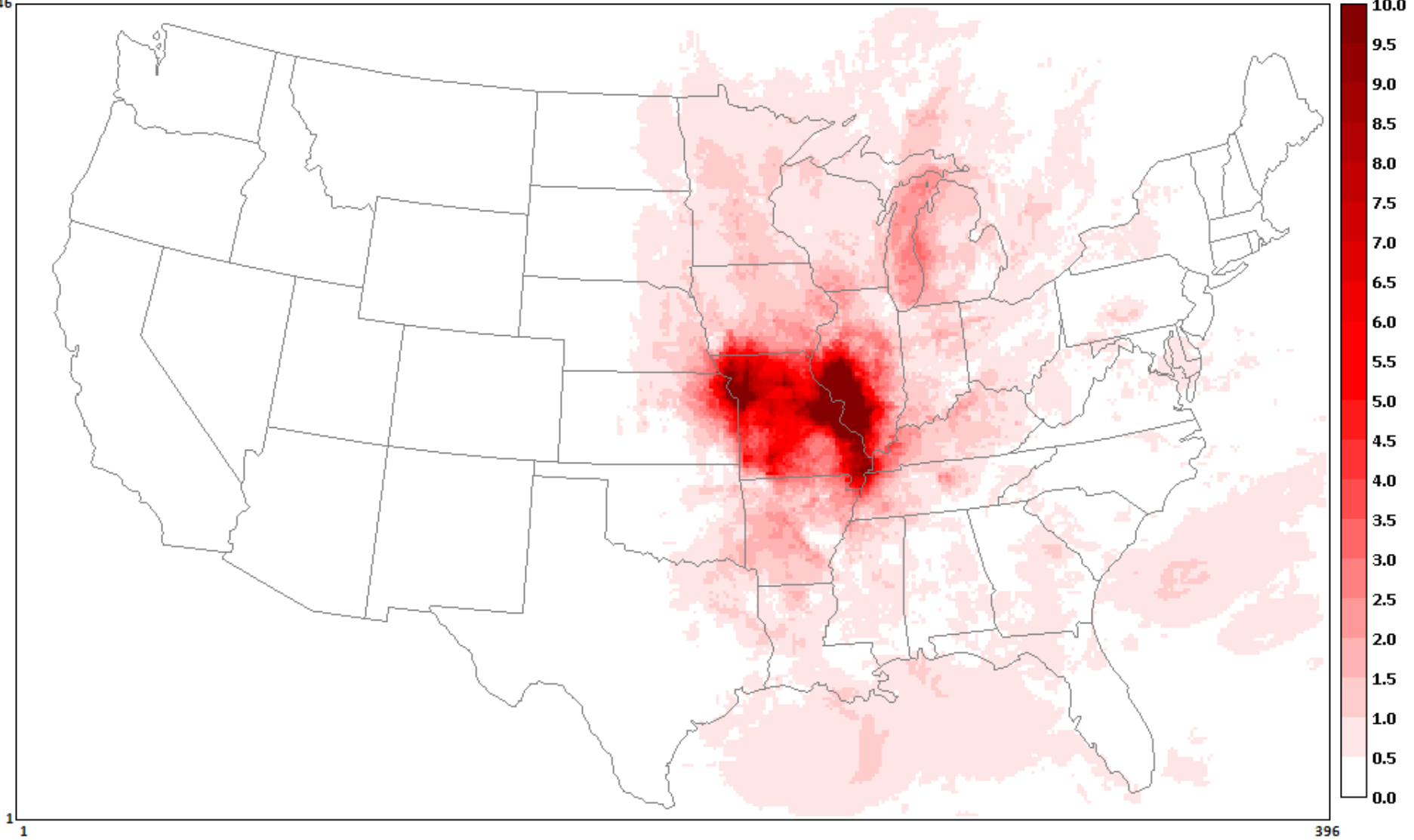
246



data = [11]2023gf_ussa_apca.tagged.O3NV.12US2.camx.O3_8hrmax_LST.5-9.top10avg.ioapi

Missouri

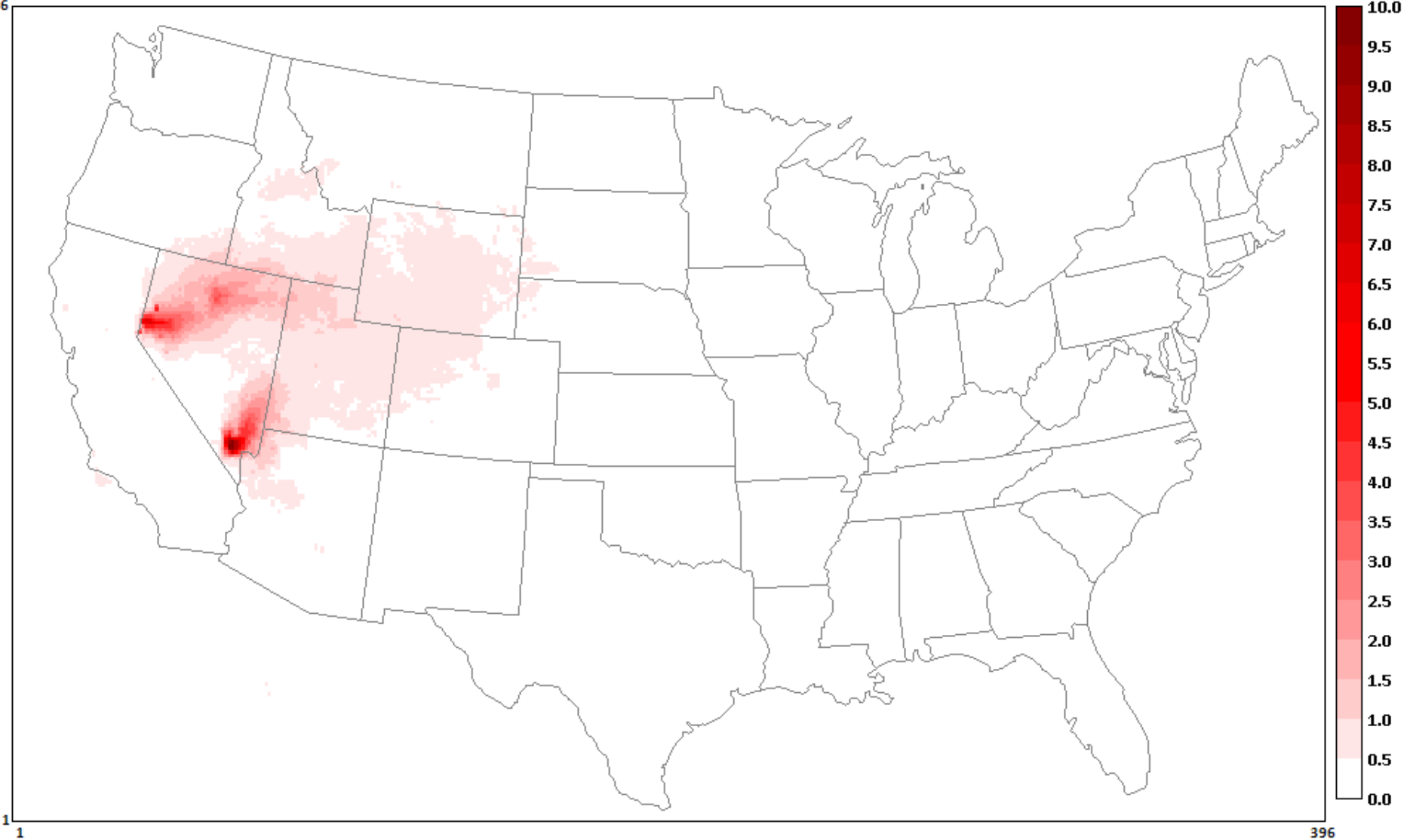
246



data = [11]2023gf_ussa_apca.tagged.O3NV.12US2.camx.O3_8hrmax_LST.5-9.top10avg.ioapi

Nevada

246



data = [11]2023gf_ussa_apca.tagged.O3NV.12US2.camx.O3_8hrmax_LST.5-9.top10avg.ioapi

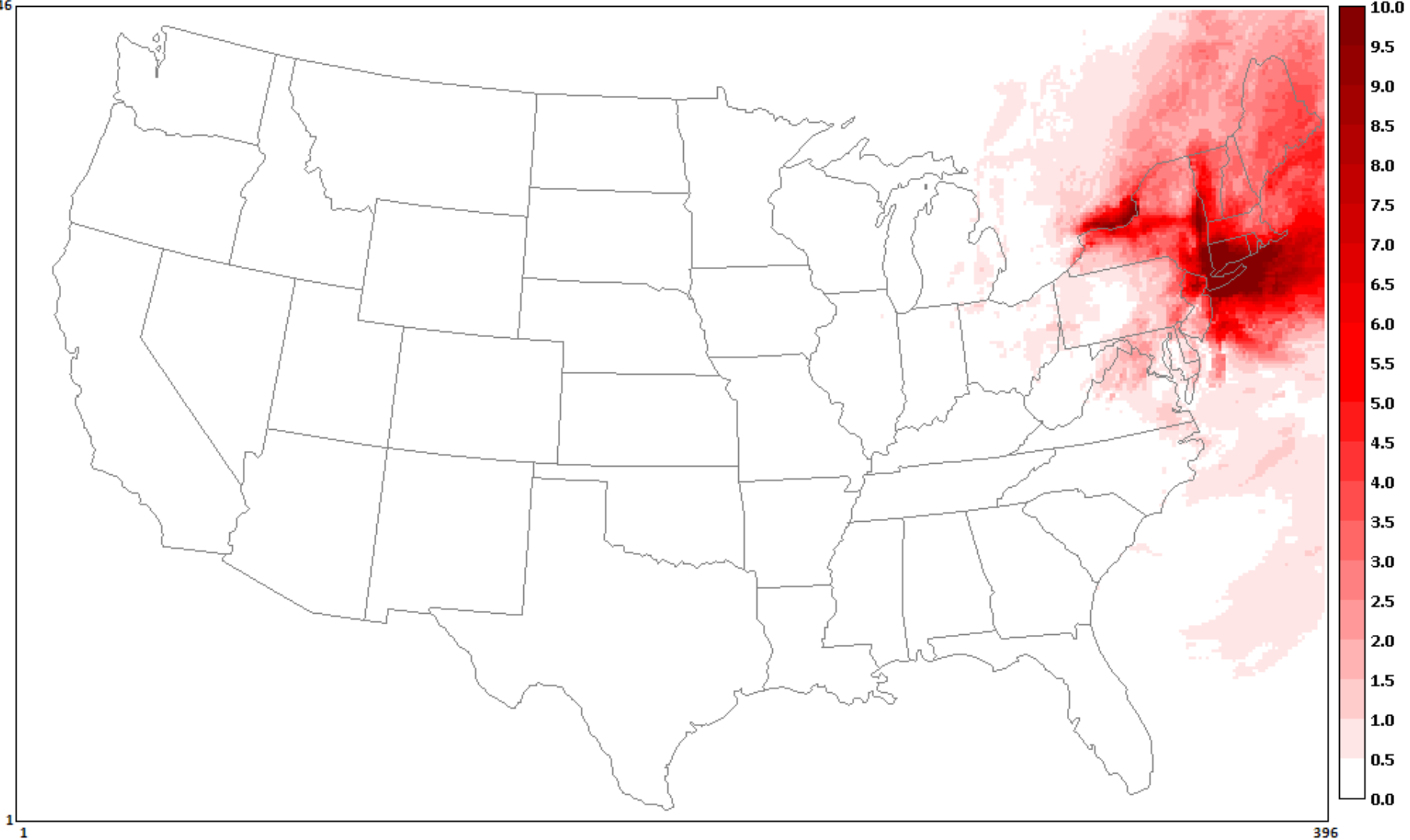
New Jersey



data = [11]2023gf_ussa_apca.tagged.O3NV.12U52.camx.O3_8hrmax_LST.5-9.top10avg.ioapi

New York

246



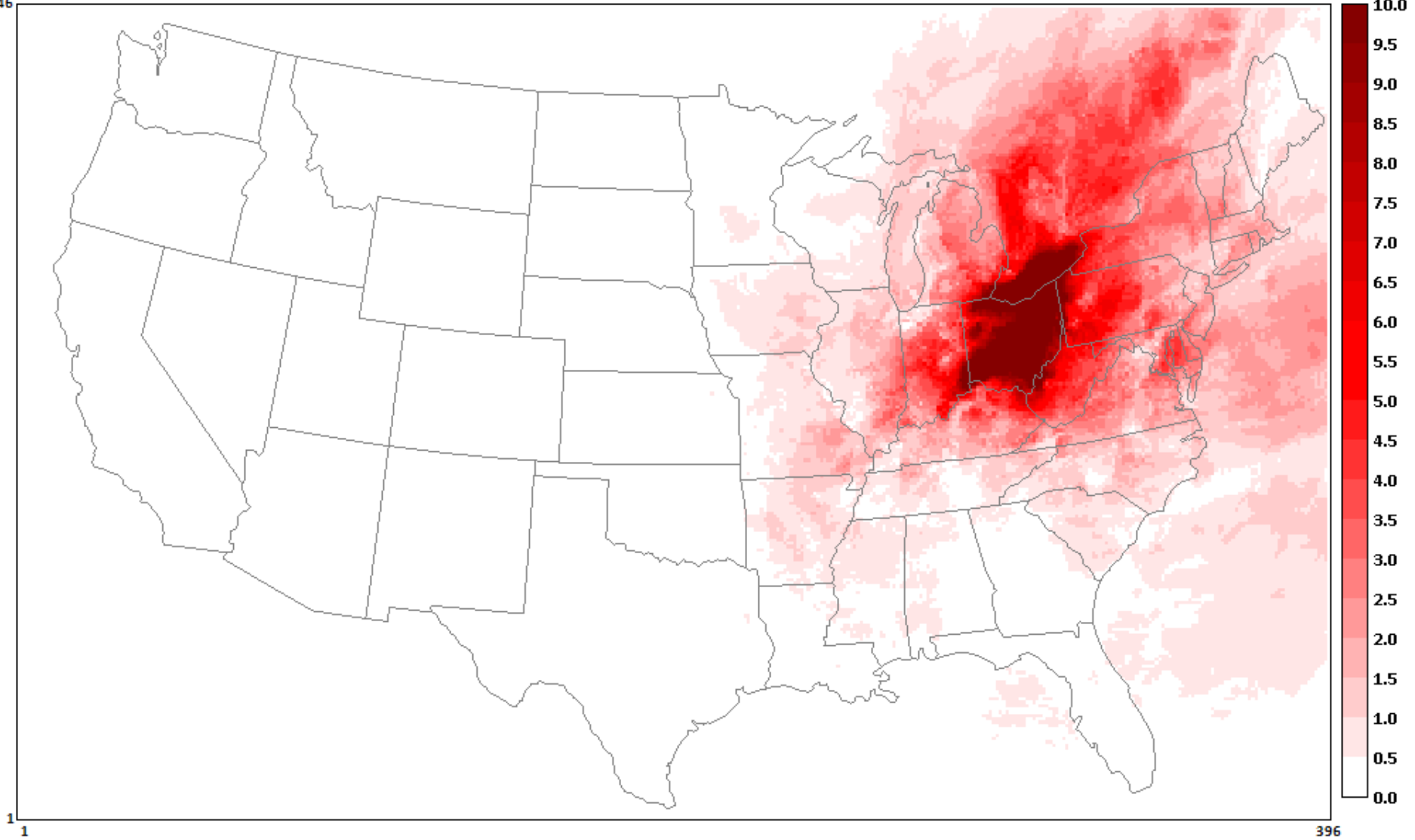
1

396

data = [11]2023gf_ussa_apca.tagged.O3NV.12U52.camx.O3_8hrmax_LST.5-9.top10avg.ioapi

Ohio

246

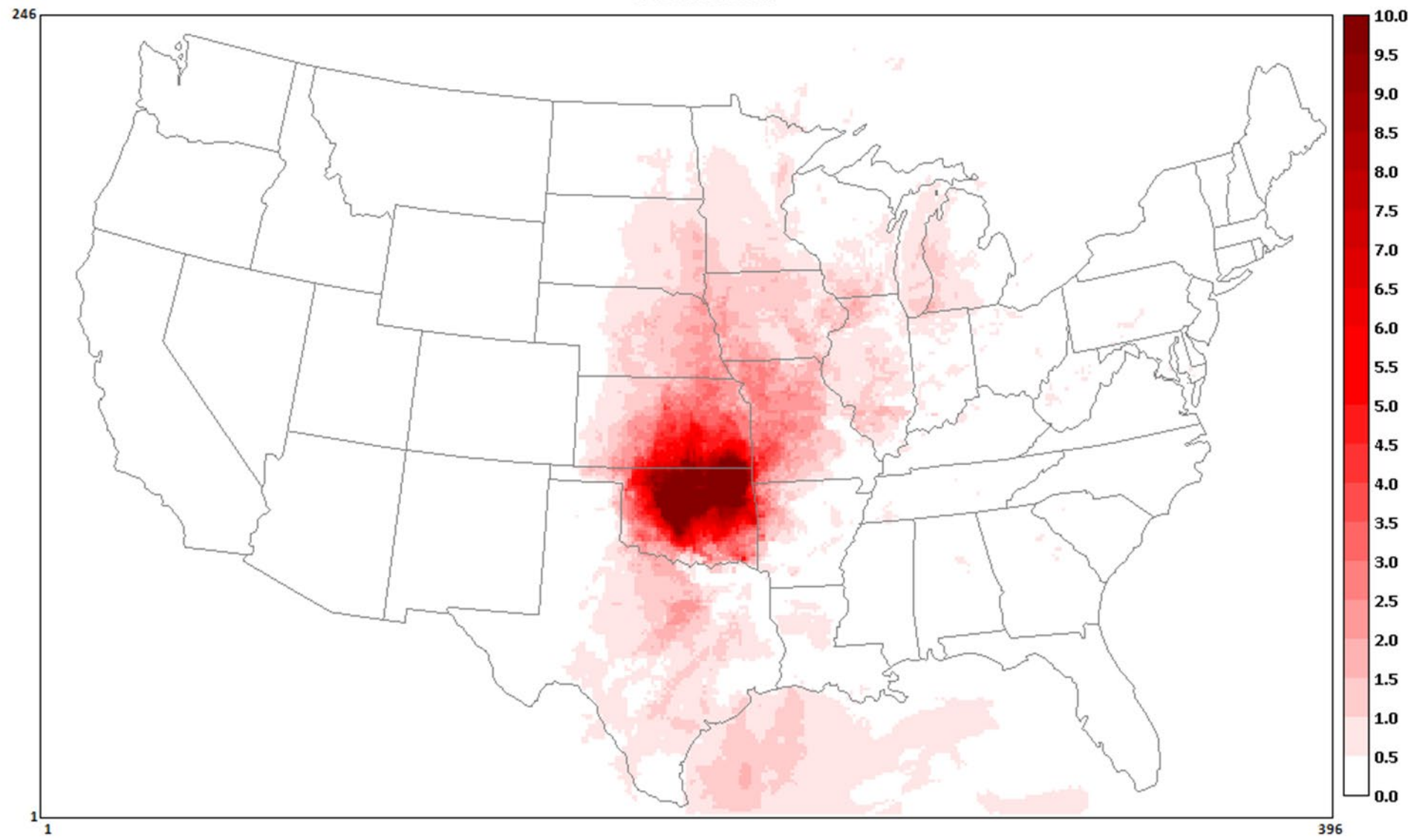


1

396

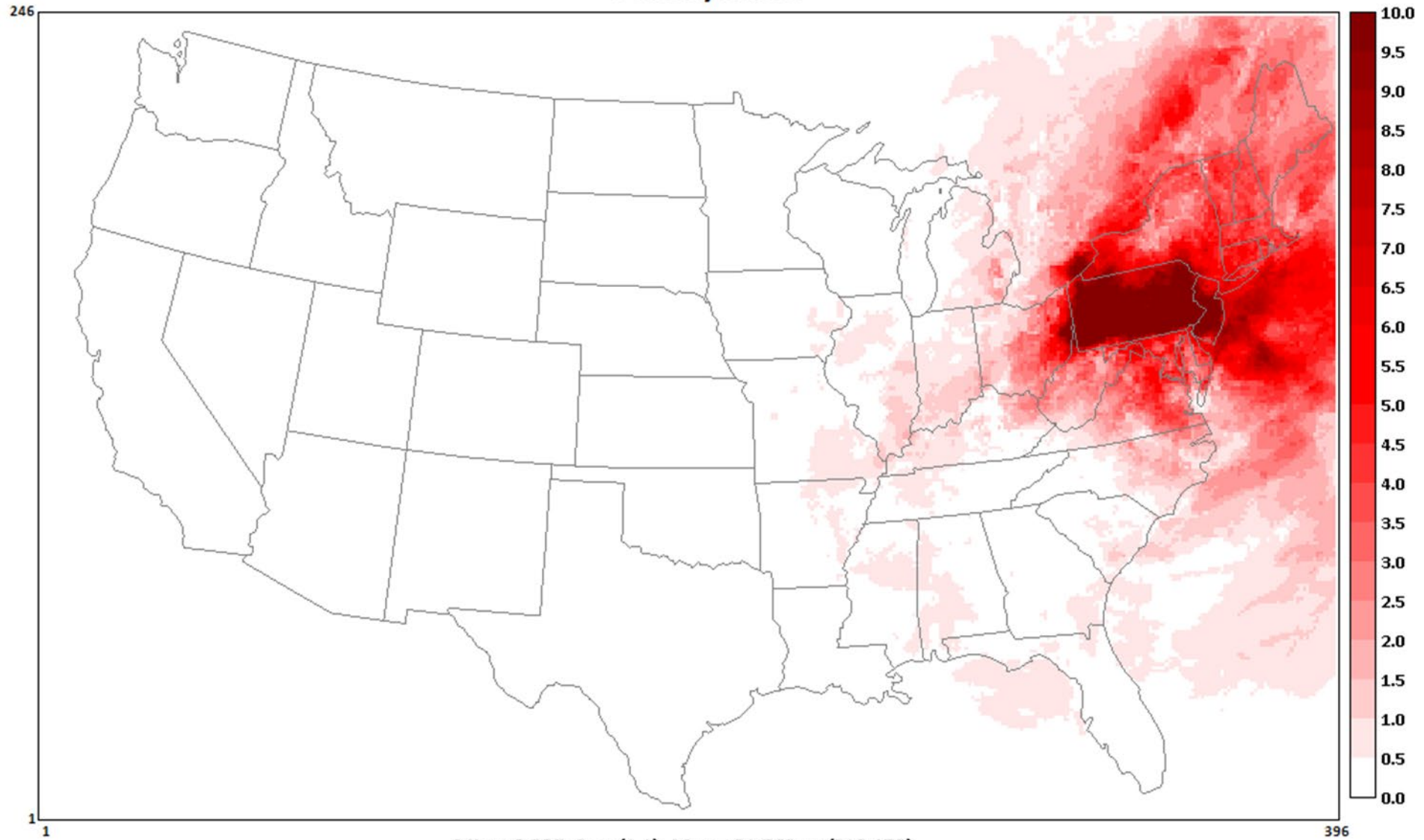
data = [11]2023gf_ussa_apca.tagged.O3NV.12US2.camx.O3_8hrmax_LST.5-9.top10avg.ioapi

Oklahoma



data = [11]2023gf_ussa_apca.tagged.O3NV.12US2.camx.O3_8hrmax_LST.5-9.top10avg.ioapi

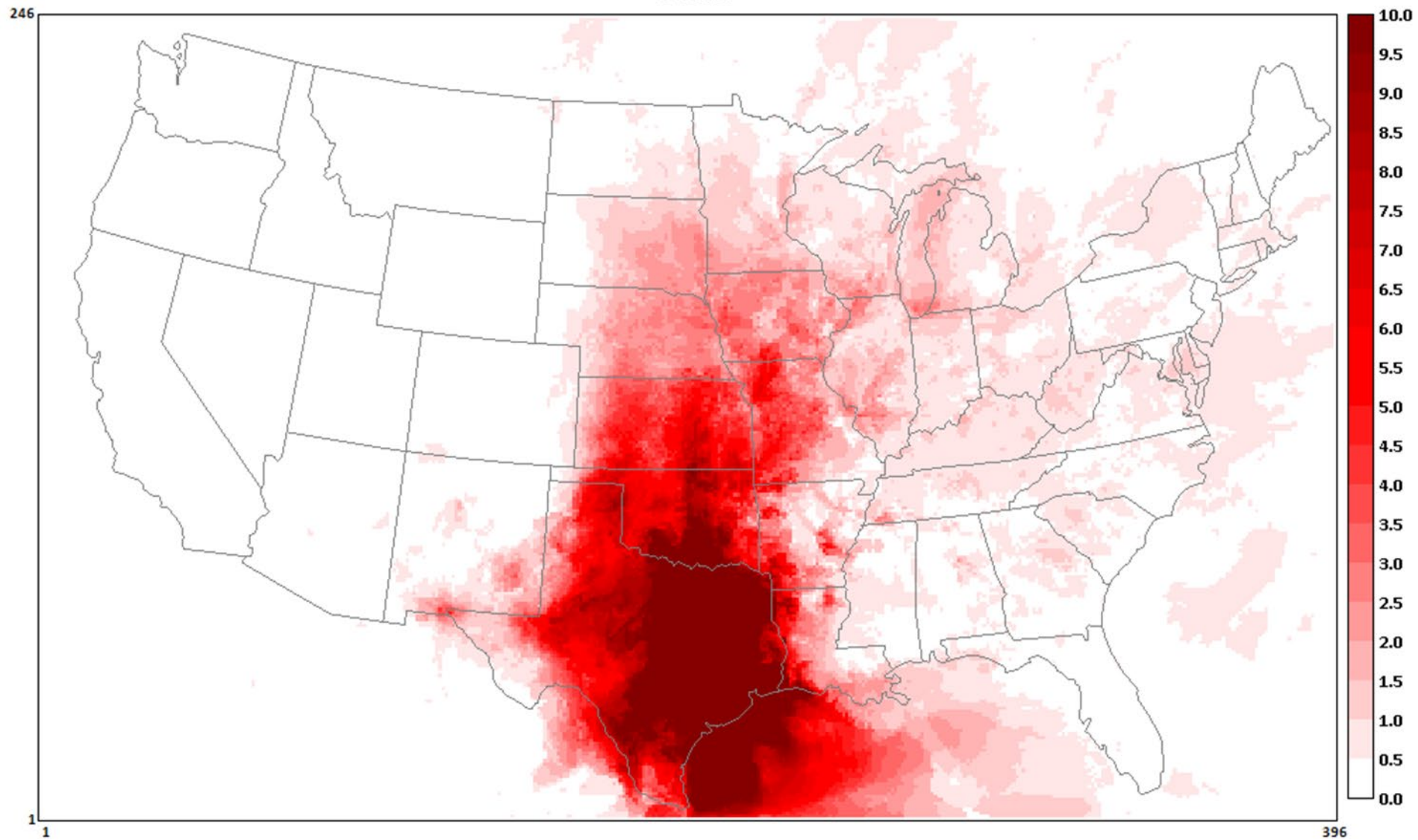
Pennsylvania



Min = 0.00E+0 at (1,1), Max = 21.560 at (319,150)

data = [11]2023gf_ussa_apca.tagged.O3NV.12US2.camx.O3_8hrmax_LST.5-9.top10avg.ioapi

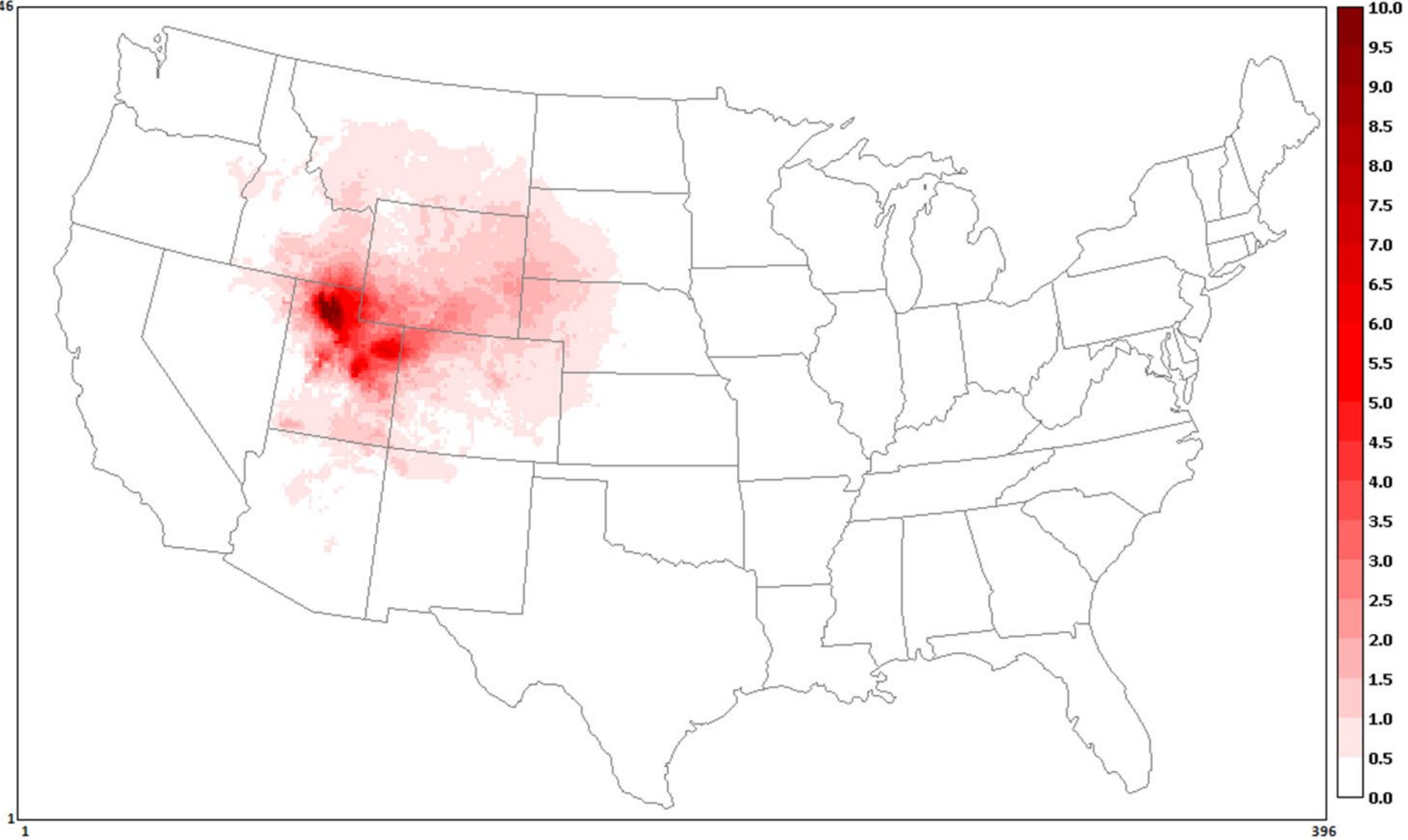
Texas



data = [11]2023gf_ussa_apca.tagged.O3NV.12U52.camx.O3_8hrmax_LST.5-9.top10avg.ioapi

Utah

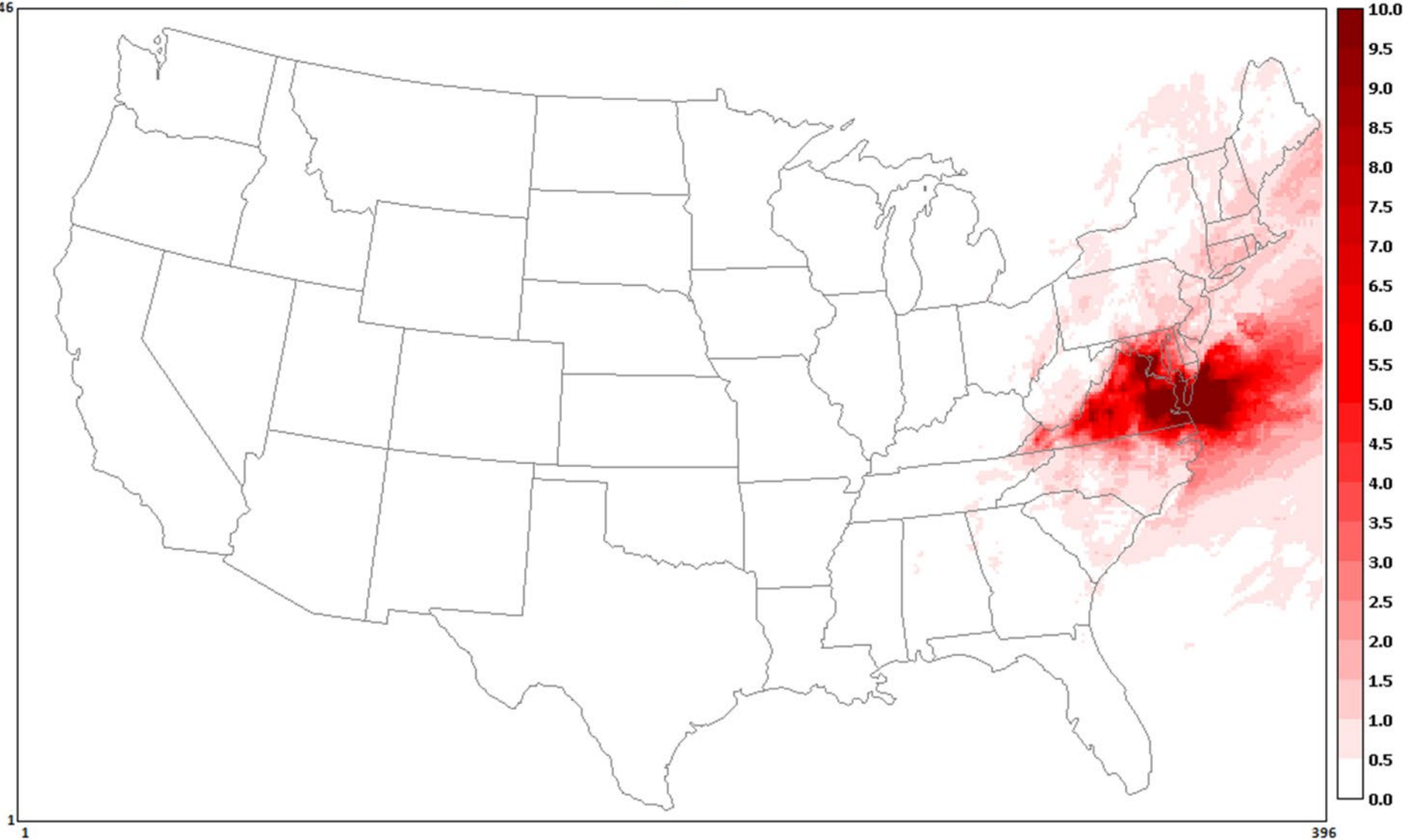
246



data = [11]2023gf_ussa_apca.tagged.O3NV.12US2.camx.O3_8hrmax_LST.5-9.top10avg.ioapi

Virginia

246



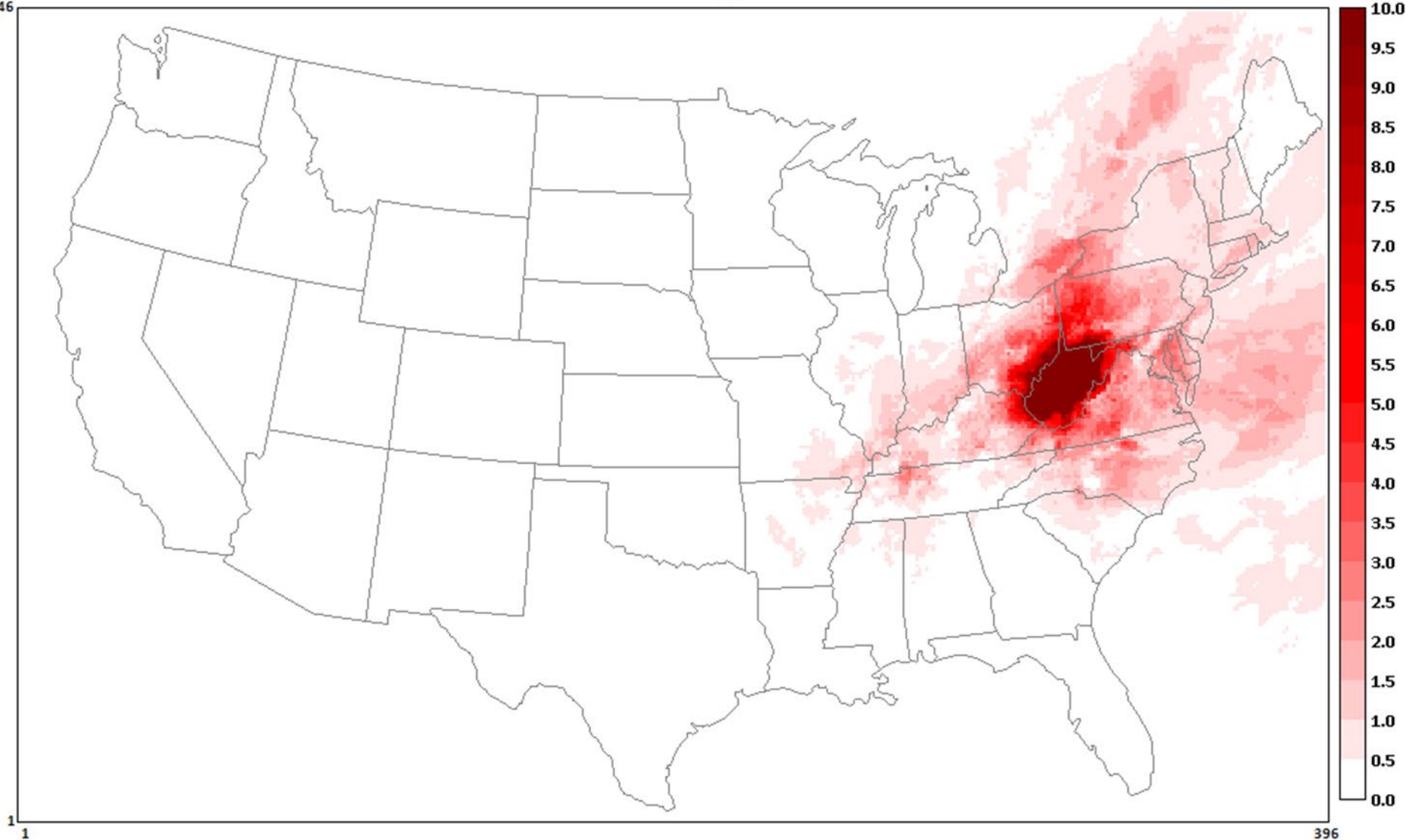
1

396

data = [11]2023gf_ussa_apca.tagged.O3NV.12US2.camx.O3_8hrmax_LST.5-9.top10avg.ioapi

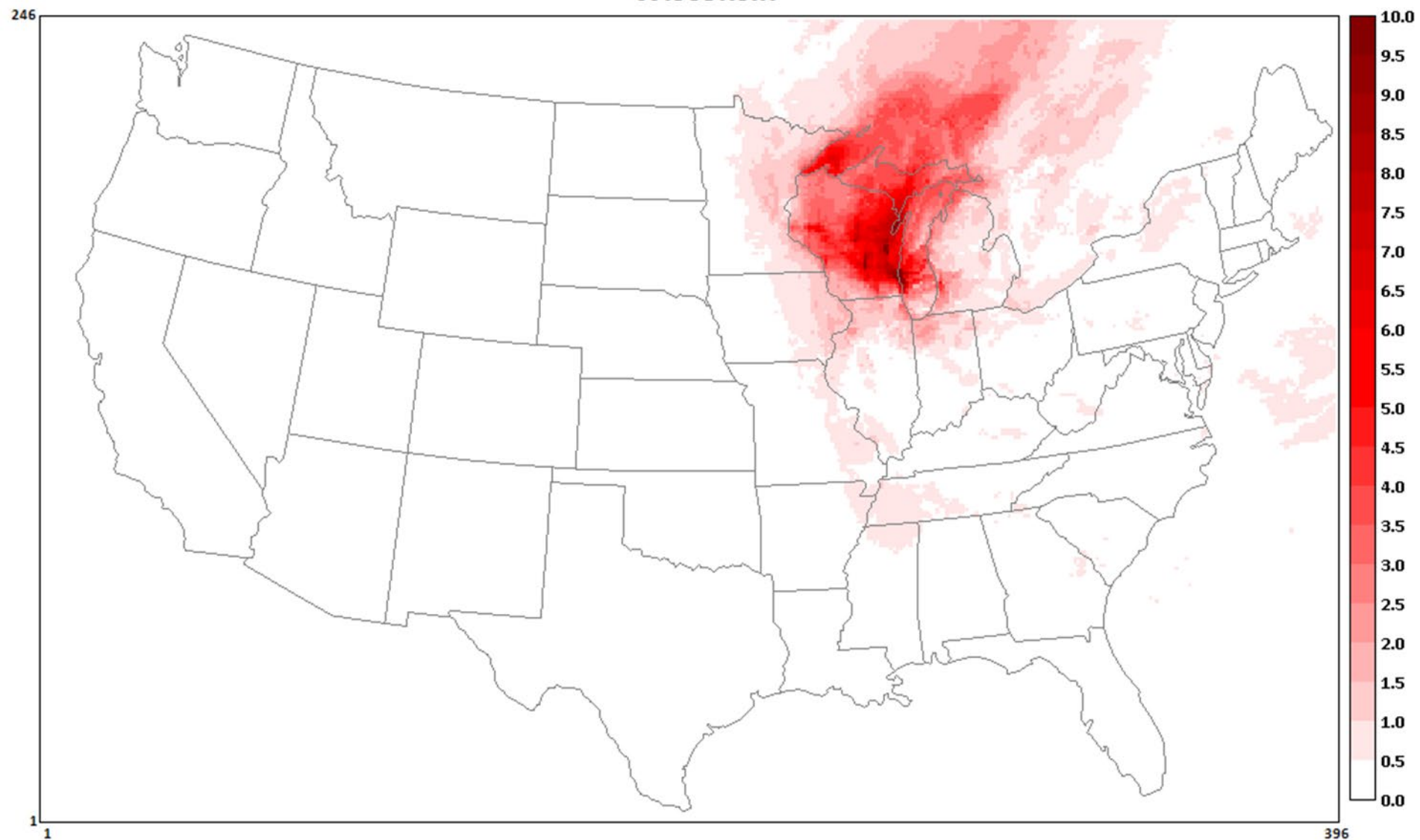
West Virginia

246



data = [11]2023gf_ussa_apca.tagged.O3NV.12US2.camx.O3_8hrmax_LST.5-9.top10avg.ioapi

Wisconsin



data = [11]2023gf_ussa_apca.tagged.O3NV.12US2.camx.O3_8hrmax_LST.5-9.top10avg.ioapi